



TALLINN UNIVERSITY OF TECHNOLOGY
SCHOOL OF ENGINEERING

Department of Electrical Power Engineering and Mechatronics

Developing rehabilitation device for people with
acquired muscle stiffness of lower limbs

MASTER THESIS

MECHATRONICS PROGRAM

Student Dmytro Tkachivskyi

Student code 156353MAHM

Supervisor Mart Tamre
 Maito Hiiemaa

Tallinn, 2017

AUTHOR'S DECLARATION

Hereby i declare, that I have written this thesis independently.

No academic degree has been applied for based on this material.

All works, major viewpoints and data of the other authors used in this thesis have been referenced.

Thesis is completed under the supervision of Mart Tamre and Maido Hiiemaa.

“.....” 201....

Author:

/signature/

Thesis is in accordance with terms and requirements

“.....” 201....

Supervisor:

/signature/

Supervisor:

/signature/

Accepted for defence

“.....” 201....

Chairman of theses' defence commission:

/signature/



TALLINNA TEHNIKAÜLIKOOL
INSENERITEADUSKOND

Elektroenergeetika ja mehhaproonika instituut

Seadme arendus inimese alajäsemetes omandatud lihasjäikuse taastusraviks

MAGISTRITÖÖ

MEHATROONIKA ÕPPEKAVA

Üliõpilane

Dmytro Tkachivskyi

Üliõpilaskood

156353MAHM

Juhendaja

Mart Tamre

Maido Hiiemaa

Tallinn, 2017

AUTORIDEKLARATSIOON

Deklareerin, et käesolev lõputöö on minu iseseisva töö tulemus.

Esitatud materjalide põhjal ei ole varem akadeemilist kraadi taotletud.

Lõputöös kasutatud kõik teiste autorite tööd ja seisukohad ning materjalid on varustatud vastavate viidetega.

Töö valmis Mart Tamre ja Maito Hiiemaa juhendamisel.

“.....” 201....a.

Töö autor:

/allkiri/

Töö vastab lõputööle esitatavatele nõutele

“.....” 201....a.

Juhendaja:

/allkiri/

Juhendaja:

/allkiri/

Lubatud kaitsmisele

“.....” 201....a.

..... õpperekava lõputööde kaitsmiskomisjoni esimees:

/allkiri/

THESIS TASK

Student

Dmytro Tkachivskyi, 156353 MAHM

Study programme, main speciality:

MAHM 02/13, Mechatronics

Supervisor:

Mart Tamre, Maido Hiiemaa

Thesis topic:

(in English): Developing rehabilitation device for people with acquired muscle stiffness of lower limbs

(in Estonian): Seadme arendus inimese alajäsemetes omandatud lihasjäikuse taastusraviks

Thesis proposal:**1. Introduction**

The purpose of this Master Thesis is to build device that helps to work out and stretch lower limbs those people who suffer from stiffness of muscular tissues.

Respective phenomena possess a progressive nature, meaning that injured person does not experience much discomfort on the essential stages of disease. However, in time, patient slowly loses its mobility, as his or her legs do not stretch enough anymore.

Therefore, the first and main task to be solved by conducting this research is to build the machine helping to regain muscle flexibility via limb stretching. Particularly, this apparatus will be designed for person moving in a wheelchair. Thus, the device will be adapted for using in a small area (e.g. an apartment) and will perform smooth linear movements of a special carriage with a foot strapped to it, making knee joint unbend. Meanwhile patient stays seated in the wheelchair, mechanically linked with machine's frame.

The second goal is to make this device from standard parts and materials presently available on the market, using as few custom details as possible.

A product of this research could potentially be employed separately by medical institutions as well as healthcare industry in general. Also, private customers might expose an interest to buy it, if the end price is affordable enough.

2. Background

Presently, there are very few types of rehabilitation devices designed for lower limbs of human body. However, upon closer examining even those few, either conceptual or commercial solutions, it turns out that all of them seem to be meant for different kind of injury, not the one this research is conducted for. Thus, neither of them can be used for regaining muscle flexibility by patients on a wheelchair.

The closest by its functionality device is called “You bike”. [1] It is a commercial product. Despite the only similarity - being capable to work in conjunction with wheelchair - it is purely mechanical device, where legs move being strapped to lower pair of pedals as long as patient has to spin manually upper pair of pedals with his own hands. The link between upper and lower pedals is done by mechanical chain/belt transmission of momentum. This technology is also inappropriate as it does not imply the linear movement, which is strongly required when muscle flexibility is almost lost.

Another similar commercial product is called “Berkelbike” which is designed to be used outside mostly. [2] Also there exists a patent for generic device for indoor use. [3] It is heavy and bulky machine, which also seems to be very costly when it comes to mass production.

Next type of rehabilitation devices is CPM machines for post-surgical rehabilitation. [4] This type of equipment is already employed by many hospitals around the globe. Nevertheless, its main drawbacks are price (usually over \$1000 [5]) and relatively fragile structure, which only fits to short periods of post-surgical rehabilitation, when limbs are basically healthy. [6]

The rest of devices is grouped into third type – a wearable equipment. These are devices which patient ought to put on, in order to benefit from it. There is a subgroup of locally wearable devices, that are designed to be worn on a certain region of a limb, mostly on the knee joint [7] [8] [9] and devices that are designed for whole leg. [10] [11] These are relatively customizable and adjustable solutions. But they are meant to be an assistive devices for patients who can walk. Therefore, these prototypes also are not beneficial in the given case, although some of applied engineering solutions are worthy to be employed in this study.

3. Methodology

- Describe your approach to address the problem, identify any key new insights and/or approaches:
 - 1) Background research on existing prototypes and commercial mass-production solutions.
 - Analysis of different engineering approaches. Classification of theirs complexity.
 - 2) Developing a conceptual CAD model:
 - Justifying its design and technical parameters;
 - Choosing building materials;
 - Choosing actuators (generic).
 - 3) Research on different kinds of actuators (pneumatic, hydraulic, electric):
 - Price, maintainability and simplicity of setting;
 - Stress simulation under working conditions.
 - 4) Research on dynamical properties of the system (limb+device):
 - Genesis of pathology of lower limbs muscle stiffness;
 - Physical and mathematical model of the injured organ.

- 5) Choosing and justifying of control algorithm (neuro-controller, PID-controller, fuzzy-controller):
 - Comparison of respective types of controllers;
 - Creating of control algorithm with regards to given task.
- 6) Modelling, validation and analysis of obtained results.
- 7) Creating of technical documentation (manufacturing drawings etc.).
- 8) Ordering materials and actual assembly of the prototype.

- Describe how the success of the research will be measured:

Under given conditions, the research may be considered as successful when technical problem is solved. Particularly, the problem is solved when patient who suffers from muscle stiffness can work out his muscles on the lower limbs with measurable therapeutic progress.

4. Research schedule

	Name of chapter done	Date range
1.	Background research	20.02 – 24.02
2.	Developing a conceptual CAD model	27.02 – 3.03
3.	Research on different kinds of actuators	15.03 – 17.03
4.	Research on dynamical properties of the system (limb+device)	27.03 – 31.03
5.	Choosing and justifying of control algorithm	6.04 – 10.04
6.	Modelling, validation and analysis of obtained results	24.04 – 28.04
7.	Creating of technical documentation	3.05 – 5.05
8.	Ordering materials and actual assembly of the prototype	8.05 – 2.06

5. References

- [1] "Rehabilitation Engineering," 2017. [Online]. Available: <https://www.anatomicalconcepts.com/youbike/>. [Accessed 18 February 2017].
- [2] "Rehabilitation Engineering," 2017. [Online]. Available: <http://www.berkelbike.co.uk/>. [Accessed 18 February 2017].
- [3] "US patent," 2017. [Online]. Available: <https://docs.google.com/viewer?url=patentimages.storage.googleapis.com/pdfs/US20120329611.pdf>. [Accessed 18 February 2017].
- [4] "CPM Machine after knee replacement," 2017. [Online]. Available: <https://www.verywell.com/do-i-need-a-cpm-following-knee-surgery-2548662>. [Accessed 18 February 2017].

- [5] "Online auction," 2017. [Online]. Available: https://www.alibaba.com/product-detail/Continuous-Passive-MotionNew-Products-Health-Leg_60361849022.html. [Accessed 18 February 2017].
- [6] "Rehabilitation Engineering," 2017. [Online]. Available: <http://www.chinesport.com/catalogue/rehabilitation-equipment/continuous-passive-motion-lower-limbs/XRI003-fisiotek-3000e/>. [Accessed 18 February 2017].
- [7] "The James Dyson Foundation," 2017. [Online]. Available: <http://www.jamesdysonaward.org/en-GB/projects/powered-leg-brace/?cookies=true>. [Accessed 18 February 2017].
- [8] A. M. Dollar and H. Herr, "Design of a Quasi-Passive Knee Exoskeleton to Assist Running," Acropolis Convention Center, 22-26 September 2008. [Online]. Available: https://www.eng.yale.edu/grablab/pubs/dollar_IROS08.pdf. [Accessed 18 Feruary 2017].
- [9] M. R. Tucket, A. Moser, O. Lambery, J. Sulzer and R. Gassert, "Design of a Wearable Perturbator for Human Knee," 2013 IEEE International Conference on Rehabilitation Robotics, 24-26 June 2013. [Online]. Available: <https://infoscience.epfl.ch/record/189717/files/Tucker%20MR%202013%20Design%20of%20a%20wearable%20perturbator%20for%20human%20knee%20impedance%20estimation%20during%20gait.pdf>. [Accessed 18 February 2017].
- [10] K. Goher and S. Fadlallah, "Design, Modelling, and Control of a Portable Leg Rehabilitation System," Journal of Dynamic Systems, Measurement, and Control, 2017. [Online]. Available: <http://dynamicsystems.asmedigitalcollection.asme.org/pdfaccess.ashx?url=/data/journals/jdsmaa/0/ds-16-1410.pdf>. [Accessed 18 February 2017].
- [11] E. Garcia, D. Sanz-Merodio, M. Cestari, M. Perez and J. Sancho, "An active knee orthosis for the physical therapy," Centre for Automation and Robotics, CSIC-UPM, 28500 Arganda del Rey, Madrid,, [Online]. Available: <http://digital.csic.es/bitstream/10261/133286/1/603130.pdf>. [Accessed 18 February 2017].

Student: “.....” 201....

Supervisor: “.....” 201....

Supervisor: “.....” 201....

CONTENTS

Introduction	12
1. Background research.....	13
1.1 Introduction	13
1.2 Wearable/mobile devices.....	13
1.3 Stationary devices.....	16
1.4 Analysis of existing concepts	18
2. Genesis of pathology of lower limbs muscle stiffness.....	20
2.1 The research.....	20
2.2 Physical model of the injured organ	22
3. Developing solution using CAD	27
3.1 Building materials.....	27
3.2 Design and technical parameters	27
3.3 Chosing generic actuators.....	31
3.4 CAD concept summary	34
3.5 Simulating human muscle in mechanical domain	35
4. Comparison of different types of actuators.....	38
4.1 The overview	38
4.2 Electric actuators	38
4.3 Pneumatic actuators	42
5. Developing of control algorithm	47
5.1 The overview	47
5.2 Creating of control algorithm	49
6. Technical parameters and validation of device's design.....	54
6.1 General technical data and cost of the project.....	54
6.2 Validation of device's design	54
Summary	60
Kokkuvõte	61
References	62
Appendices	71-102

LIST OF ABBREVIATIONS AND SYMBOLS

(HK)AFO – (hip-knee-) ankle-foot-orthosis

SMS – Stiff man syndrome

GAD – glutamic acid decarboxylase

EMG – electromyogram

REC – rectus femoris

VAS – vastus lateralis; vastus medialis

GLU – gluteus maximus

HAM – hamstrings

GAS – gastrocnemius

SOL – soleus

PCA – physiological cross-sectional area

SM – semimembranosus

ST – specific tension

CAD – computer aided design

PID – proportional-integral-derivative (control)

EC – emergency controller

CE – contractile element

SE – seres (elastic) element

PE – parallel (elastic) element

DC – direct current

VAC – volts of alternating current

RPM – rounds per minute

NC (switch) – normally closed (switch)

TI – Texas Instruments

PC – personal computer

ADC – analog - digital converter

DAC – digital - analog converter

DOF – degree-of-freedom

PREFACE

The Thesis topic was initiated by the Department of Mechatronics at Tallinn University of Technology. The major Thesis works were made using facilities and resources of Tallinn University of Technology, particularly library and computer laboratories with specialized software installed for simulation purposes. This study may contain certain interest for the people involved in medical or engineering field, who work on medical rehabilitation problems.

The author of this study would like to thank the Head of Department of Mechatronics at Tallinn University of Technology Professor Mart Tamre and the Research Scientist of Department of Mechatronics at Tallinn University of Technology Ph.D. Maito Hiiemaa for their assistance during working on this paper.

INTRODUCTION

The purpose of this Master Thesis is to build device that helps to work out and stretch lower limbs those people who suffer from stiffness of muscular tissues.

Respective phenomena possess a progressive nature, meaning that injured person does not experience much discomfort on the essential stages of disease. However, in time, patient slowly loses its mobility, as his or her legs do not stretch enough anymore.

Therefore, the first and main task to be solved by conducting this research is to build the machine helping to regain muscle flexibility via limb stretching. Particularly, this apparatus will be designed for person moving in a wheelchair. Thus, the device will be adapted for using in a small area (e.g. an apartment) and will perform smooth linear movements of a special carriage with a foot strapped to it, making knee joint unbend. Meanwhile patient stays seated in the wheelchair, mechanically linked with machine's frame.

The second goal is to make this device from standard parts and materials presently available on the market, using as few custom details as possible.

A product of this research could potentially be employed separately by medical institutions as well as healthcare industry in general. Also, private customers might expose an interest to buy it, if the end price is affordable enough.

1. Background research

1.1 Introduction

Nowadays there are plenty of rehabilitation devices for human lower extremities available on the market. In parallel, there are numerous of researches on new variants of prototypes going on worldwide.

Generally, all of them, either already made or those yet to be produced, differ in one principal feature: that is stationary or wearable/mobile usage. Another significant difference is in devices' construction themselves, which is determined by the type of prescribed medical rehabilitation. Be it ordinary post-surgical recovery of knee joint of the healthy person, the construction of the machine most likely will not be of heavy duty type.

On contrary, if a patient has been struggling with muscular or neurological disease for years, then it is being considered as chronic and because of that more intensive exercising is involved. Thus, the rehabilitation process requires reliable equipment, being able to withstand abnormal training conditions.

1.2 Wearable/mobile devices

In majority of cases this kind of rehabilitation equipment is meant for people who are still in command of their lower extremities, having some medical disorders though. The whole design of the device is dictated by the fact that a patient can walk or at least to stand.

A wearable rehabilitation device for lower human extremity can be of the following types: AFO (ankle-foot-orthosis), KAFO (knee-ankle-foot orthosis), HKAFO (hip-knee-ankle-foot orthosis).

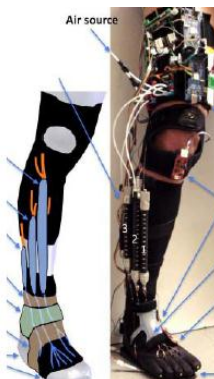


Figure 1.1. Bio-inspired AFO [12]

Figure 1.1 demonstrates a prototype of active orthotic device for ankle-foot pathology [12]. By utilizing the advantages of the pneumatic artificial muscle actuators, an inspired biological musculoskeletal system with a muscle-tendon-ligament structure was introduced as the design of this orthosis system. Three types of sensors are used for the control system: the first is a strain sensor for measuring ankle joint angle changes; the second is an internal measurement unit (IMU) to measure the orientations of the lower leg and the foot; and the third is a pressure sensor to identify the foot ground contacts and gait cycle events [13].



Figure 1.2. KAFO [14]

Above, Figure 1.2 demonstrates a typical knee-foot orthosis, which is used for the treatment of patients with paraplegia after thoracic and/or lumbar spinal cord injuries [14]. While these orthoses provide excellent stability during steady-state standing, they are not convenient for daily home use. As a result, the rate of continuous use of orthoses is low, and they tend to be worn only for standing and exercise in the home setting. Even in the clinical setting, these orthoses are not frequently used because of problems associated with their weight, size, appearance, and comfortableness [15].

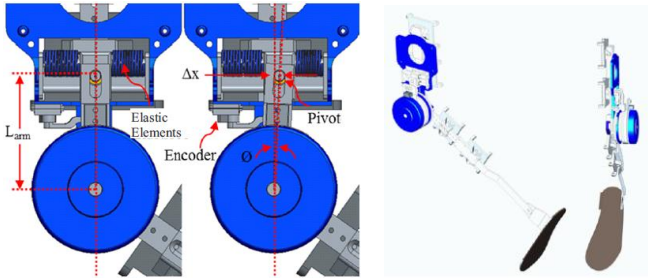


Figure 1.3. KAFO with spring deflection [11]

Figure 3 illustrates yet another approach to designing of knee-ankle-foot orthosis. It shows CAD design of the MB-ActiveKnee. It is an AKAFO (Active Knee Ankle Foot Orthosis), where the ankle joint responds passively. The brace extends down to the foot to provide better grip and stability on the subject. The shank link is adjustable in extension from 20 cm to 70 cm [11].

This project is a joint work between the Centre for Automation and Robotics and Marsi Bionics. It has been conceived to provide active knee control in the leg stance providing the necessary rigidity, and active power during swing. Therefore this active brace compensates for the lack of knee mobility or quadriceps weakness, present in MS, Stroke and PPS [11].

The orthosis ALEX along with force-field controller has been developed for gait rehabilitation of stroke survivors. Its aim is to help in retraining the gait pattern by using assist-as-needed approach which allows the patient to participate more actively in the retraining process compared to other currently available robotic training devices (Figure 1.4) [15] [16]. It belongs to HKAFO type (hip-knee-ankle-foot orthosis).

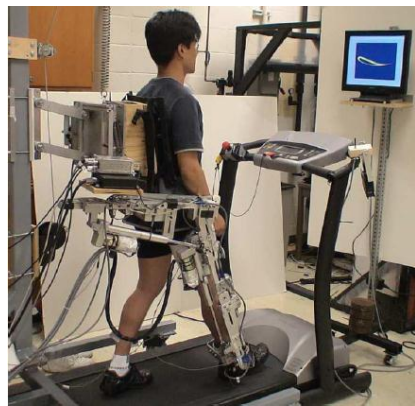


Figure 1.4. Motorized HKAFO ALEX [15]

The RoboKnee (Yobotics, Inc., Cincinnati, OH, USA) is a 1-degree-of-freedom powered knee exoskeleton, for adding power at the knee to assist in stair climbing and squatting during load-carrying (Figure 1.5) [17]. The RoboKnee may be used for the patients who are suffering from weakness in their lower extremities, such causes including cerebral vascular trauma (stroke), post-polio syndrome, multiple sclerosis, muscular dystrophy, and aging. The device consists of a linear series-elastic actuator connected to the upper and lower portions of a knee brace, with the help of which low impedance is achieved just below the hip and on the calf, respectively [15] [18].



Figure 1.5. RoboKnee [15]

The Mobility Device (Tempe, Arizona, USA) allows patients with a wide range of impairments to walk over ground safely (Figure 1.6). It is enforced with a battery operated power lift actuator that lifts patients: weighing up to 159kg (350lbs), from sit to stand. To make the effort easier, the Mobility Device is designed to assist both patient and therapist [15] [19].



Figure 1.6. LiteGait mobility device [15]

The Walking Trainer (Ropox A/S, Naestved, Denmark) is a device to provide a normal walking pattern by controlling weight bearing, balance and posture during walking therapy. It can lift patient from sitting position, with the help of attached to the device lifting actuator. Training can normally be done by one therapist [15] [20].

The WalkTrainer (Cyberthosis, Monthei, Lausanne, Switzerland) is equipped with orthoses for the legs and pelvis, body weight support, and with CLEMS (Closed Loop Electrical Muscle Stimulation) [21], this system allows near perfect mimicking of walking movements with the aim of stimulating nervous system plasticity (Figure 1.7). The WalkTrainer is composed of body weight support, active winch, harness, pelvic orthosis, gait orthesis, motorized wheels, battery, electrostimulator, electrodes and control unit. The main function of the walking frame is to follow the patient while moving. It serves as a mobile support for all the other components [15].



Figure 1.7. WalkTrainer [15]

The BerkelBike (BerkelBike BV, Sint-Michielsgestel, Netherlands) [2] is a combination of a hand and a recumbent bike and is driven by arm as well as leg power (Figure 1.8). It provides support to both muscle groups helping to rehabilitate and keep the muscles stronger and fitter. The benefits of cycling for impaired patients are to overcome overweighting due to lack of activities. The BerkelBike

is for patients with spinal cord injury, polio, multiple sclerosis or stroke (CVA). The BerkelBike (Classic, Home or Pro) is equipped with a sensor that tells the Impuls stimulator the position of the legs. The software in the stimulator uses this information to calculate which muscles to stimulate and the strength of electric pulse required. The electric pulses generated are passed to the muscles via a pair of Impuls electrode shorts. These are like cycling shorts with a number of electrodes embedded within them. The electric pulses stimulate the muscles, causing them to contract at the appropriate time, allowing the person to cycle again [15] [2].



Figure 1.8. BerkelBike Connect [15]

1.3 Stationary devices

The stationary rehabilitation devices can be distinguished by several criteria. One of the most important distinctive characteristics of rehabilitation devices is the nature of the compensation force, which can be passive or active. The compensation force can be considered as passive if it is created by a non-motorized element [15].



Figure 1.9. Ergys2 rehabilitation system [15]

Figure 1.9 depicts stationary system called “Ergys2” (Therapeutic Alliances Inc, Ohio, USA). It is a rehabilitation system for treating neuromuscular disorders and diseases, which is, in fact, an embodiment of a patent # US20120329611 A1 [3].

This device uses computerized functional electrical stimulation (CFES) to allow people with little or no voluntary leg movement to actively pedal [22].

Computer generated, low-level electrical pulses transmitted through surface electrodes cause coordinated contractions of the leg muscles: quadriceps, hamstring, and gluteus. Sensors located in the Ergys2 provide continuous feedback to a computer which controls the sequence of muscle contractions as well as resistance to pedaling [15].



Figure 1.10. Lokomat system [15]

The Lokomat (Hocoma AG, Volketswil, Switzerland) consists of a robotic gait orthosis and an advanced body weight support system (Figure 1.10) [23]. This system adds the ability to measure the patient's activity by a way of force transducers fitted directly on the motors and offers the possibility to adjust the level of gait assistance for each leg between full and zero guidance force [15].



Figure 1.11. MotionMaker rehabilitation device [15]

The aim of MotionMaker (Cyberthosis, Switzerland) (Figure 1.11) is to maintain, or increase muscular volume and capacity for patients in the chronic phase, to reinstate mobility of the joints, to train cardiac capacity and prevent neurological osteoporosis. This innovative concept not only allows automation of the treatment, but also an active participation of the patient's muscles.

The patient's limbs can be mobilized passively or workactively in an electro-stimulated manner and/or voluntarily against resistance loads created by the motors [21].

The MotionMaker has shown the advantages of combining robotics and controlled electrostimulation to improve voluntary control [24]. The activation of muscles in exercises of neurological re-education brings patients not only the recovery of muscle strength and joint mobility, but also the proprioceptive information essential for recovering the ability to activate by themselves their paralysed muscles [15].



Figure 1.12. HapticWalker robotic walking simulator [15]

The HapticWalker [25] comprises two programmable foot platforms with permanent foot machine contact (Figure 1.12). One of the applications of the machine is the gait rehabilitation for neurologically impaired persons such as afterstroke or spinal cord injury.

The machine is equipped with electrical direct drive motors, enabling highly dynamic footplate motions. For force feedback 6-degrees-of-freedom force/torque sensors are mounted under each foot platform.

The HapticWalker is designed as a scalable and modular system with a unit-by-unit extensibility. The basic unit enables movements in 3-degrees-of-freedom per foot in the sagittal plane. Each footplate can be extended to up to 6-degrees-of-freedom, plus an additional metatarsal joint drive. The system is able to simulate not only 'smooth' trajectories like walking on plane floor, stepping staircases up/down, but also walking on rough ground or even stumbling. The machine is controlled by a full-featured robot control software and hardware [15].

The Erigo (Hocoma AG, Volketswil, Switzerland) is an innovative tilt table with integrated robotic stepping functions (Figure 1.13). It combines simultaneous dynamic leg movement and physiological loading of the lower extremities of long bed rest patients or of neurological patients in the early phase of rehabilitation. The purpose of the Erigo is to provide the opportunity of intensive movement therapy and physiological loading of the lower limbs at an early stage after onset combined with the possibility of simultaneous up-righting of the patient [15] [26].



Figure 1.13. Erigo [26]

1.4 Analysis of existing concepts

Among considered approaches there is one thing in common for all of them: a patient to whom either of this apparatus should be applied, is expected to be of command of his/her lower extremities. This requires patient's ability to stand or even walk while respective machinery facilitates this process, but only in assistive way.

It, however, turns out to be insufficient when dealing with stiffness of lower extremities muscular tissues. Whoever happens to have disorder of a kind experiences its slow progressive nature, which comprises full patient's immobility on late stages.

Therefore, for flexing injured muscles a completely new approach is needed. Considering the worst case scenario when patient has already lost ability to walk and is being wheelchaired, the design should be of a stationary type, yet should not make patient leave his/her wheelchair. In this situation having a stationary construction mechanically connected to a wheelchair frame seems to be a reliable solution.

From this point of view BerkellBike (Figure 1.8) and Ergys2 (Figure 1.9) systems look like decent examples to start research from. However, neither of them capable to solve the specific issue of this study. Another technical solution being worthy of emphasizing is HapticWalker (Figure 1.12). Being based on a rigid and light construction from aluminum profiles makes it interesting from the financial point of view.

Having a movable foot-platform, similar to one proposed in Ergo rehabilitation system (Figure 1.13), connected to linear actuators, stretching out lower human extremities, would become extremely effective under given conditions. Additionally, implementing a robust and sensitive feed-back control would eliminate the necessity of medical worker helping with rehabilitation session and make it possible to become a daily routine.

2 Genesis of pathology of lower limbs muscle stiffness

2.1 The research

In order to choose actuators with right technical characteristics it is, first of all, necessary to understand the processes that happen in the injured organs and express these processes mathematically (quantify).

This is only possible if preceded by comprehensive research regarding genesis of exploring disease.

As such, lower limbs stiffness has been occurring since long ago, deteriorating life of people of different age, gender, ethnicity and life style. Only in the middle XX century Moersch and Woltman [27] were those scientists who for the first time made an effort to systematize and describe this phenomenon, which was known “stiff person syndrome” (some sources may denote it as “stiff man syndrome” or “SMS”) ever since. Particularly, mentioned work describes this syndrome like of “progressive fluctuating muscular rigidity and spasm”. However, despite the number of cases [28] that have been reported and respective studies conducted over the last 6 decades, the pathophysiology of the stiff man syndrome remains uncertain. Moersch and Woltman found no significant pathological changes at autopsy [29].

Nevertheless, over the years the disease has been carefully studied which made possible to differentiate its sub-cases and develop a treatment to each of them. The finding of antibodies to glutamic acid decarboxylase (GAD) in approximately 60% of patients has suggested an autoimmune basis [30].

Following there are mentioned names of SMS-based deviations: “Jerking SMS”, “Focal SMS”, “Paraneoplastic SMS”, “Progressive encephalomyelitis with rigidity (PER)” [30].

Despite of similarity of symptoms of conventional SMS with case of concrete patient, that is being considered in this paper, there exist another probable causes of rigidity, worthy of mentioning:

- spinal cord lesions and rigidity
- Isaac's syndrome and acquired neuromyotonia
- Schwartz-Jampel syndrome
- Benign physiological cramps [30].

However, none of them seem to fit to given problem.

An additional, more complex, form of conventional stiff man syndrome has been reported.

There then remain a group of patients who may have the classical ‘stiff man syndrome’ or a related syndrome. When strict diagnostic criteria are used, patients with the stiff man syndrome uniformly have axial rigidity, and about 90% are found to have antibodies against glutamic acid decarboxylase. Treatment response and prognosis are excellent. Stiff persons with ‘plus’ signs, particularly those with rigidity of a distal limb, are unlikely to have the classical stiff man syndrome. They have a poorer treatment response and prognosis.

Clinically, stiff persons with ‘plus’ signs may be divided into three groups according to the aggressiveness of the pathology and its relative distribution. Encephalomyelitis with rigidity follows a relentless subacute course, leading to death within 3 years [29]. Overall, following simplified explanation can be given to explain the difference between classical SMS and SMS ‘plus’: classical SMS does not include any additional complications, while SMS ‘plus’ cases are usually reported as well containing an encephalomyelitis of different severity.

In their papers aforementioned researchers P. Brown and C.D. Marsden (1999) claim the level of antiGAD bodies in classical SMS to be in 90% of cases, whereas their opponent prof. P.D. Thompson

(2001) have got not so optimistic results – only approx. 60% of patients had antibodies to glutamic acid decarboxylase (GAD).

Analysing works of T. Bartsch, T., Herzog, J., Baron, R. *et al.* J Neurol (2003) [31] and P. Brown, J. C. Rothwell, C. D. Marsden (1997) [32] it evidently becomes clear that the presence of antiGAD bodies in patient's serum and/or cerebrospinal fluid (CSF) is a reliable marker of resistivity of the immune system and overall responsiveness to treatment, and thus can be used for making diagnoses and prognosis.

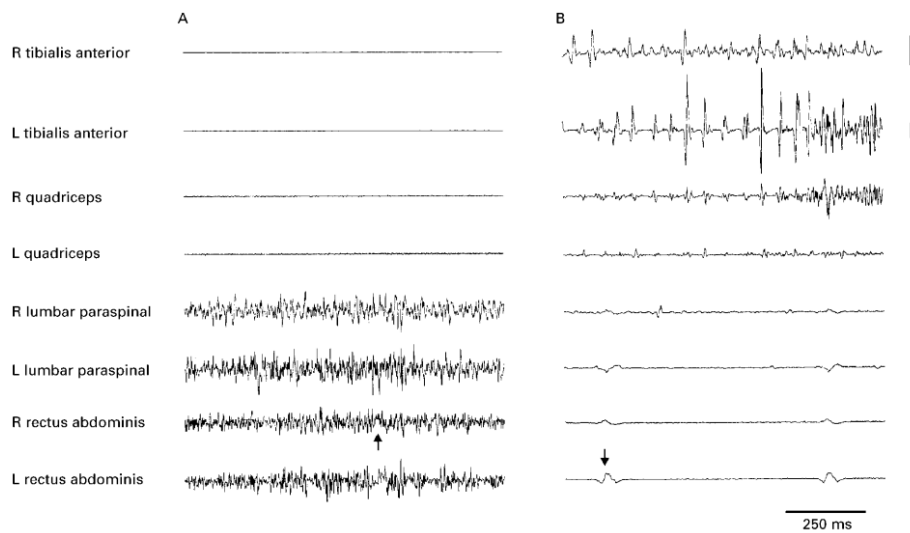


Figure 2.1. EMG comparison of patients with antiGAD and without antiGAD bodies [28]

Figure 2.1 demonstrates (A) unrectified surface electromyogram (EMG) activity during spontaneous spasms in a patient with chronic axial rigidity (stiff man syndrome) and positive anti-GAD antibodies, and (B) in a patient with rigidity of the distal lower limbs (stiff limb syndrome) who was anti-GAD antibody negative. (A) The spasm is confined to the muscles of the trunk, and EMG activity is indistinguishable from that recorded in a voluntary contraction. (B) The spasm is confined to the lower limbs, and EMG activity in the left (L) tibialis anterior tends to segment into large, but brief discharges [28].

It is noticeable, that patients who develop antibodies to GAD do not suffer from lower extremities disorders (tibialis anterior and quadriceps graphs are flat; contractions are absent). Contrary, patients lacking antiGAD bodies in their organisms are tend to have “stiff limb syndrome”.

In other studies, Bartsch *et al.* report about 69 years old woman case, whose antiGAD bodies level was increased by the time of conducting his study. It is described that she could walk, even though her posture was slightly distorted due to flexed plantar of right foot. At the same time, 4 patients of different age (35F, 60M, 35F, 52M) described in work of P. Brown *et al.* were not spotted to have antibodies to GAD at all. Consequently, none of them were able to walk independently, each having their disease progressing in a rapid pace. Obviously, the level of antiGAD bodies plays a significant role in treatment from stiff man syndrome.

It is interesting that in both above mentioned works their authors refer to subject of their research as “stiff leg syndrome” (Brown *et al.*) and “stiff limb syndrome” (Bartsch *et al.*). Apparently, it is not the classical SMS and a new term for sub-case of lower limbs stiffness has been incorporated for better distinction.

A. Hajjioui *et al.* (2010) [33] in his study reports a case that is very much alike to the case of interest of this paper: “*A 49-year-old male patient presented with a progressive stiffness and painful spasms of his both legs resulting in a difficulty of standing up and walking. The diagnosis of stiff limb syndrome was supported by the dramatically positive response to treatment*”. In his research A.

Hajjioui describes classical treatment method, using medicines, which, however, is not of interest of this study.

Nevertheless, supplementary rehabilitative techniques may contain an interest, being performed additionally to conventional medical treatment. Particularly, mechanical muscle stretching applied alongside with medicines can lead to a faster recovery.

2.2 Physical model of the injured organ

The composition of physical and mathematical models requires physical characteristic, such as mass, volume, force etc. They all can be obtained from anthropological measurements, summarized in biomechanics books.

Specifically, David A. Winter in his book “Biomechanics and motor control of human movement” have gathered and summarized numerous of case studies that pertain to field of biomechanics [34].

At one of the chapters it is given human’s body segment dimensions as fraction of the height (p.60). Figure 2.2 illustrates it.

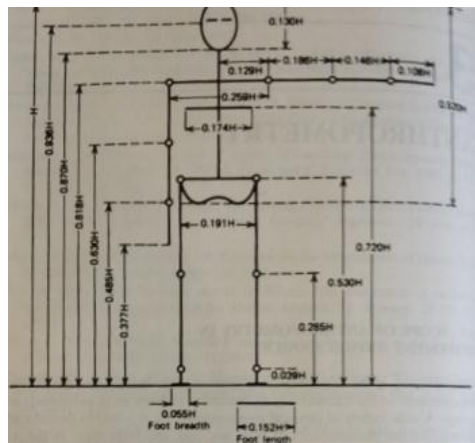


Figure 2.2. Body segment lengths expressed as a fraction of body height [34]

According to it a whole length of leg (foot+shank+thigh) is equal to $0,530 \cdot H$, and the length of foot + shank equals to $0,285 \cdot H$, where H is a human height. Thus, the length of thigh itself is $(0,53 - 0,285) \cdot H$ or $0,245 \cdot H$.

In their work Estonian scientists Lintsi and Kaarma (2006) report the average height of Estonian man is 179 cm [35]. Taking this as basis for calculation patient’s anthropometrical parameters (since specific data are unavailable), the leg measurements than are:

$$L_{shank} = 0,285 \cdot 179 = 51 \text{ cm}$$

$$L_{thigh} = 0,245 \cdot 179 = 44 \text{ cm.}$$

Here, for the sake of compactness, length notation for foot and shank was marked as L_{shank} .

In the same book [34] (p. 63) there is presented a table with theoretical weights of human body organs, expressed as fractions of total body mass. Particularly, mass of thigh $M_{thigh} = 0,1 \cdot M$, and mass of foot + leg $M_{leg} = 0,061 \cdot M$, where M represents whole body mass.

That is, assuming patient’s weight is 70 kg (since specific data are unavailable), his leg parts are of the following masses:

$$M_{thigh} = 0,1 \cdot 70 = 7 \text{ kg}; M_{leg} = 0,061 \cdot 70 = 4,27 \text{ kg.}$$

Before creating physical model as such, it is reasonable to get acquainted with distribution of forces that implicitly generated by different groups of muscles.

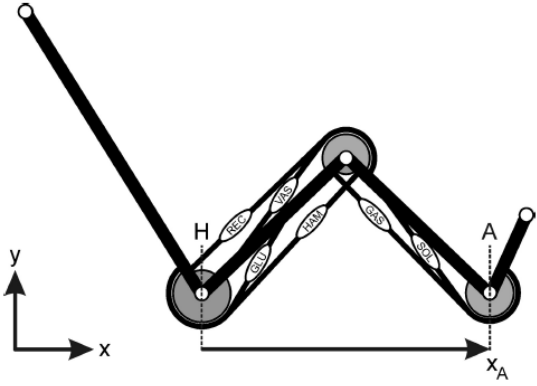


Figure 2.3 Musculoskeletal model [36]

Figure 2.3 schematically represents the interconnections of muscles in human lower extremities as mechanical system. The letters *H* and *A* are used to denote respective hip and ankle nodes. Here are the meaning of abbreviations shown on above illustration:

REC – *rectus femoris*

VAS – *vastus lateralis and vastus medialis*

GLU – *gluteus maximus*

HAM – hamstrings group (*biceps femoris, semitendinosus, semimembranosus*)

GAS – *gastrocnemius*

SOL – *soleus*.

Among them, there are only two groups of muscles that are of the biggest interest for this study: *quadriceps* (*REC + VAS*) and *hamstrings* (*HAM*). That is because they contribute to knee flexion/extension the most.

In scientific world it is a common practice to define *quadriceps* as *agonist* muscles and *hamstring* group as *antagonist* muscles respectively, as during the knee extension agonist muscles start the movement up while antagonist muscles are meant to slow down the limb, in order to prevent knee injury. In some way, this mechanism reminds a puppet pulled by strings. However, in this case the puppet-master is patient's brain itself [37].

Figure 2.3 can be presented simpler, excluding unnecessary information, as follows:

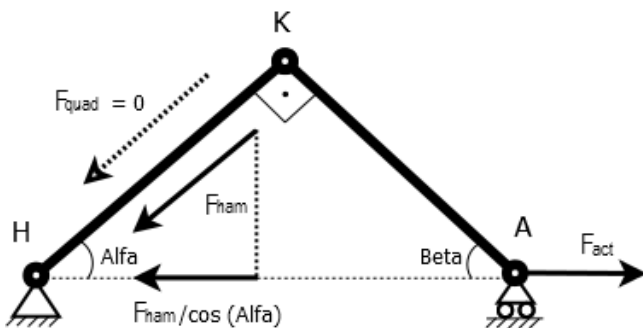


Figure 2.4. Derived physical model

Figure 2.4 depicts parts of lower extremity, shown as mechanical system with one degree of freedom. Node *H* (hip) shows that patient's hip is grounded, since pelvis bone is positioned in a wheel-chair. Node *A* (ankle) represents patient's foot being strapped to moving platform of rehabilitation device. There is right angle between them, at the node *K* (knee), which copies current patient's leg posture.

On the picture above, link *HK* corresponds to thigh and link *KA* corresponds to shank and foot, such that:

$$HK = L_{thigh} = 44 \text{ cm}; KA = L_{shank} = 51 \text{ cm}.$$

Thus,

$$HA = \sqrt{HK^2 + KA^2} = \sqrt{44^2 + 51^2} \approx 67 \text{ cm} \quad (2.1)$$

In order to calculate locomotion force of actuator F_{act} , the horizontal component of each force (F_{quad} , F_{ham}), generated by respective muscle group, must be found. To do that, it is firstly needed to find approximate values of angles α and β . They determine the horizontal inclination of patient's thigh and shank, at the beginning of rehabilitation procedure.

$$\alpha = \arccos(44/67) \approx 49^\circ,$$

$$\beta = \arccos(51/67) \approx 41^\circ \text{ or } (180^\circ - 90^\circ - 49^\circ) \quad (2.2)$$

By nature, quadriceps are stronger than hamstrings [38] [39], therefore, the explanation as to why lower limb can not freely stretch by 180° might be the antagonist (*hamstring*) muscles stiffness dominates over agonist (*quadriceps*) muscles ability to stretch.

Similarly, the patient, whose case is considered in this study, has been assumed to have the force F_{quad} exerted by quadriceps equals 0, that is, stiffness of the hamstring muscles prevents the leg from full knee extension; whereas quadriceps muscles have drastically weakened over the time of disease progressing.

In the essence of phenomenon of generating power by human muscle, there is a principle of varying of its physiological cross-sectional area (*PCA* or *PCSA*) [40]. That is, when muscle internally extends (lengthens) it simultaneously becomes thinner, decreasing its *PCA*. Oppositely, when muscle internally contracts (shortens) it becomes thicker, increasing its *PCA*. The external muscle length always stays constant though.

Nowadays, it has become possible to measure *PCA* *in vivo* (on the live subjects), using ultrasonography or magnetic resonance imaging, whereas up to middle of XX scientists where ought to make experiments *post mortem* (after patient's death), working with cadaveric material.

One of the most significant contributions to the field of *PCA* studying has made an American surgeon Thomas L. Wickewicz, M.D. Specifically, in his work "Muscle architecture of the human lower limb" (Wickewicz et al., 1983) he presents comprehensive study about architectural features of the major knee extensors, including anthropological measurements of all muscles of lower limb [41]. For the scope of this study Dr. Wickewicz's work is interesting by the measurements of hamstring muscles, specifically their *PCAs*. Below, Table 2.1 presents measures hamstring measurements, according to aforementioned study:

Table 2.1. Architectural features of the hamstrings

	Cross-Sectional Area, cm^2			
	I	II	III	Mean
SM	18,6	18,1	13,9	16,87
BF	16,4	14,7	17,4	16,17
ST	6,3	4,4	-	5,35

In Table 2.1 *SM* stands for *semimembranosus*, *BF* stands for *biceps femoris*, *ST* stands for *semitendinosus*. The values of pennate angles have not been considered as their influence is negligibly small.

All measures were taken from cadaveric material. Knowing this, it is additionally assumed that the equivalent of muscle rigidness, that occurs to people with stiff limb syndrome or any similar disorder,

is of the same nature with that observed from recently died people. This equivalent is called “specific tension” and quantitatively is expressed as relation between force, which muscle potentially can generate, and its *PCA* [42]:

$$F_{total} = PCA \cdot ST, \quad (2.3)$$

where F_{total} is total force, exerted by muscle, *PCA* is physiological cross-sectional area, *ST* is specific tension.

From above mathematical expression it is obvious though, that as thinner muscle becomes, as more tension its inner structure experiences, thus, causing the muscle rigidness. The units of specific tension, therefore, are:

$$ST = F_{total} / PCA \text{ [N}\cdot\text{cm}^{-2}\text{]} \quad (2.4)$$

Several biomechanical scientists in their studies [43] [44] had used value of specific tension equals to $61 \text{ N}\cdot\text{cm}^{-2}$ to calculate maximum isometric with derived from Dr. Wickewicz's *PCA* measurements. Because to date quite a few researches have been done regarding narrow field of *specific tension in hamstring muscles*, the same value of $61 \text{ N}\cdot\text{cm}^{-2}$ is used for calculations in this paper.

This value of specific tension is higher than the range of values ($11\text{-}47 \text{ N}\cdot\text{cm}^{-2}$) reported previously [45], and larger than the experimentally measured value of mammalian muscle of $22,5 \text{ N}\cdot\text{cm}^{-2}$ [46] [44]. It indeed makes sense that all these values are less than $61 \text{ N}\cdot\text{cm}^{-2}$, as they were obtained from living subjects with flexible muscles, and, thus, are not applicable to this study.

Lastly, the approximate force of stiffed hamstring muscles can be calculated:

$$PCA_{HAM} = PCA_{BF} + PCA_{SM} + PCA_{ST} = 16,17 + 16,87 + 5,35 = 38,39 \text{ cm}^2;$$

$$F_{HAM} = 38,39 \cdot 61 = 2342 \text{ N} = 2,342 \text{ kN}; \quad (2.5)$$

$$F_{HAMx} = 2,342 / \cos(49^\circ) = 3,57 \text{ kN}.$$

Since Table 2.1 presents data from 3 cadavers, the mean values of *PCA* from each experiment, that have been calculated previously, were now summed to acquire total mean value PCA_{HAM} . Then, this number was multiplied by value of *ST* (specific tension) to find the force, exerting in muscles. Last step was to calculate *x*-component of this force, by projecting it on the horizontal axis. Figure 2.5 schematically shows forces diagram from Figure 2.4 applied to CAD view.

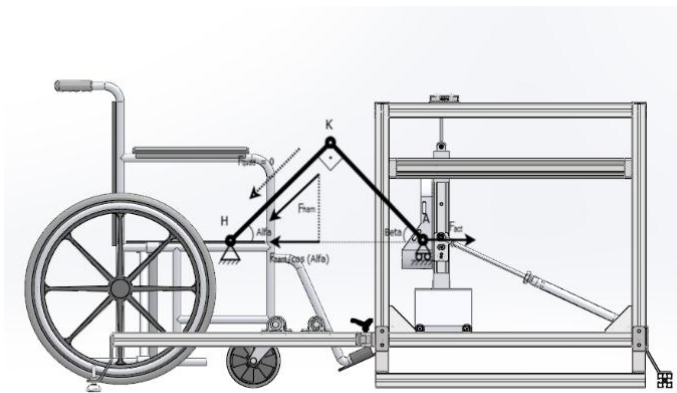


Figure 2.5. Working scheme

A friction resistance of rolling-sliding elements of rehabilitation device was neglected due to its insignificance regarding the scale of the project.

The above calculations conclude that actuators installed on rehabilitation device cumulatively must produce at least 3,6 kN of thrust to overcome the resistance of stiff muscles and stretch patient's leg.

Comparatively, a value of actuating force F_{ACT} needed for healthy people would be only 1,76 kN. This number derives from previously calculated force contributions of healthy hamstring muscles [38], such that $F_{HAM} = 1,155$ kN (p.66, Table 4). It has been taken during running and jumping exercises, which makes specific tension even bigger. However, the $F_{HAMx} = 1,155/\cos(49^\circ)$ is still 2,05 times smaller than that which is needed to extend a stiff muscle.

To solve described problem, the conceptual device was developed. It comprises number of features from rehabilitation devices mentioned in subchapter 1.3 "Stationary devices" (specifically "Ergys2", "Haptic Walker" and "Erigo"). The process of developing CAD model of device is thoroughly described following, in chapter 3, which is a part of the complete developing cycle schematically shown on Figure 2.6 below:

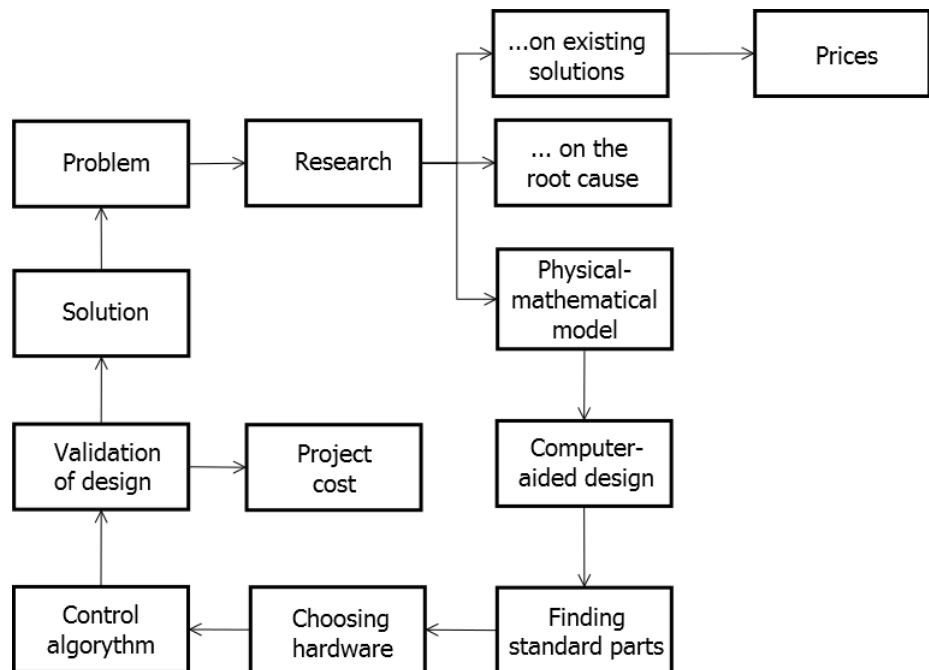


Figure 2.6 Stages of complete developing cycle

3 Developing solution using CAD

3.1 Building materials

Considering the degree of complexity of given case, when patient is being permanently immobilized and therefore ought to use a wheelchair, it was decided to build a rehabilitation device of stationary type. Moreover, it must be capable of mechanical connecting to the frame of wheelchair, so during dynamical exercising both constructions should behave like one solid body.

One of the crucial aspects of this project is cost. Using many custom-made parts will inevitably lead to budget increasing. Thus, it is reasonable to build up a machine from standard parts which are always available on the market.

Most appropriate building material seems to be a square aluminum profile. The supplying company name is “MiniTec” [47]. The profile possesses all necessary features for framing such as lightweight and rigidness. Figure 3.1 demonstrates profile’s look.

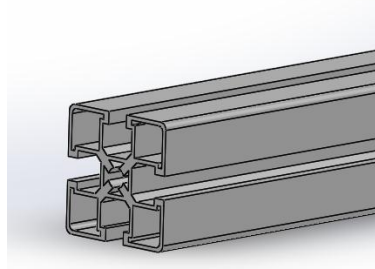


Figure 3.1. Profile 45 X 45 UL [48]

Another advantage of this profile is its symmetric shape with grooves. This allows to attach profiles between themselves by special fasteners. They fit to shape of grooves and slide along until they are tied (Figure 3.2).

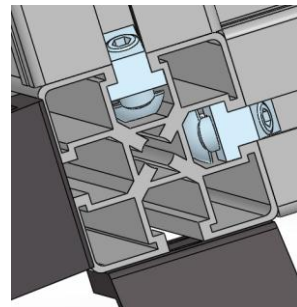


Figure 3.2. Profile lock-fastener [49]

Also, being a company that specializes on various mechanical solutions, “MiniTec” seems like an appropriate vendor for majority of ready-made mechanical units for this project. The company has its affiliations around the world, including Estonia [50]

3.2 Design and technical parameters

Before being supplied to customer, the needed length of profile is cut. In order to keep low cost of project, a variety of parts also must be narrowed down to minimum. Particularly, in case of profiles it is possible to achieve if the device’s main frame is of a cubic shape. Only in this case profiles of the same length are required (Figure 3.3).

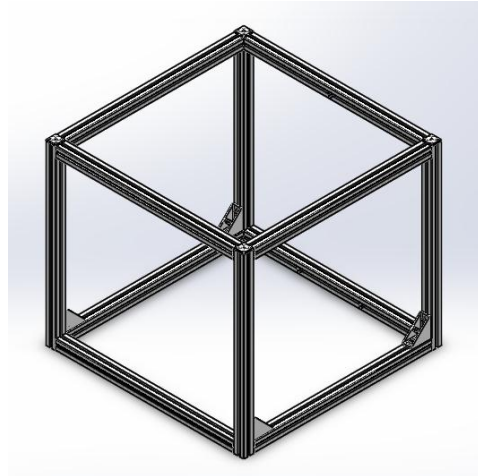


Figure 3.3. Main frame

The above frame is assembled from 12 identical profiles, each 775 mm of length. This certain length is dictated by dimensions of an ordinary wheelchair, overall width of which (including wheels) is up to 640-670 mm [51].

While main frame is meant to be stationary, a special foot platform moves within its space. Figure 3.4 illustrates this part, that is not a standard one. It needs to be produced as custom detail.

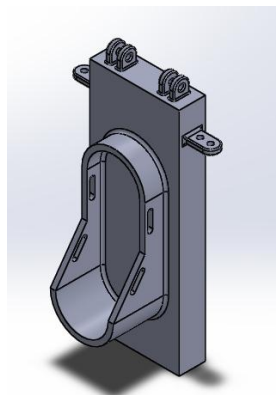


Figure 3.4. Foot platform

It can be produced by milling of solid piece of metal with further welding or 3D printing a whole part at once. The first method seems to be more reliable, but more expensive one, while second method is appropriately reasonable in terms of its cost.

The given part consists of slab with dimensions 438 x 170 x 50 mm, a foot cradle and two types of connecting loops (4 in total) welded to it, on both sides and on top. The foot cradle also has 4 cut outs for putting straps through for fastening patient's foot. The welded loops are placed where locomotion force from actuators is supposed to be applied.

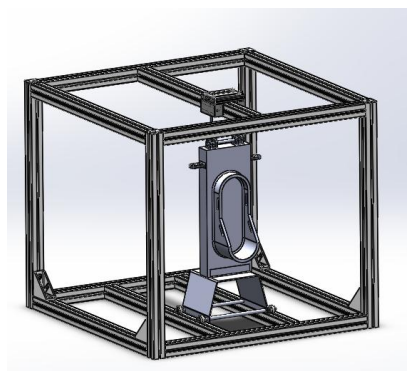


Figure 3.5. Dynamic assembly

Figure 3.5 depicts assembly of movable foot platform embedded into main frame with help of support units. These are custom made lower support carriage, which, however, uses some standard parts (rolling elements) [52] and upper support unit that itself is entirely a standard detail [53].

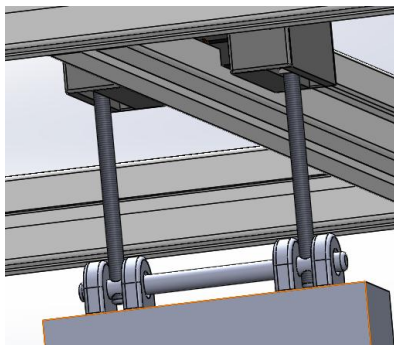


Figure 3.6. Upper connections

The connections between upper slider and foot platform are made through conjunction of two threaded bars with one custom drilled bar (Figure 3.6).

For stability and smoother movement of foot platform a lower rolling support was developed (Figure 3.7). It is made of bended sheet metal of 3 mm of thickness, custom milled axes with standard rollers on their ends. The rollers are equipped with bearing mechanism that allows to roll into profile grooves with ease.

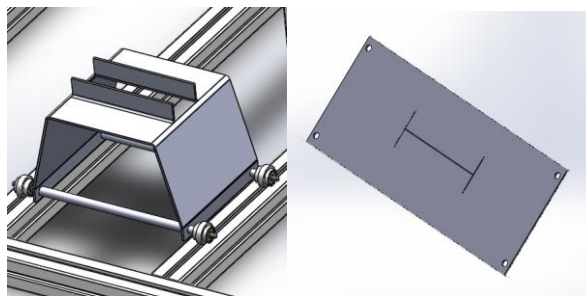


Figure 3.7. Lower support assembly (left) and flatten sheet metal (right)

For mechanical connection with wheelchair two supplementary subassemblies were developed entirely from standard parts. First subassembly is shown on Figure 3.8. It consists of two moving profiles attached to swinging standard profiles, which, however, can be fixated with help of fixable angle bracket [54].



Figure 3.8. Mechanical links for wheelchair

For height adjusting, on the other end of each profile there are attached angle bracket [55] and leveling foot [56].

Two standard bars [57] whose purpose is to block the frame of the wheelchair, can be easily removed from support bearings [58] to let wheelchair park and leave the space next to the rehabilitation device (Figure 3.9).

The support bearings themselves move easily along profile's groove, therefore this fixation type is applicable to any geometry of wheelchair's frame.

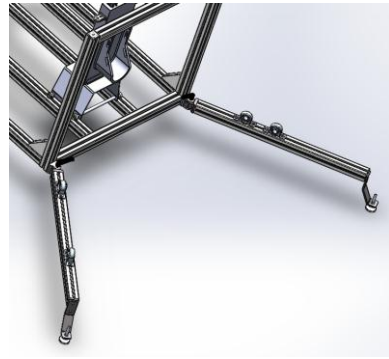


Figure 3.9. Links are opened for parking

The second supplementary subassembly is illustrated on Figure 3.10. It is assembled from same 6 angle brackets [55] and 3 aluminum profiles of same type [48] but of longer length - 860 mm.

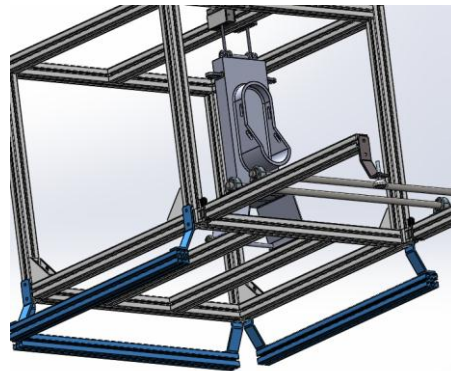


Figure 3.10. Height adjusting subassembly

Particularly, the reason for adding this addition to the main construction lays in personal anthropomorphic features of different patients' bodies, such as height.

With help of this simple upgrade the patient gets ability to adjust device accordingly to his or her anatomy better. Also, a whole construction gets better stability as its base becomes 165 mm wider.

Figure 3.11 shows the whole construction mechanically link with a wheelchair model [59]. The CAD model of a wheelchair is in compliance with international standards of wheelchair production [60], thus it can be used for verification of prototype's geometry.

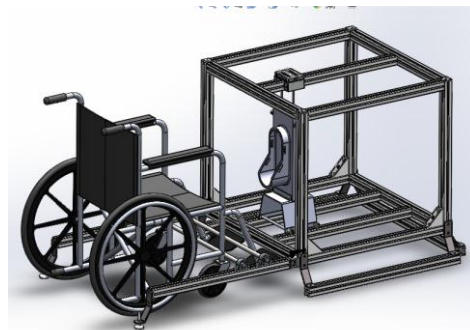


Figure 3.11. The construction with mechanically linked wheelchair

3.3 Chosing generic actuators

To put foot platform in motion by actuators it is necessary to place them as close as possible to each other. Having a firm and rigid profile construction, it was decided to pick linear rodless actuators as a primary source of motion and attach them to existing ribs (Figure 3.12).

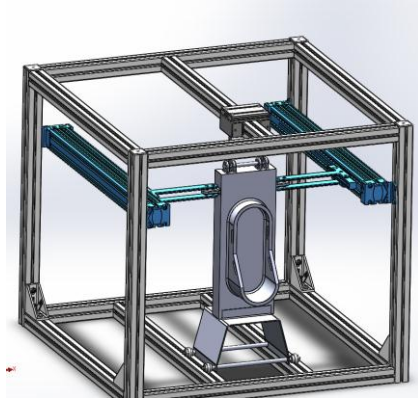


Figure 3.12. Mounted linear actuators

To transfer momentum from actuators to foot platform, special T-shaped link was designed (Figure 3.13). It is to be made of metal, presumably steel (DC 01), with at least 6 mm of thickness. The results of respective preliminary stress tests will be presented in next chapter.

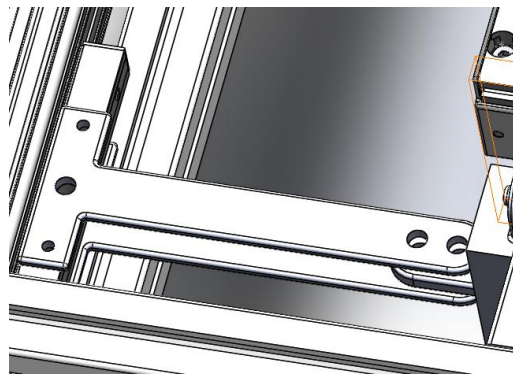


Figure 3.13. Paired T-shaped links

To ensure that foot platform moves at the smoothest way possible, a secondary pair of actuators has been added to the system. Figure 3.14 depicts their position and the connecting principle.

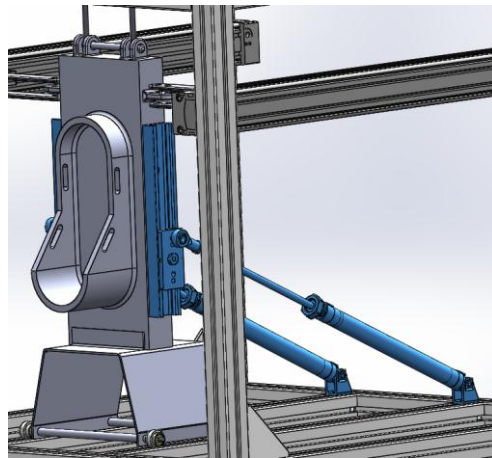


Figure 3.14. Mounted secondary actuators

The secondary actuators work in shifted mode regarding primary actuators, that is when linear actuators finishing their working cycle, the cylinder ones are at the middle of their working cycle. The main reason of incorporating secondary actuators as such is providing a smooth movement of

foot platform. It becomes possible using standard rail sliders, attached to foot platform [61] [62] (Figure 3.15).

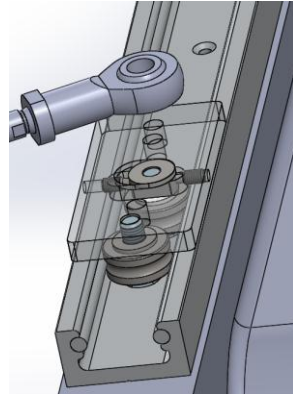


Figure 3.15. Rail slider with inner components

Since it is a preliminary model being presented in this chapter, it is not much detailed and, therefore, missing some insignificant details, such as fastening bolts and nuts. Particularly, in Figure 3.15 the rod end is only concentrically mated with upper whole of the slider, for modelling purposes. However, in real life a manual drilling will be needed to increase hole size from 7 mm to 10 mm and further connecting two elements with bolt.

Due to choosing of new actuating equipment, which is being discussed in great details in chapter 4, the corresponding CAD model has been updated accordingly, as shown on figure below.

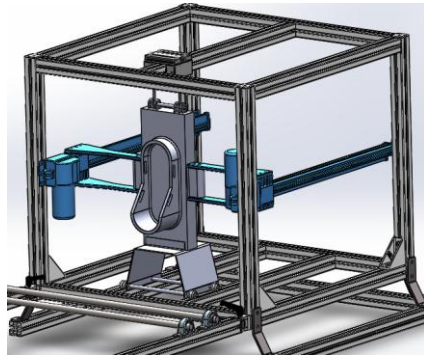


Figure 3.16. CAD model with new actuators

Since each of them is capable of delivering 2 kN of thrust, it was decided to exclude two auxiliary rod-type actuators that were in the previous version of model, as they put additional cost to project and are not essential parts. Additionally, two custom links that transfer torque from motor to moving platform were redesigned to match new geometrical requirements (Figure 3.17). It is planned to produce them from solid piece of steel with thickness of 7-10 mm, to withstand momentary mechanical stress created by motors.

The creating of control algorithm includes hardware and software part, and is being thoroughly discussed in chapter 5. Particularly, it includes explanation regarding choosing a time-of-flight optical sensor, microcontroller and shows its interaction with external PID controller made of operational amplifiers, and its interaction with simple emergency controller (EC). Additionally, in this chapter a suggestion is given regarding layout of electronical components in controlling scheme. Also, there are developed wiring diagram for electrical connections, as well as programming script for microcontroller.

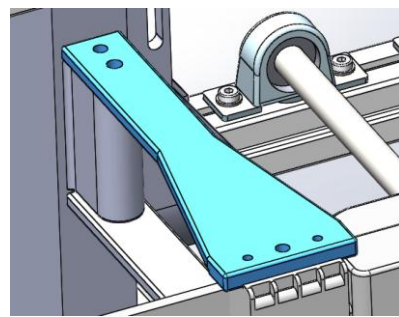


Figure 3.17. Redesigned side link

Additionally, because naturally human plantar can not stay in vertical position for a long time it was decided to modify current design of foot platform towards making it more ergonomic (Figure 3.18).

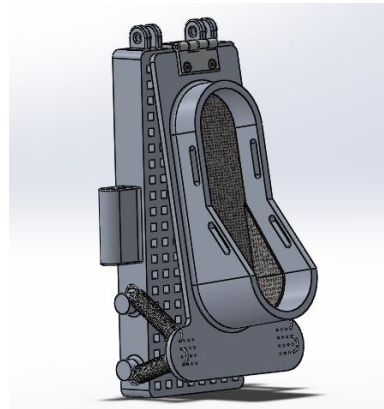


Figure 3.18. Ergonomic design of foot platform

The previous version was split in two parts, one of which is now movable. It provides angular movement for 15° maximum off the vertical by incorporating a steel door hinge from MiniTec [63] and two spring from each side.

To restrict angular movement of foot pad to 15° a certain spring must be chosen. An approximation was made for this purpose as shown below:

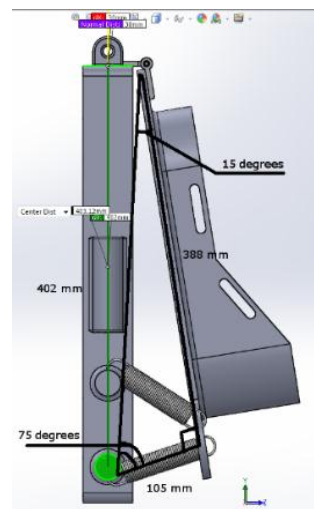


Figure 3.19. Calculating spring's length

It was found that length of stretched spring should be around 105 mm. For given case it is calculated as difference between spring's stationary length and its stretched length. Below is shown parameters of spring that was chosen as most appropriate (T32860):

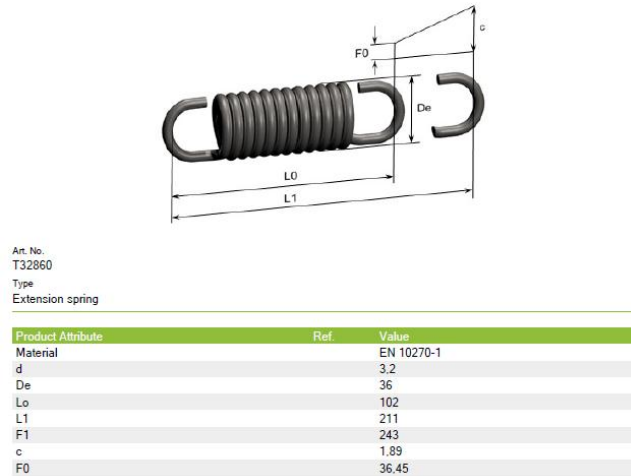


Figure 3.20. Parameters of supporting spring

Here, the difference between L₁ and L₀ is 109 mm which makes it appropriate for the restricting function. In case when foot pad is not inclined from foot platform, the spring is assumed to be sagged.

The upper spring was added for redundancy and will not be taken into account in stress simulations.

3.4 CAD concept summary

The aim of this chapter was to present a conceptual model of rehabilitation device, justifying its design and choice of building materials.

There were used numerous of standard parts as well as few custom-made details. Also, certain models of real life industrial actuators were found for this concept. These actuators, however, remain unnamed in this chapter due to its insignificance. The thorough analysis of any possible type of actuator will be made in Chapter 3, with all information about models revealed.

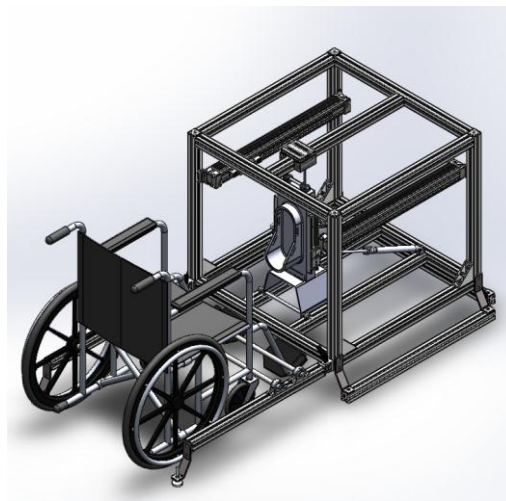


Figure 3.21. Complete look of prototype model

Currently, there are two types of actuators used in the model: stationary rodless linear actuators with 490 mm of working distance and swinging cylindrical piston-based actuators with 250 mm of working distance.

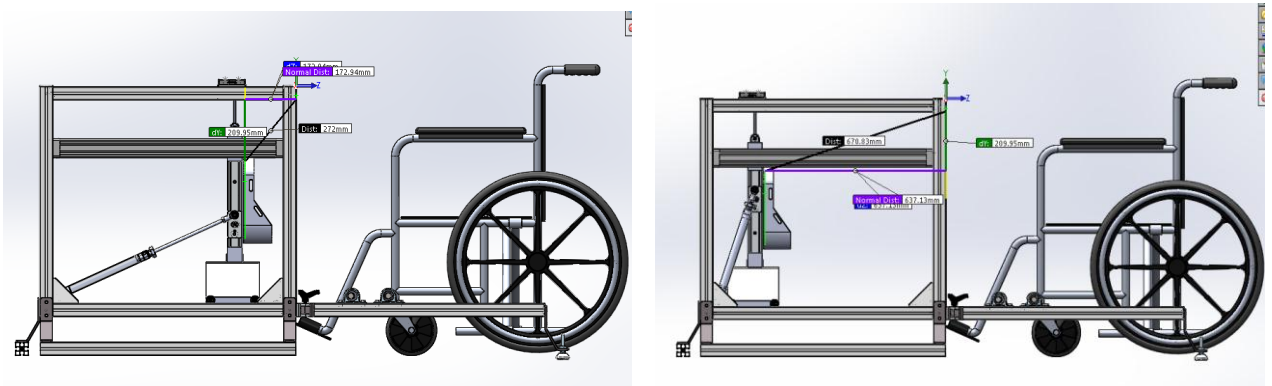


Figure 3.22. The initial (left) and furthest (right) positions of foot platform

With first type of actuators chosen it was possible to achieve ultimate operating distance of the device as big as 464 mm (Figure 3.22). However, after it was decided to switch to different type of actuators, the working distance had increased and became even more. It is now 594 mm. It seems like quite enough distance for majority of people. The comprehensive analysis about interacting human body and device will be made in Chapter 4.

Additionally, to increase or decrease the gap (if needed) it is possible to adjust position of a wheelchair by moving two stopping bars back and forth along the grooves of aluminum profiles.

3.5 Simulating human muscle in mechanical domain

As reported (Hill, 1938), a behaviour of any biological muscle can be simulated by simple mechanical system, that consists of 3 components: contractile element (*CE*), series elastic element (*SE*) and parallel elastic element (*PE*) (Figure 3.23) [64].

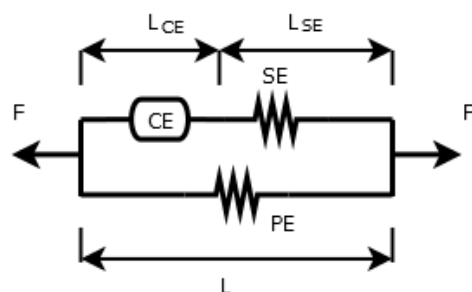


Figure 3.23. Hill's elastic muscle model

Here F is force, applied to a tendon, contractile element (*CE*) defines the ability of muscle to generate power, series element (*SE*) simulates dynamic characteristics of all connective tissues in series with *CE*, parallel element (*PE*) simulates behaviour of connective tissue that surrounds *CE* and acts much like an elastic band [34].

A set of mathematical expressions can be defined for the presented model:

$$L = L_{PE}; \quad L = L_{CE} + L_{SE}, \quad (3.1)$$

where L is full lenght of muscle that always remains constant, L_{CE} is lenght of *CE*, L_{PE} is lenght of *PE*, L_{SE} is lenght of *SE*. Stretching of series element *SE* can only occur when contractile element *CE* shortens on the same distance [65].

$$F = F_{PE} + F_{SE};$$

$$F_{CE} = F_{SE} \Rightarrow F = F_{PE} + F_{CE}, \quad (3.2)$$

where F_{CE} is an active force due to active role of contractile element in creating the motion. Oppositely, F_{PE} is a passive force because it does not produce any dynamics. A viscous damper may be also included in this system to simulate the effect of viscoelasticity. It may occur when the dynamics of the second-order critically damped twitch is regarded [65]. Its properties can be described by following equations:

- linear viscous damper: $F = k \dot{x}$;
- nonlinear damper: $F = k \dot{x}^a$; $F = k (e^{\dot{x}} - 1)$ [34] (p.222) (3.3)

There are, however, deviations of the classical Hill's muscle model. Figure 3.24 shows the complete model, which incorporates the contractile element, a linear damper B to model any viscous or velocity-dependent (in the contractile element and connective tissue), a linear spring K to represent the series elastic elements (in tendon, fascia, and cross-bridges), and a mass element M to represent the effective mass of muscle tissue that must be accelerated as the force impulse wave travels from the motor end plate region toward both tendons [34] (p.224-225).

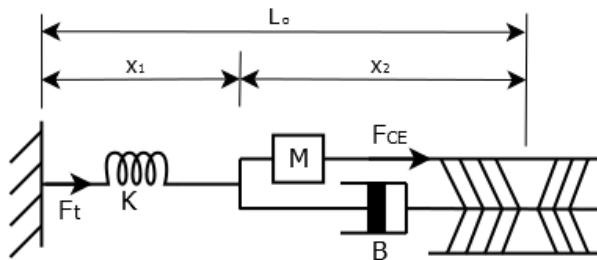


Figure 3.24. Biomechanical model of a muscle during isometric contraction

F_{CE} is modeled as an impulsive contractile element force acting on an equivalent mass M , a linear damping element B , and a series elastic element K . F_{CE} acts on the mass to accelerate it, but to do so mass acts on the damper and spring elements. Thus, the equations of motion are:

$$\begin{aligned} x_1 + x_2 &= L_o = \text{constant} \\ F_{CE} &= M\ddot{x}_1 + B\dot{x}_1 + Kx_1 \end{aligned} \quad (3.4)$$

The tendon force F_T is seen only if the series elastic spring increases its length beyond resting length:

$$F_T = Kx_1 \quad (3.5)$$

The final part of the model is to determine K , B and M for the muscle. However, there is no need to measure them separately. Rather, a fact can be used that the twitch wave form is quite close to that of critically damped second-order system [66]. For a mass-spring-damper system that is critically damped, the twitch time T allows to calculate the correct ratios, $T = 2M/B$, $B/M = 2/T$. Also, $B = 2\sqrt{MK}$. Therefore, $K/B = B/4M = 1/2T$ [34] (p.226).

Because it was not found an appropriate value of T for hamstring muscles, the value of calf muscle group was used due to its close biomechanical characteristics. Particularly, a value for *medial gastrocnemius* muscle was adopted. The mean value of twitch time $T_{mean} = 79$ ms (52-100 ms) [34] (p. 209).

According to D. Winter's book "Biomechanics and motor control of human movement", the mathematical model of twitching muscle can be built as follows [34] (p. 225):

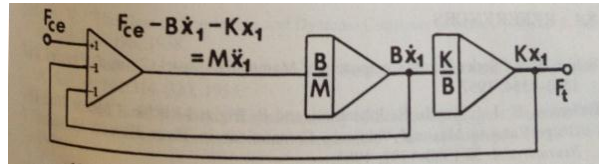


Figure 3.25. Reference model [34]

In Matlab, a mass-spring-damper system was built, using anthropological parameters of current case. Also, a mean mass of 149,93 g for stiff *medial gastrocnemius* muscle was taken from work of Dr. Wickewicz [41]. To simulate healthy muscle a mass of 158 g was used [34] (p.79).

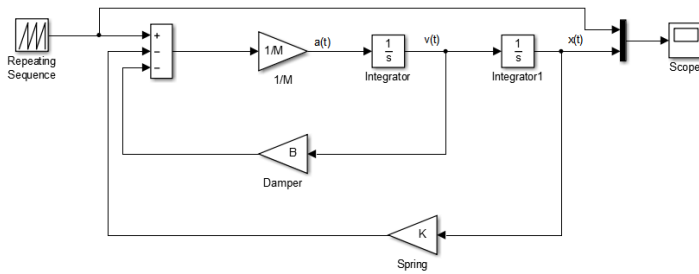


Figure 3.26. Simulation of muscle contraction

At first, a simulation for healthy muscle has been run. The input was set to perpetuate linear increase, with 2.34 kN in its peak (value of F_{HAM}) and cycle time of 10 seconds.

The magnitude of B and K was calculated and inserted into a model, which showed the displacement of series elastic component *SE* around 9 mm (Figure 3.27a). In the next run coefficients K and B were assigned 3 times bigger values to simulate an increased stiffness in tendons and muscle surrounding tissues, respectively. The stretching potential of muscle fibers had decreased to approximately 3,1 mm (Figure 3.27b).

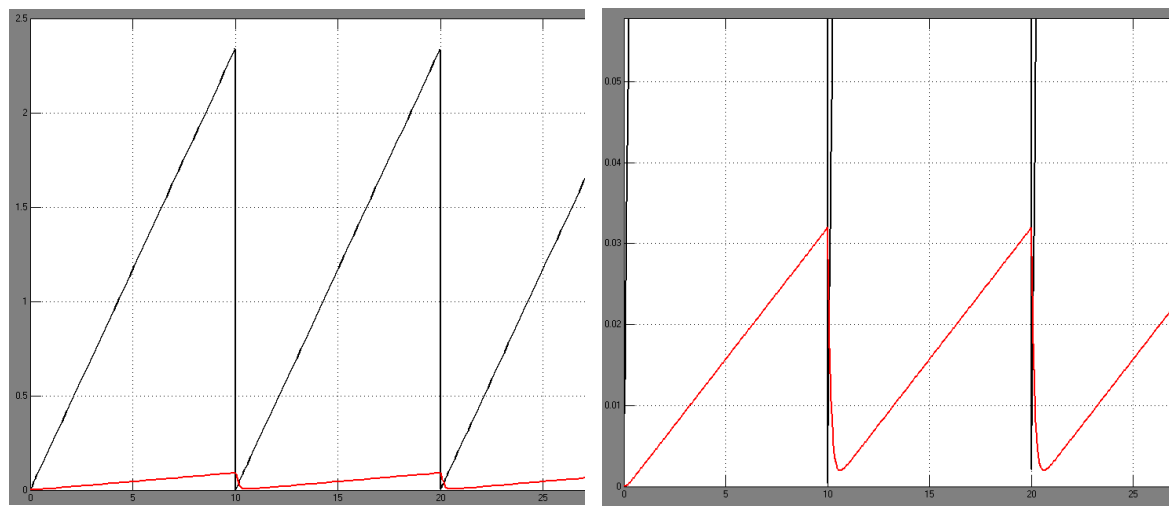


Figure 3.27. a) Healthy conditions with muscle contraction length equal to 9 mm (left); b) Stiff muscle with approx. 3,1 mm of stretching potential (right)

The purpose of simulation was to show the change in stretching dynamic of calf muscle (*medial gastrocnemius*), which was used due to lack of studies made on hamstrings group. The graphs had shown linear correlation between increasing of stiffness parameters B and K and decreasing stretching potential of the muscles. Even though the simulation is maximally close to reality, the nature of muscle stiffness, however, possesses much more complex nature and is a subject of further studies.

4 Comparison of different types of actuators

4.1 The overview

In Chapter 3 there was presented a conceptual design of rehabilitation device for stretching lower limbs with stiffness. This design requires linear actuators to be symmetrically attached to side profiles, providing reciprocal motion to the foot carriage.

Despite a huge variety of different actuators presently available on the market, their classification can be narrowed down to very few distinct technologies. These are, hydraulic, pneumatic and electric actuators. The latter one comprises more wide nomenclature, such as ball screw, roller screw, acme (lead) screw or belt drive.

Hydraulic actuators utilize the non-compressing nature of fluids. It is nearly impossible to compress any fluid by any significant value, thus, it is widely used for delivering robust and extremely precise actuating. Hydraulic actuators can produce forces 25 times greater than their pneumatic opponents of the same size. This technology is perfect for handling heavy duty tasks, i.e. lifting and holding vehicles. The downside of these actuators is often fluid leakage and demanding a numerous of companion parts, such as fluid reservoirs, pumps, valves and heat exchangers. A noise is another drawback of hydraulic actuating systems.

Because of aforementioned negative sides, it was decided not to consider hydraulic actuators as appropriate actuating solution for designing rehabilitation device, yielding pneumatics and electrical actuators the right to be compared.

4.2 Electric actuators

This type of actuators has good range of accuracy and low operable cost. Unlike pneumatics, the setup made with electric actuators does not need supplementary devices, such as stepper or servo motors to move the valves or air compressor and maintain pressure level. Of course, electric actuators contain motors (servos or steppers) in their construction by default. But this case differs from pneumatics, as these motors are already included in actuator's price, which may vary from few hundred to few thousand euros (or dollars, respectively).

Another advantage of electrical actuators is their strict correlation between applied force and velocity of the moving carriage, such that, as lower velocity is, as greater value of force is being exerted.

As to level of comfortable, electric actuators are far ahead comparing to all other technologies. In terms of noise, they produce much less pollution than pneumatic or hydraulic actuators. Additionally, because there is no fluid inside, leakage contamination is excluded. Finally, electric actuators are exclusively driven by motor. Together with inner low voltage circuitry, they consume far less power, thus is more appropriate for domestic usage.

Generally, there are four different inner arrangement types of electric actuators: ball screws, roller screws, acme screws and belt drives.

Majority of linear actuators nowadays run ball screw mechanism due to its robustness and efficiency (up to 95% [67]). In its essence stands the interaction of miniature metallic balls, rolling in the screw grooves, converting rotating movement of balls to linear movement of carriage, or vice versa. Actuators of this type, may, however, be quite expensive.

Roller screw actuators is an upgraded version of ball screw drives, where instead of miniature metallic spheres, roller bearings are used. Typical stroke lengths range from 5 mm to 2 m; speeds can reach 70 in./sec. In short, roller screws have the speeds of ball screws, but much higher thrust capacity and force density because of the line (not point) contact on the screw flights. The downside of roller screw

technology is its low availability: Because the technology is relatively new, there are few manufacturers, so lead-time and prices are typically 40 to 100% higher than those of ball screws [67].

Acme screws are low cost. Unlike ball or roller screws, acme screws do not incorporate any additional mechanical elements in their construction. They are also known as lead screws and are one of the simplest mechanisms for converting rotary movement to linear. They employ a plastic or bronze solid nut that slides along the threads of a screw like an ordinary nut and bolt. However, because there are no rolling ball bearings, as on a ball screw or roller screw, acme screws transfer only 30 to 50% of the motor's energy to driving the load [67].

Belt drive systems do not have critical limitations in speed, having fewer moving parts with minimal wearing of the components. However, such design possesses poorer repeatability and accuracy and may require a planetary gear system to overcome the inertias from load and actuator itself. The maintenance of such products is often low, while the price is bigger than of acme screws but does not reach roller screw's expensiveness level.

In scope of this study it seems appropriate to use an actuating equipment driven by acme screw, due to its low cost, enough efficiency and simple maintenance.

Such equipment was found among products of “Progressive automations” [68], which specializes on manufacturing of linear actuators and linear motion control solutions. Particularly, linear actuator PA-18 was examined (Figure 4.1). The available stroke range is 2 - 60 in (5,08 - 152,4 cm).



Figure 4.1. PA-18 track actuator [69]

It is an electrical rodless actuator, driven by acme screw mechanism, which has a big range of dynamical forces available (Table 4.1).

Table 4.1. Force-velocity options of PA-18 model

#	Force, kN (lbs)	Velocity, cm/s (in/s)
1.	0,667 (150)	3,81 (1,5)
2.	1 (225)	4,32 (1,7)
3.	2 (450)	1,98 (0,78)
4.	3 (675)	0,99 (0,39)
5.	4 (900)	0,64 (0,25)
6.	5,78 (1300)	0,58 (0,23)

Because manufacturer offers only fixed length strokes, the most appropriate value of it is 24 in (609,6 mm). In Table 4.1 the actuator with proper force-velocity ratio seems to be number 3: 2 kN of thrust and maximal velocity of 1,98 cm/s. It is planned there will be two actuators working in parallel, delivering 4 kN of thrust cumulatively, to overcome 3,57 kN of muscle stiffness. The available velocity range is also acceptable, that is ~ 1,016 – 1,98 cm/s (0,4 – 0,78 in/s).

The given model has IP54 protection class, which gives it a limited protection against dust and gentle splashes of water.

The manufacturer only presents technical data and price for two models – 150 lbs and 900 lbs of thrust [70]. Thus, based on available data an approximation (red graph) about force-velocity characteristic for chosen actuator has been made (Figure 4.2).

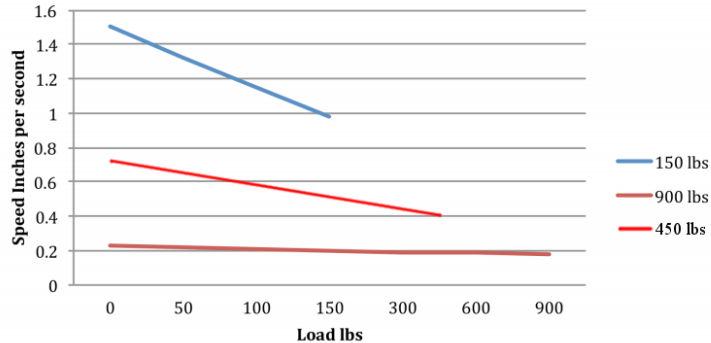


Figure 4.2. Force-velocity dependency [70]

The price for chosen actuator should not exceed \$185,99 (approx. €176) [69] as this is a price of more powerful model with 4 kN (900 lbs) of dynamic force.

To control the speed of actuator's extension a speed regulator is needed. The DC speed controller AC-14 [71] can be obtained from the same enterprise for \$31,99 (approx. €30) (Figure 4.3).



Figure 4.3. DC speed controller for electric actuators [71]

In this setup two relays and rocker switch are also needed to maintain simultaneous work of both actuators with 8A of full load per each. These items are available from Progressive Automations at \$18 (approx. €17) [72] for the rocker switch RC-03 and \$17 (approx. €16) [73] for each relay AC-22 (two relays are needed). Figure 4.4 shows these items.



Figure 4.4. Relay AC-22 (left) [72] and rocker switch RC-03 (right) [73]

A power supply PS-11 and wiring kit AC-17 cost \$85,99 (approx. €81) and \$29,99 (approx. €28) respectively [74] [75].



Figure 4.5. Power supply 120-220 VAC - 12 VDC, 25A (left) [75] and wiring kit (right) [74]

The manufacturer also presents wiring schematics for plugging all the devices together. Particularly, there is a setup scheme with two actuators working independently, such that each of them is controlled by separate DC speed controller [76]. These schematics, however, do not quite fit to simultaneous control task, and thus, have been modified as follows:

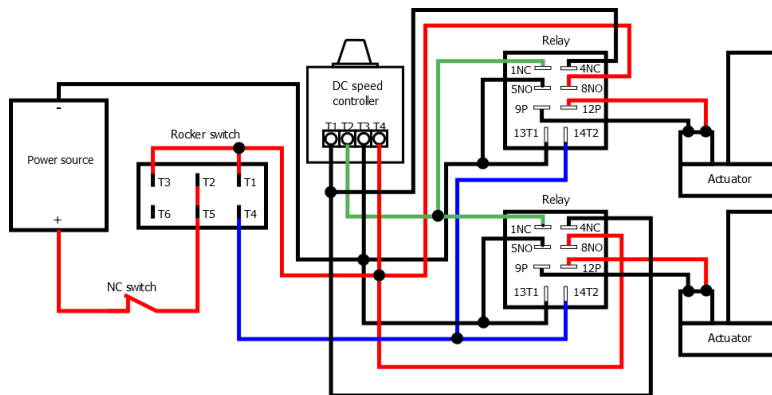


Figure 4.6. Wiring diagram for setup with 2 electric actuators

Figure 4.6 shows a simple setup scheme for plugging two actuators, controlled by one speed controller and rocker switch. The rocker switch is ON-OFF-ON type and it provides extending and retracting movement, when either of ON positions is pressed. Normally closed switch (NC switch) is supposed to work as an emergency button, in case if patient wants to terminate the procedure.

Also, there is an opportunity to purchase premanufactured external limit switch [77] for \$24,99 (approx. €23). But this device requires a controlling block which additionally costs \$119,86 (approx. €113) [78] and is only meant for 110VAC of input. Hence, these devices are considered for this case as optional ones.

Another optional feature could be a Hall effect control, which gives possibility to measure motor's RPM rate inside of the actuator (Figure 4.7) [79]. The downside of this device is its price - \$275 (approx. €260) and unnecessary features, such as dual wireless remote control dongles. The wiring diagram with this device included, would become more complex, respectively.



Figure 4.7. 12 VDC synchronized dual Hall effect actuator control [79]

As an alternative for feedback on velocity and displacement a controlling PID algorithm will be used. It will be programmed onto Texas Instruments MSP430 Launchpad, which has been discussed previously. The process of creating controlling algorithm is described more detailed in next chapter.

Following, Table 4.2 contains the total cost of components for electric actuators:

Table 4.2. Total cost of the components for electrical actuators

Name	Q-ty	Price, €
Linear actuator [69]	2	176
DC speed controller [71]	1	30
Rocker switch [72]	1	17
Relay [73]	2	16
Power supply [74]	1	81
Wiring kit [75]	1	28
MSP430 Launchpad [80]	1	9
NC switch	1	2
	Total	551
Optional devices		
External limit switch [77]	1	23
Control block with built-in power supply (110 V) [78]	1	113
Hall effect control [79]	1	260
	Total	396

As seen, a setup with electrical actuators from aforementioned manufacturer can be much cheaper. Of course, not all vendors set as low prices as these. Moreover, many of them do not disclose prices for their products at all, if one is not a privileged customer.

While writing this chapter, it has been made few unsuccessful attempts to get price list for either pneumatic or electrical actuators from several authoritative brands, such as Festo, Parker and Tolomatic. Besides, those products are meant for industrial purposes, offering features that are not required in given case, but, nevertheless, must be paid for.

4.3 Pneumatic actuators

Unlike electrical or hydraulic, pneumatic actuators use compressed air as working substance. Because gases are easy compressible a loss of thrust may occur due to decreased pressure. But for non-critical tasks this is not an issue. The relationship between force of pneumatic actuator and pressure supplied to it can be described as follows:

$$Force = Pressure \times Area, \quad (4.1)$$

where *Force* is a magnitude of thrust, *Pressure* is the value of pressure provided by compressor, *Area* is the mathematical area of piston which is connected to actuated mechanism.

Much like hydraulic, pneumatic actuators require supplementary parts, among which the bulkiest one is an air compressor. An example of air compressor of such kind is demonstrated on Figure 4.8.



Figure 4.8. 3,5 liters capacity air compressor [81]

Its operating voltage is either 110 or 220 VAC and flow rate is ~0,47 l/s. The noise level is 30 dB, which is equivalent to sound of computer fan or quiet public library.

The shown compressor operates at 116 psi (approx. 0,8 MPa) and weights 17 kg. Suppose, if the linear pneumatic actuator with piston area of 40cm² was chosen to work with this compressor, the force generated by this tandem would be following:

$$F = 0,8 \cdot 10^6 \cdot 40 \cdot 10^{-4} = 3200 \text{ N} = 3,2 \text{ kN} \quad (4.2)$$

In previous chapter the needed magnitude of thrust, produced by all actuators cumulatively, was calculated to be greater than 3,57 kN. This means, that if paired with mentioned compressor the actuator with 40 cm² of piston area is too powerful because it alone provides almost all needed thrust. Since the rehabilitation device is designed to have two actuators working in the same direction, an actuator with smaller piston area (e.g. 25 cm²) could be purchased, therefore, saving funds. In this case each actuator would deliver 2 kN of thrust, which is quite enough for given task.

Of course, it must be pointed out that all numbers were calculated at peak performance, thus, it is always better to choose slightly more powerful equipment, to avoid its rapid wearing out.

To set an air compressor to work for the first time user must manually attach air filter onto the special nozzle, to make sure that compressor works only with filtered air. Also, a lubrication oil needs to be poured into the system until prescribed level is reached. Additionally, it requires monthly condensate draining and frequent oil lubrication of inner moving parts. Operating of such compressor are as simple as turning tumbler on the command module to ON and adjusting desired level of pressure on the regulator.

As of 28.03.2017 the price of this compressor was set to \$1 036 (approx. €970). This particular type of compressors has a storage tank. This makes compressor more expensive comparing to those without a tank. They need to work constantly in order to maintain needed pressure.

The proposed construction of the rehabilitation device is based on square aluminum profiles. They have grooves on each plane for fastening different parts by bolts. The distance between two vertical profiles is 775 mm (Figure 4.9). In order to use as much space as possible from available 775 mm, it was decided to choose a rodless type of actuators.

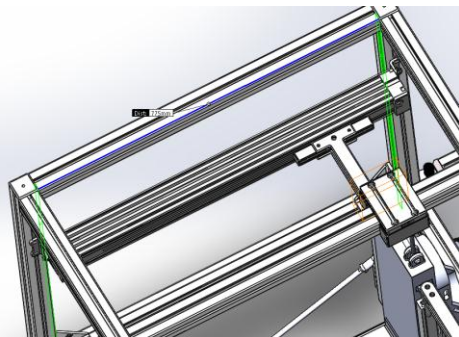


Figure 4.9. Linear actuator attached between two vertical profiles

On figure above there is shown a pneumatic rodless actuator Festo DGC-K-40-490 [82]. This particular model does not have a moving rod. Instead, actuating happens because of moving of a carriage, driven by inner piston (Figure 4.10).

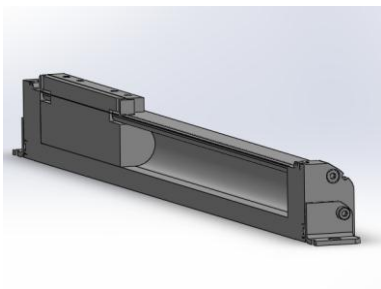


Figure 4.10. The inner structure of rodless pneumatic cylinder

The area of piston is 40 cm^2 , and its stroke length is 490 mm. This model was used for demonstration in conceptual CAD model because of its total length. It is 790 mm which fits perfectly between two profiles. However, according to manufacturer's specifications, given model with 40 cm^2 of piston area produces only 754 N of linear thrust, which is far less than needed (even when two actuators work simultaneously). The most appropriate model, producing 1,87 kN of thrust, would be an actuator with 63 cm^2 of piston area and stroke length 890 mm. This length does not fit into device's design, therefore, a replacement for this actuator would have to be found.

The cost of rodless pneumatic actuator varies from \$370 (approx. €350) [83] for used one to £527 (approx. €620) [84] for new actuator. However, these prices may differ at the time of actual purchasing.

Maintenance of such actuators requires qualified workers [85]. Some manufacturers, however, claim their products lifetime as big as $40 \cdot 10^6$ cycles or even “endless” [86].

A velocity of actuator plays an important role for rehabilitation process. For given tasks, it is important to have an adjustable velocity, so the leg can be stretched without sudden spikes, that may cause an injury.

In contrast to electromechanical actuators, pneumatics does not have correlation between produced force and velocity of moving carriage. That is because the force only depends on externally generated pressure and construction of actuator's inner parts. Nevertheless, there is a way to control velocity of moving element by installing threaded fittings onto air inflow and outflow bores (Figure 4.11). They cost \$17 (approx. €16) a pair.



Figure 4.11. Fittings with air speed control [87]

There is also an opportunity to include in airline a device for actuating the moving carriage. Figure 4.12 shows two types of them existing: electrical solenoids [88] and manual levers [89]. The price of electrical solenoid is around £10 (approx. €12), whereas manual lever costs £25 (approx. €29).



Figure 4.12. Electrical solenoid (left) [88] and manual lever (right) [89]

Figure 4.13 demonstrates a setup of these parts:



Figure 4.13. Air speed control set up [90]

The only thing that could be automated in this set up is starting up and turning off the actuator. This can be done by including a microcontroller into the system. However, its speed still needs to be adjusted manually by turning caps of air fittings clockwise or anticlockwise.

For controlling purposes Launchpad MSP430 [80] by Texas Instruments can be used (Figure 4.14). It costs \$10 (approx. €9) + shipping expenses.



Figure 4.14. MSP430 Launchpad development board [80]

Optionally, to automate a speed of air intake a miniature stepper motors can be used, as drivers for fittings (Figure 4.15). This approach is described in a study of McKibben type actuators (Parandyk et al., 2015) [91].

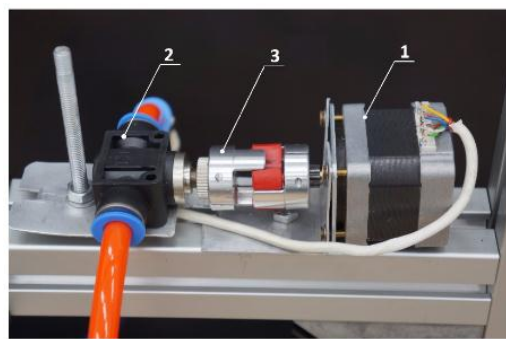


Figure 4.15. Airflow control components: 1 – stepper motor, 2 – throttle valve, 3 – sliding clutch [91]

Beside main actuating function “expand/retract” described earlier, this is meant to be a second electrical contour which needs to be controlled through additional stepper motor controller. Figure 4.16 schematically depicts probable composition of the whole pneumatic system with two controlling contours.

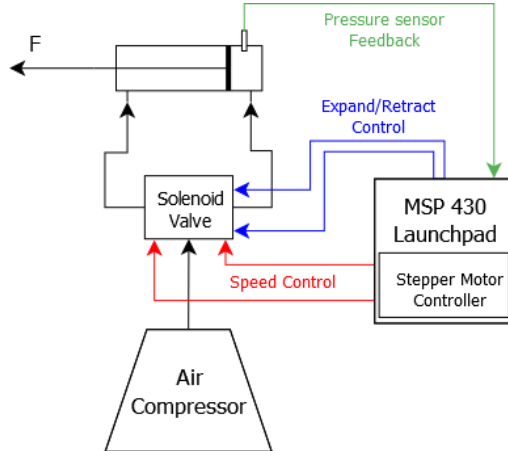


Figure 4.16. Control diagram for one actuator

It adds complexity due to additional wiring and increases the cost of the project in total. Table 4.1 sums up an average cost of minimum items needed for pneumatic set up.

Table 4.3. The cost of pneumatic components

Name	Q-ty	Price, €
Linear actuator [84]	2	1340
Compressor [81]	1	970
Electrical solenoid [88]	1	12
Fitting [87]	2	16
MSP430 Launchpad [80]	1	9
Stepper motor with driver [92]	2	20
Miscellaneous (airlines, electric wires etc.)		20
	Total	2387

Overall, this setup tends to be bulky and costly and seems like not an appropriate solution for given task. However, the Launchpad MSP 430 by Texas Instruments is a good choice to perform any kind of control, including electrical actuators. It will be used as a platform for developing control algorithm in chapter 5.

5. Developing of control algorithm

5.1 The overview

Prior to developing control algorithm for biomechanics-related problems it is essential to decide on type of control technique. Among known approaches for given case the analysis was narrowed down to neuro-controller and conventional PID- and Fuzzy-control.

To chose most appropriate between mentioned types a set of certain criteria must be pointed out. These to be stress in organic tissues (leg) that are being exercised, the easiness of use of device controlled by chosen algorithm, the stress in mechanical construction of device and its electrical circuits. The stress in organic tissues can be of two types: the mechanical stress and neural stress, Each of them is feeling subjectively by patient.

Considering controller based on neural networks, its resource demanding must be mentioned. Because very complicate structure a neural algorithm makes possible transition from pure control to prediction of operator's intentions. This, in its turn, offers much better user experience. For case of this study this means a neural controller can possibly adjust to each patient exclusively by developing a unique control type. Suppose, a million of patients with leg muscle stiffness have been offered to test a million of new rehabilitation devices in manual mode for certain time. Meanwhile controllers based on neural algorithm were gathering data from each individual and store them into one database. Ultimately a universal controlling algorithm would be developed, which fit to million of different people because it was able to recognize and predict men intensions. The drawback of its approach is, of course, its demand for both time and financial resources, thus it was decided do not consider it in this study.

Fuzzy controller possesses somewhat simpler approach in matter of implementation but still requires lots of "if-then" rules to describe different states of linear-nonlinear system (machinery-human) conjunction. Nevertheless, if spending some significant time on programming is not an issue a decent algorithm capable of recognizing patient's intentions can be developed too, much like its neural counterpart but significantly cheaper. As an option, additional mini-fuzzy controller could be developed only for emergency button (which is part of controlling hardware block) because precision of fuzzy controller is not applicable to thorough control of whole system, if number of "if-then" statements is not big enough.

The dynamical model of controlled device can be described by set of following equations:

$$\begin{aligned} T &= \vec{r} \times \vec{F}; \quad F = m \cdot a \Rightarrow T = r \cdot m \cdot a = r \cdot m \cdot \ddot{x}; \\ F &= kx + b\dot{x}, \end{aligned} \tag{5.1}$$

where T is torque of the motor, r is a radius of acme wheel that transforms angular movement of rotor shaft into linear movement of the carriage, F is a force exerted by actuator's carriage, m is mass of leg's tissues, a is an acceleration of the leg.

First equation represents forces that are applied to foot by mechanism, whereas second equation represents dissipative energy and forces that act oppositely in the leg. Following from (5.1) a unified equation of mechanical equilibrium that connects torque, displacement and velocity can be derived:

$$\frac{T}{r} = kx + b\dot{x} \tag{5.2}$$

Considering electrical part, the dynamical model of motor is following:

$$T = K \cdot I; \quad V = K \cdot w, \tag{5.3}$$

where T is torque of the motor, K is constant of proportionality, V and I are, respectively, voltage and current across the motor's electrical ports.

These equations describe smooth motion of dynamical system, which by definition can not tolerate any sudden impulses. Thus, it is reasonable to use differential controllers, among which most widespread is PID type. Another argument in favor of using PID controller for solving controlling task in given case is PID's popularity in robotics due to its relative simplicity and ability to be autotuned.

The cheap yet fully functional PID controller can be assembled from simplest electronical components, as follows [93]:

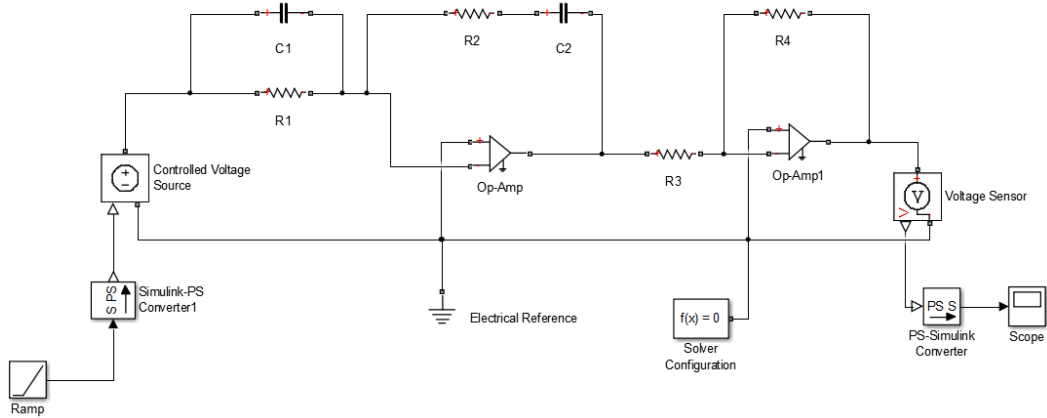


Figure 5.1 PID controller built on operational amplifiers (for larger image see Appendix 29)

This diagram shows the simple prototype of controller with constant nominals of elements and tuned for concrete case, whereas advanced state-of-art controllers have already adjustable electronics. However, since in given case there is no frequent retuning required, this diagram can be included in validation model (Figure 5.2), having pre-defined nominals of electronical components. In details, the process of device's design validation itself is described in chapter 6.

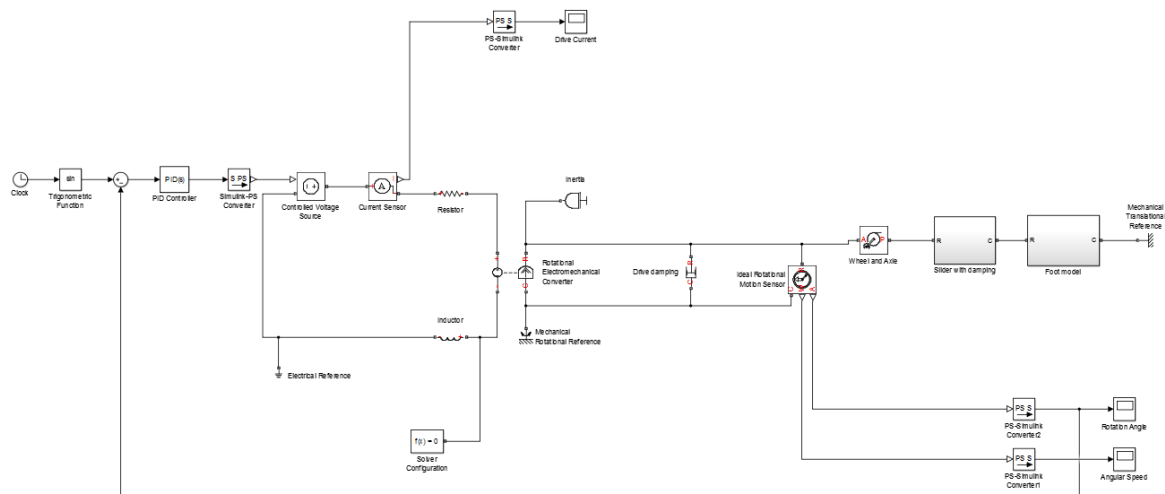


Figure 5.2 Validation model (for larger image see Appendix 30)

This model incorporates sine wave block as the training input for the system. Following, the system is being linearized to calculate values of PID block components and voltage is being sent to the motor as control signal. Between motor's input and output of PID block there is a converter to match signal types of Simscape and Matlab environments. The feedback loop reads the rotational displacement of motor's shaft (rotation angle), which is in direct correlation with linear movement of the motor's

carriage that is driven by acme screw mechanism (Figure 4.10). In the upper part of model there is “Wheel and Axle” block which converts rotational movement into that of linear type. The value of “Wheel and Axle” block is set to 2,5 cm, which corresponds to the radius of spinning shaft in actuator’s housing.

From the shown model a set of coefficients for conventional PID controller was obtained (Figure 5.3):

Proportional (P):	0.370678187393386
Integral (I):	0.0619732509130511
Derivative (D):	0.446847980814572
Filter coefficient (N):	4.56372895722713

Figure 5.3 Values of coefficients for PID controller

To build respective PID controller, as shown on Figure 5.1, from simplest electronical components, respective ratios were calculated:

$$c_1 = \frac{4,29}{R_1}; \quad R_2 = \frac{1,69}{c_2}; \quad \frac{R_4}{R_3} = 0,62 \cdot R_1 \cdot c_2 \quad (5.4)$$

Choosing of components’ nominals is dictated by working tasks, conditions (current, voltage) and controller’s efficiency in terms of consumed energy.

On average, the developing and simulating of mathematical model takes about 5 working days or 40 working hours. Approximate salary rate of the specialist (engineer, mathematician, physicist) capable of fulfilling this task is about €30/hr. Therefore, whole task cost is €1200. It is included in total project cost as one time investment (see Appendix 1).

To given task of medical rehabilitation PID controller is also applicable because it incorporates:

- proportional element, that makes controller sensitive to linear displacement (of motor carriage)
- integral element, that makes controller sensitive to control errors of any kinds
- derivative element, that makes controller sensitive to rapid movement changes

Speaking of PID’s downside, same as neural and fuzzy controllers’, it neither is capable of measuring mechanical stress in construction of device nor neural stress in patient’s leg. However, because it is possible to track the displacement of motor’s carriage and consequently transmit these data to PID controller, an approximate mechanical stress in patient’s leg can be estimated. Additionally, such dynamical parameters as velocity and acceleration can be computed as first and second order derivatives respectively.

5.2 Creating of control algorithm

To implement closed-loop system based on PID logic it is necessary constantly compare present state of controlled object with its desired state. In given task it was decided to measure position of motor’s carriage with help of time-of-flight distance sensor Adafruit VL53LOX (Figure 5.4). It is miniature and affordable mini-lidar that works in range 30-1000 mm. Its cost is only \$14,95 (approx. € 13,6).

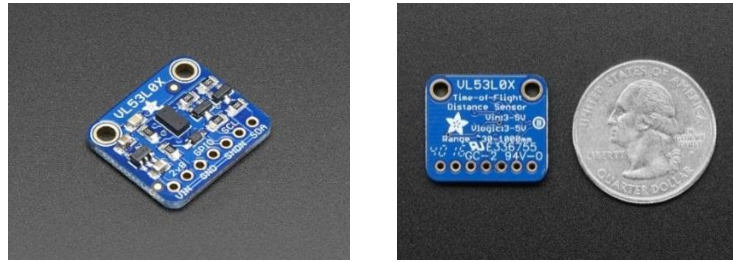


Figure 5.4 Time-of-flight distance sensor Adafruit VL53L0X [94]

The sensor contains a very tiny invisible laser source, and a matching sensor. The VL53L0X can detect the "time of flight", or how long the light has taken to bounce back to the sensor. Since it uses a very narrow light source, it is good for determining distance of only the surface directly in front of it. Unlike sonars that bounce ultrasonic waves, the 'cone' of sensing is very narrow. Unlike IR distance sensors that try to measure the amount of light bounced, the VL53L0X is much more precise and doesn't have linearity problems or 'double imaging' where you can't tell if an object is very far or very close [94].

To fasten such a small sensor safely to profile's frame a special custom enclosure was designed (Figure 5.5a). It is meant to be 3D printed and attached to frame facing upper slider which moves reciprocally back and forth. For effective attachment a sheet metal steel brace was designed to complete an assembly. The enclosure was made with an additional space for battery pack 3,7 V of voltage and 150 mAh of capacity manufactured by Adafruit [95] (Figure 5.5b). The addition of battery pack should make this unit autonomous in terms of power supply, as it is situated remotely from remote control. The cost of battery pack is \$5,95 (approx. €5,4).

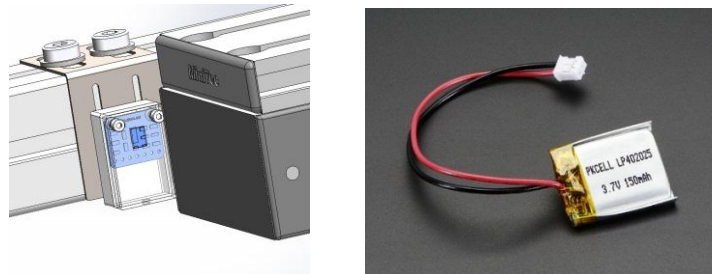


Figure 5.5 Custom enclosure for a) Adafruit VL53L0X and b) Adafruit battery pack [95]

To gather all electronics (except distance sensor) in one place a special remote control enclosure was designed (Figure 5.6). In this 3D printed box it is presumed 7 elements to be set:

- controller Launchpad MSP 430 (Texas Instruments);
- two relays AC-22 (Progressive Automations);
- rocker switch RC-03 (Progressive Automations);
- generic potentiometer;
- emergency button S533000 Red (Valeo 533 seriен [96]);
- battery pack 3,7 V of voltage and 6600 mAh of capacity (Adafruit [97]).

The enclosure has three wall perforations: on the side wall there are wholes for controller inputs and mini-usb connection for reprogramming or writing the log file to the computer and on the rear wall a whole for output from relays to actuators is situated.

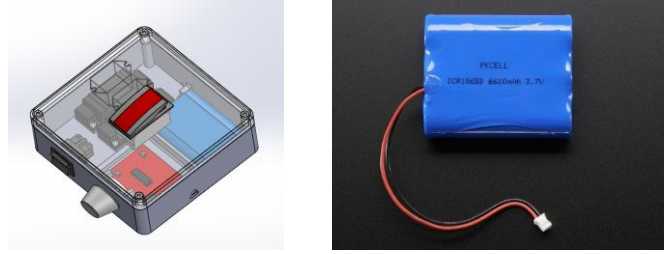


Figure 5.6 a) Remote control enclosure with electronics inside; b) Adafruit 3,7 V 6600 mAh battery pack [97]

The battery in this unit is shown only as possible option, because this layout is meant to be powered via wall power supply (Figure 4.5), through voltage 12V to 3,6 V converters [98] (Figure 5.7).

Additionally, it was decided to exclude DC speed controller AC-14 (Figure 3.3), presented in previous “manual” version of control wiring diagram (Figure 3.6). In new schematics it is now controller’s job to “decide” whether human turns potentiometer too intensive or too weak. Turning potentiometer’s knob changes the first input signal value. The second input is voltage from sensor Adafruit VL53LOX, which transmits the position of foot platform, and thus, patient’s foot itself.

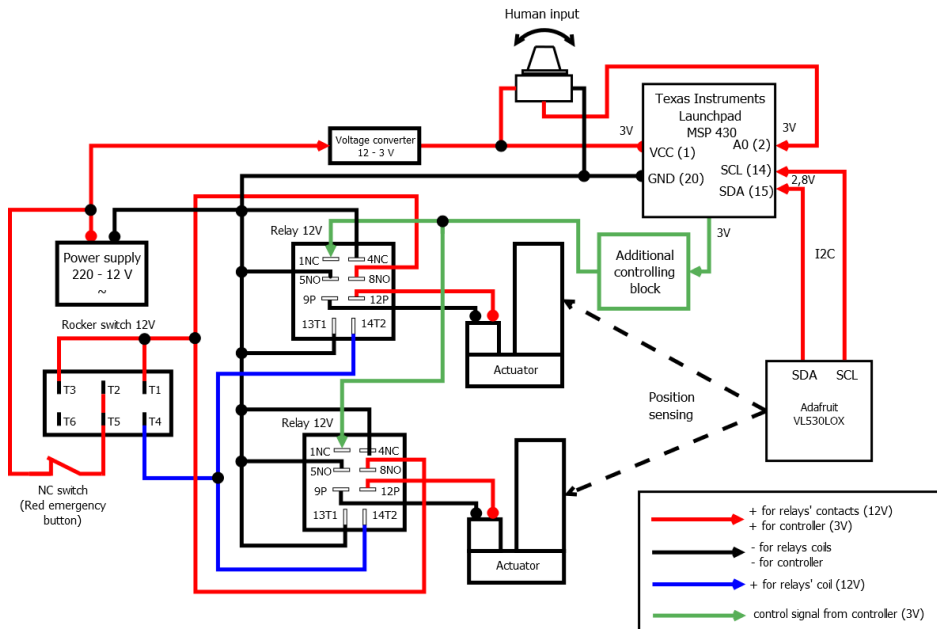


Figure 5.7 An updated control wiring diagram

A new unit named “Additional controlling block” (framed green) has been added to schematics in order to add an emergency control mode. This unit “decides” whether control signal from PID controller (logic 1) or emergency controller (EC) (logic 0) must be sent to an end actuator (Figure 5.8). If the signal from PID controller is not satisfying, it is being assigned logic 0 and contacts *a*, *c* and *e* are opened, therefore, controlling is done through EC. The EC is realized on simple RC-filter, that makes motor slowly retract moving carriage back to starting position. *Error* is the annotation for difference of desired and actual input to PID controller.

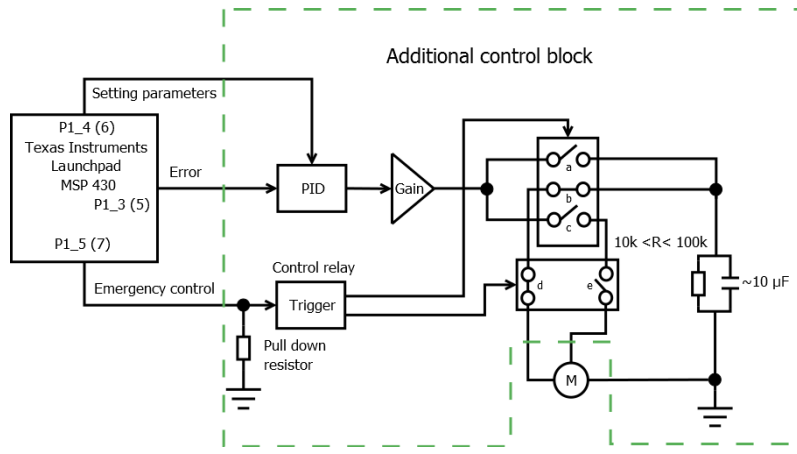


Figure 5.8 Circuit diagram of additional controlling block. The logic “0” state is shown.

The name “Additional controlling block” is rather symbolic as this unit incorporates sub-units that might be placed remotely, regarding each other. Particularly, there are PID controller, 2 relays that trigger between logic “0” and logic “1” states, the simple emergency controller, that is made of capacitor and resistor, and the amplifier that increases low-level signal from PID controller. A pull-down resistor is used to ensure there is no floating in the input signal. Its nominal should be at least 10 times bigger than impedance of input pin.

Concerning realization PID algorithm on the Launchpad’s MSP 430 basis, there were two options: either to write embedded program using custom library or to set it working with external PID device. Even though first option looks better in theory, in practice due to controller’s architecture the embedded algorithm running would cause significant delays and overall system’s responsiveness would decrease.

Launchap M430 is not meant to calculate the value of P, I and D components themselves, as they are obtained from linearization of Matlab model.

According to this, the functions of TI Launchpad MSP 430 are overwriting the P, I and D components of PID controller, initiating training mode when needed and storing information damp for late analysis on PC.

The program logic for TI Launchpad MSP 430 is following:

1. Setting up the controller (sets all controller’s parameters, initial parameters of devices, controlling programs):
 - a) *setting up of ADC – obtains data from sensor (optical sensor Adafruit VL53LOX);*
 - b) *setting up of DAC – for transferring of control signal to PID;*
 - c) *setting up of timers – calculating and assigning of working schedule and intervals, that provides appropriate performance of controller and control algorithm;*
 - d) *setting up of serial port for exchanging data with PC;*
 - e) *setting up of indicators (LEDs, external displays) – for indicating working mode, measuring data etc.;*
 - f) *granting access for interruptions – last step before control mode is ON; after this control is enabled.*

2. The main program loop (indicating of working mode, measuring data and possible errors):
 - a) *indicating of working mode;*
 - b) *indicating of measuring data (indicators, LEDs; PC – if the interactive mode is enabled);*
 - c) *indicating of possible errors;*
 - d) *switching between working modes and device's settings.*
3. The main control program (the main working mode is timer interruption, ADC, DAC etc.):
 - a) *Interruption of timer A: a quick interruption that controls upper parts of drivers – reading data from ADC and PID;*
 - b) *Interruption of timer B: a slower interruption that requires more time; controls the data conversion and responsible for necessary calculations of working schedule (waving working mode or any other), sets the control signals on controlling outputs.*

The program code itself is available on the optical disk, containing additional materials of this work. On average, the developing of control algorithm takes about 5 working days or 40 working hours. Approximate salary rate of the specialist (engineer, mathematician, physicist) capable of fulfilling this task is about €30/hr. Therefore, whole task cost is €1200. It is included in total project cost as one time investment (see Appendix 1).

6. Technical parameters and validation of device's design

6.1 General technical data and cost of the project

In this chapter a brief technical data are presented in a written form together with comprehensive cost estimation of the whole project. Set of manufacturing drawings for all custom-made parts and assembly drawings for 6 subassemblies and 1 complete assembly are attached as appendices 10-28 (scaled versions, to fit A4 format).

The invention being developed in this study is 1 degree of freedom (1 DOF) electromechanical device aiming to facilitate rehabilitation process for people with acquired muscle stiffness of lower extremities. The rehabilitation device is meant to be for stationary use. Its dimensions 930 x 1030 x 1865 mm (expanded) or 930 x 1030 x 940 mm (folded).

The device is meant to be powered by public electrical network (110V; 220V) via proprietary 3d party power supply convertor. The internal voltage of device's electrical chains is 12V for electrical end-actuators and 3,6V for computational electronics. The sequencing of these voltages is done through proprietary voltage converters.

The actuators and supplementary electric devices were meant to be purchased from "Progressive Automations" [68]. The computational electronics represented by Launchpad MSP 430 (or of similar functionality) is presumed to be obtained from "Texas Instruments" [99].

The total mass of construction is 78,9 kg. It incorporates such materials as aluminum alloy, steel alloy, 3D printing of plastic and rubber material. The producing of aluminum custom made details require weldments of sub-parts. The producing of sheet metal steel parts require plasma cut and bending. There are designed 5 steel bars requiring milling or engraving M8 thread on them. 13 aluminum profiles require internal M8x15 thread in central whole to be able to fasten between themselves.

Overall, there are 12 custom made parts. All framing parts are standard parts. They are presumed to be bought from Minitec Estonia [50]. An up-to-date (28.04.2017) price list was obtained from Minitec Estonia to calculate estimated cost of the project (see Appendix 1). The final cost, together with overseas shipment and cost of producing custom parts, should not exceed €5000 for the first device or €2500 for each next series product.

6.2 Validation of device's design

The validation of design is done by simulating mechanical stress in respective parts of construction. For custom parts stress simulations have been run in "Ansys Workbench" software package to verify their suitability to routine working conditions. The simulations show deformation at time range 0 - 1 s. All details were assumed to be made of metal: the material for foot platform assembly is aluminum alloy 6061-T6 (SS) for decreasing its weight and the for rest custom parts ally steel was used with 7700 kg/m³ of density.

The mass of whole foot platform assembly is 11,5 kg. In the simulations this value is used together with an approximate mass of patient's shank of 4,27 kg (15,77 kg or 157,7 N).

The validation of mechanical parts was done by applying the working fatigue value to respective elements of the base and upper slider. The simulation process was split into such subcases because of computational restrictions of academical version of "Ansys Workbench". The respective illustrations can be found in Appendices 2-9. For all standard parts stress simulations have not been run, as initially they were chosen due to their ability to withstand similar load, according to vendor's specifications.

To simulate the behavior of biological tissues of human muscles in conjunction with electromechanical system, the respective model was built, using Simscape package of Matlab (see Chapter 5 for details). Its output is an input of “Slider with damping” block (Figure 6.2).

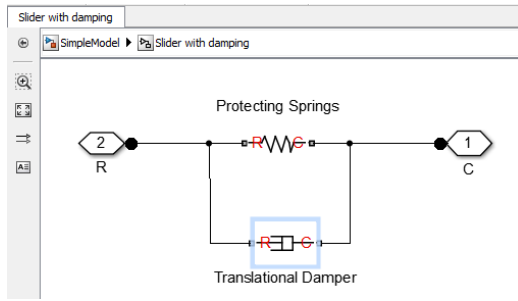


Figure 6.2 Slider with damping block that simulates behavior of linear actuator

This is the simplest block for simulation physical properties of linear actuator. The spring element represents mechanical resistance to the movement of the carriage and inner parts. The damper adds viscous effect of the motor's work. To simulate reciprocal movement of actuator's carriage that is being influenced by forces of both viscous and stiffness natures, the value of spring stiffness was set to $3800 \text{ N}\cdot\text{m}^{-1}$ (2 extension springs T32860 with spring rate of $1900 \text{ N}\cdot\text{m}^{-1}$ each [100]) and value of viscous damper was set to $100 \text{ N/m}\cdot\text{s}^{-1}$.

The value of damping is set rather insignificant due to features of given mechanical system. The most impact on damping in the considered system is done by friction, which is represented by friction of rolling of roller elements that move along the grooves in aluminum profiles. This friction can be neglected considering the scale of the project, therefore, the value of damping of $100 \text{ N/m}\cdot\text{s}^{-1}$ is justified for given case.

After “Slider with Damping” block, the “Foot model” block is placed. It splits into inertial and mechanical blocks. The entire parent block tends to copy behavior of human organic tissues as its dynamical part is arranged according to Hill's model [64] (Figure 6.3).

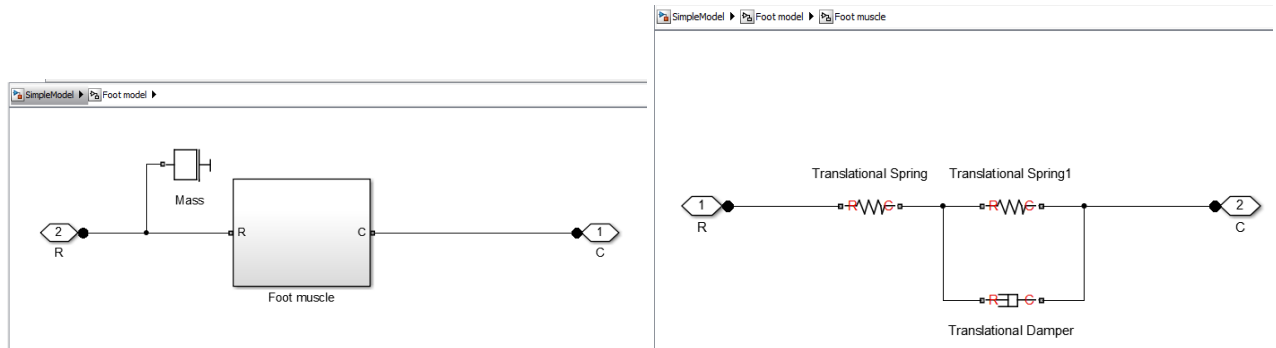


Figure 6.3 Foot muscle block: parent model with mass block for inertial parameters (left); daughter Hill's model (right)

The only deviation from classical Hill's model is the absence of function $A(t)$ in contractile element (CE), as this function pertains to healthy human muscle, specifically those capable of generating power. The other part of CE is damper, which remains in the model. In “Mass” block there is specified a mass of the whole leg (thigh + shank) as big as 11,27 kg and value of initial velocity set as 0.

The set parameters of Hill model were calculated according to formulas presented in Chapter 3: $T = 2M/B$, $B/M = 2/T$. Also, $B = 2\sqrt{MK}$. Therefore, $K/B = B/4M = 1/2T$ [34]. For single considered muscle its biomechanical parameters are following:

$$M = 149,93 \text{ g}; T = 79 \cdot 10^{-3} \text{ s}; B = 3,8 \text{ N/m} \cdot \text{s}^{-1}; K = 24,05 \text{ N} \cdot \text{m}^{-1}.$$

After tuning of PID controller the best control curve was found (Figure 6.4):

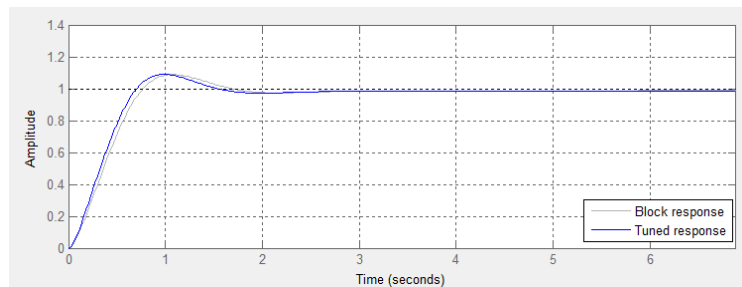


Figure 6.4 The response curve of tuned controller

The tuning goal was to shorten transient state to less than 2 seconds with the smallest overshoot possible (less than 10% of overshoot achieved). The control signal stabilizes in 1,5 seconds and remains stable ever after.

Following, there are presented comparison between tuned and untuned plots of DC drive current change, angular displacement and angular velocity for given biological conditions:

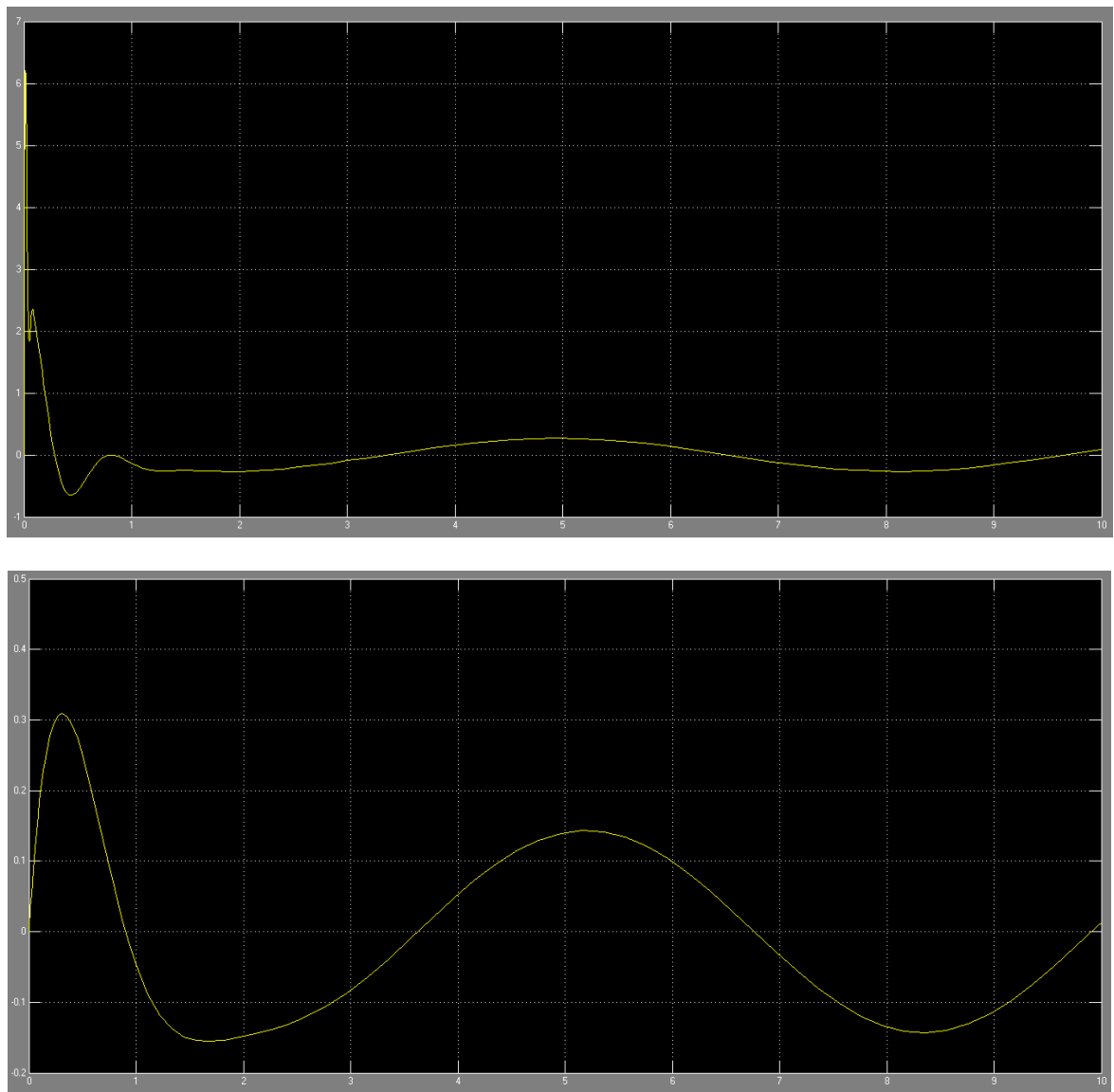


Figure 6.5 DC drive response of not tuned (upper) and tuned model (lower)

Before tuning the controller, behavior of DC motor was characterized by steep jump in the beginning (Figure 6.5, upper). The peak value reached 6,2 A, which is within 10A of actuators working range. Nevertheless, it possesses danger of rapid wearing out of the inner parts of the motor. After the first peak, there were two other drops and peaks, all during first 0,4 s.

After tuning was done the response of the current has changed positively. It smoothly increases from 0 only to 0,31 A during first 0,4 s and never goes higher than 0,15 A ever since (Figure 6.5, lower). Because there is a training sine wave signal supplied to the input, the output of all sensors is also of the same shape, with period of 6 s. On the second graph line moves without any sudden spikes or drops, within $-0,15 - + 0,15$ A. This means DC drive works in forward and reverse mode, switching every 3 seconds.

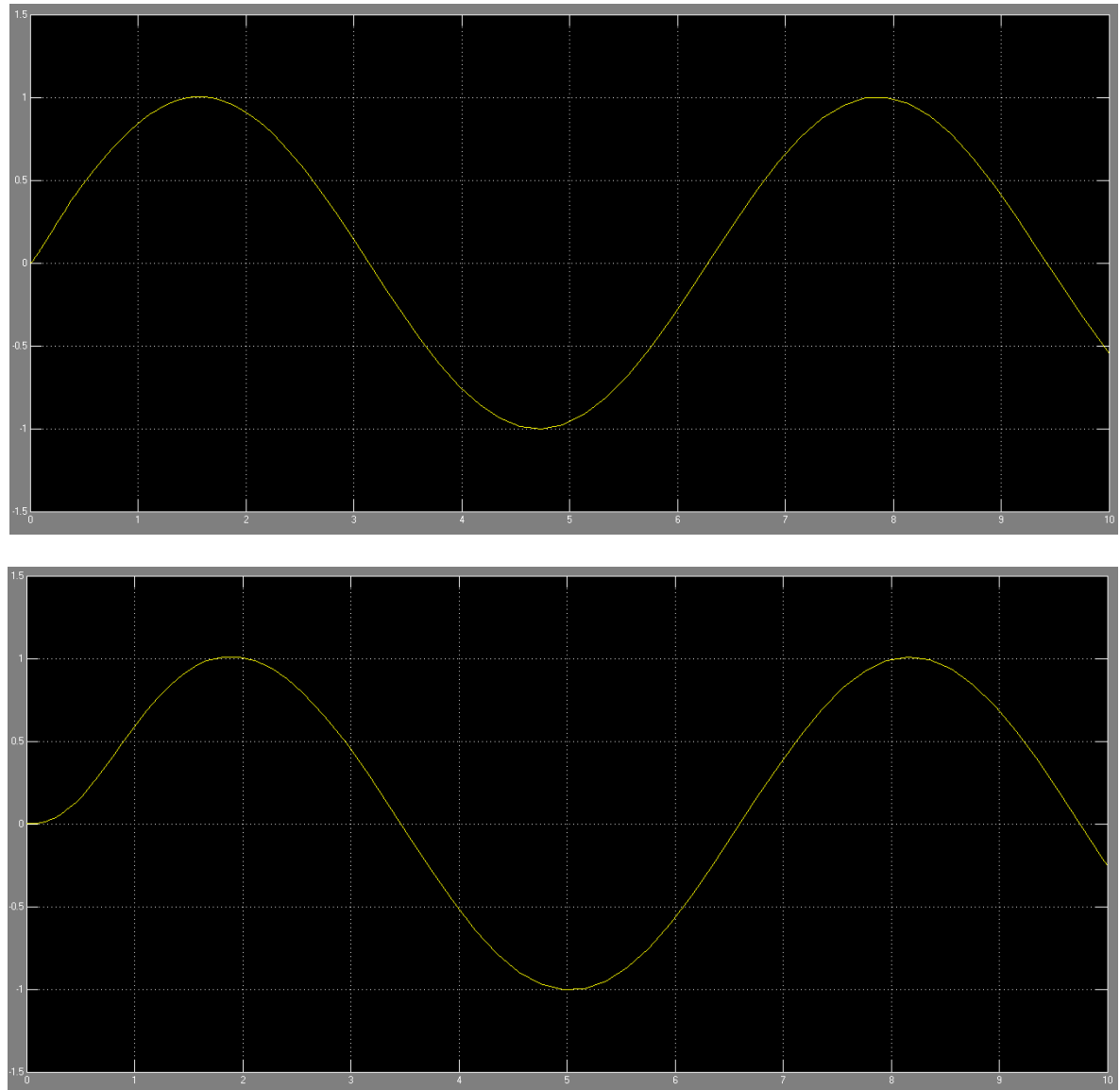


Figure 6.6 Rotation angle change of not tuned (upper) and tuned model (lower)

The rotation angle's pattern almost has not change in tuned model (Figure 6.6). The only distinct differences are shifting of signal for 0,3 s and smoother gain at the beginning, during the first second. The signal reaches its first positive peak of 1 rad ($\sim 57^\circ$) in 1,9 s – 2 s and first negative peak of -1 rad on 5th second. Because actuator's shaft driven by motor makes only approximately 1/6 of full turn in given simulation, the actuator's carriage travels very little distance. The simulation shows that it would be enough to extend the stiff muscle alone, as its being considered in scope of this simulation separated from other muscle groups. However, for extension such complex biomechanical system as

human leg, there is a full length (594 mm) of stroke foreseen. The intensity and the distance of muscle extension is up to patient's preferences.

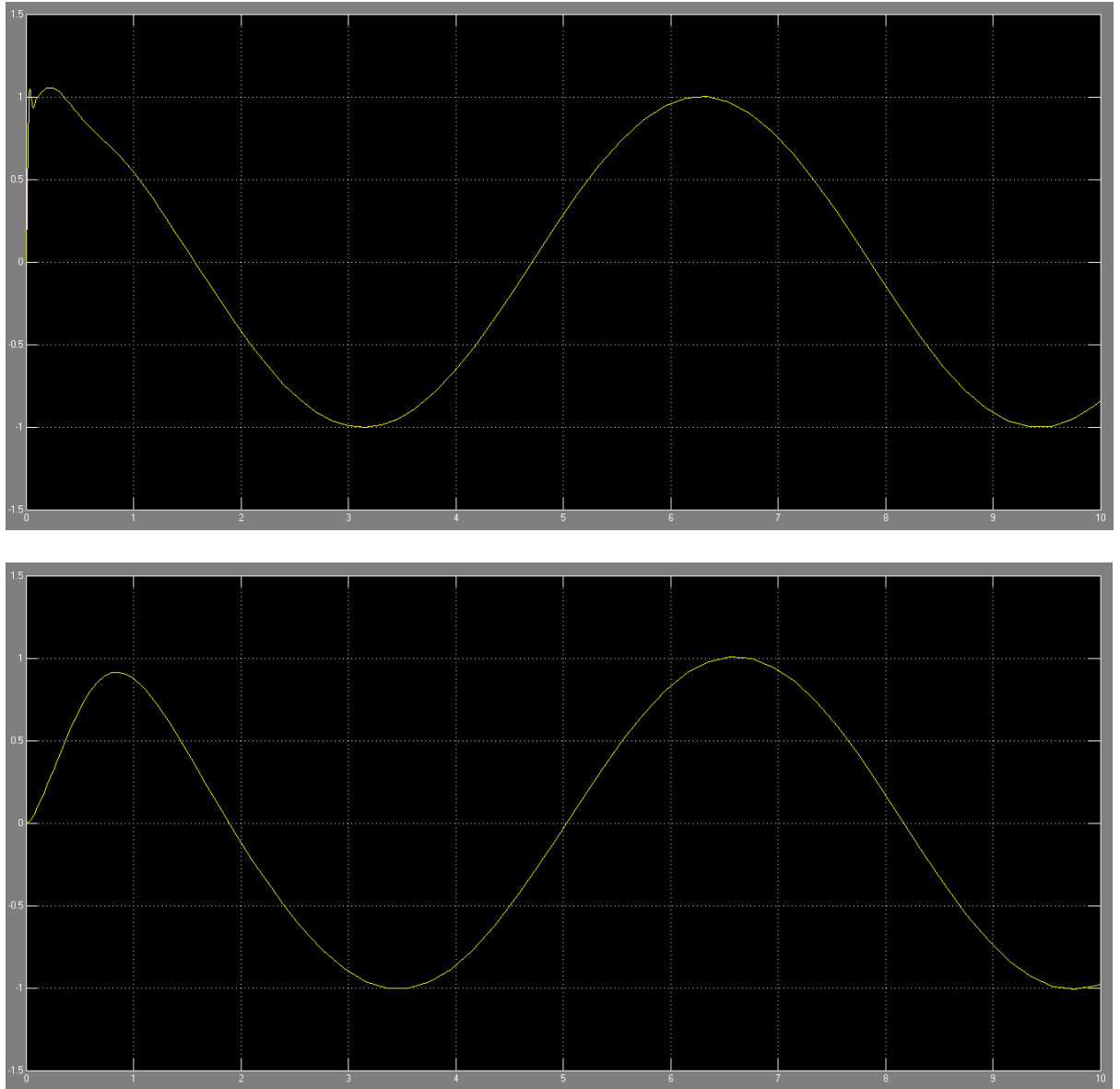


Figure 6.7 Angular speed of not tuned (upper) and tuned model (lower)

Before the system was properly tuned, the graph of motor's angular speed has been comprising sudden jerk from 0 to $1 \text{ rad} \cdot \text{s}^{-1}$ in just 0,1 s (Figure 6.7, upper). It is so because of the existing correlation between current on the motor and spinning shaft velocity itself. And much like in case of steep current increase, in case of frequent and rapid shaft turning at start, the possibility of its faster wearing out increases significantly. After tuning the smooth and safe for equipment response was achieved with slight undershoot at the first iteration (Figure 6.7, lower). The first positive peak of $0,9 \text{ rad} \cdot \text{s}^{-1}$ is now reached in 0,9 s and first negative peak of $-1 \text{ rad} \cdot \text{s}^{-1}$ is reached in 3,4 seconds.

Considering any kind of current jumps on DC motor: the initial paramters of the model were chosen in such a way, that sudden jumps in electrical part of the model had to be eliminated as such. However, if there were sudden spikes at the beginning, their nature would be of potential and not kinetical part of dynamics. That is, transferring the energy to magnetic component without influencing of system kinetics, such that initial velocities remain constant or change at insignificantly small range.

Considered system can also be defined as plastic since it possesses devices capable of easy accumulating of potential energy. These are the motor and the leg. While motor is an artificial

electromechanical system being designed in such way, the leg as biological system, that over long evolutional period has obtained tendons. The function of tendons is making sure that muscle does not experience overload and, therefore, remains integral in its structure.

Summary

The goal of this work was to create electromechanical device for medical rehabilitation. Particularly, it is supposed to target cases when patient can not stretch his or her leg for more than 90° in the knee joint. This disease is called “Stiff man syndrome” (SMS) and is characterized by increased rigidity of hamstring muscles. The invented device should help to flex these muscles via provoking their mechanical extension.

A comprehensive research was conducted on devices of the same functionality, presently available on the market. Those of commercial segment were found to be non-competitive with the product of this paper due to their function. They are meant for post-surgical rehabilitation, when patient's leg is already healthy but needs to be mechanically stretched over some short period of time. As a result, these devices comprise light materials which can not withstand some significant stress, inevitably involved in stretching leg with SMS.

To make the cost of the project as low as possible, the device was designed mostly from standard parts which can be purchased from company “Minitec Estonia”. It is a local affiliation of company “Minitec”, which specializes on fastening solutions, using aluminum profiles and sliding systems. The aluminum square profile was taken as a basis for device's frame, which is of cubic shape. Inside of it a special foot platform, to which patient's foot is being strapped, slides back and forth, making muscles stiffed in 90° position to extend to 180°.

For controlling part there were choosing electronical components, including microcontroller made by company “Texas Instruments”. A program algorithm that includes emergency case scenario was developed for this controller. Additionally, there was foreseen PID controller which works in conjunction with microcontroller. The optical sensor by company “Adafruit” provides feed back about patient's leg position. The proper linear electrical actuators that provide enough of thrust were found among products of company “Progressive Automations”.

The fully featured dynamical model of the device was created using Solid Works 2015 modelling package. The mechanical stress calculations of loaded parts were done in simulating software Ansys Workbench 16.2. To validate the system, that combines mechanical and biological structures working together, Matlab 2013b was used, a software for the mathematical simulation.

A product of this research could potentially be employed separately by medical institutions as well as healthcare industry in general. Also, private customers might express an interest to buy it, if the end price is affordable enough.

KOKKUVÕTE

Käesoleva töö eesmärgiks oli luua elektromehaaniline seade meditsiiniliseks taastusraviks. Täpsemalt on silmas peetud olukorda, kus patsient ei saa jalga põlvest üle 90° liigutada. Seda haigust nimetatakse jäiga mehe sündroomiks (Stiff man syndrome - SMS), mida iseloomustab põlvekõõluste suurenenedud jäikus. Antud seade peaks aidama nende lihaste mehaanilisi liigutusi esile kutsuma.

Läbi viidi ulatuslik uuring turul olevate sama funktsionaalsusega seadmetele. Saadaval olevaid seadmed on mõeldud operatsioonijärgseks taasturaviks, kus patsiendi jalgi on juba terve, kuid vajab aeg-ajalt sirutamist. Nende ehituses kasutatakse kergeid materjale, mis ei kannata suuremaid koormusi, mida on vaja SMS-ga patsientidel jala sirutamiseks.

Projekti maksumuse vähendamiseks on kasutatud peamiselt standardseid osi, mida on võimalik ostaa ettevõttest Minitec Estonia. Tegemist on Miniteci kohaliku esindusega, mis spetsialiseerub kinnituslahendustele kasutades alumiiniumprofiile ja liugsüsteeme. Kuubikujulise raami ehituses on kasutatud nelinurkset alumiiniumprofiili. Sees asub spetsiaalne platvorm, kuhu patsiendi jalgi on kinnitatud ja mis edasi-tagasi liikudes paneb lihased kokku tõmbuma ja lõtvuma.

Kontrollsüsteemi osadeks valiti elektroonilised komponendid, mis on valmistatud ettevõttes Texas Instruments. Kontrolleri jaoks on loodud algoritm, kus on arvestatud ka hädaolukorra stsenaariumiga. Lisaks on kasutatud ka ettenähtud PID kontrollerit, mis töötab koos mikrokontrolleriga. Patsiendi jalaasendi kohta annab tagasisidet optiline sensor ettevõttelt Adafruit. Vajalikud lineaarsed elektrilised ajamid on leitud ettevõtte Progressive Automations toodete hulgast.

Seadme kohta on loodud dünaamiline mudel kasutades Solid Works 2015 tarkvara. Mehaanilise koormuse arvutuste jaoks on kasutatud simuleerimistarkvara Ansys Workbench 16.2. Lisaks on kasutatud mehaanilise ja bioloogiliste struktuuride koostöömimiseks matemaatilise simulatsiooni tarkvara Matlab 2013b.

Antud meditsiinilist seadet võiksid kasutada meditsiinilised institutsioonid, kuid ka tervishoiu valdkond üldiselt. Samuti võib seade taskukohase hinna puhul äratada huvi ka eraklientides.

REFERENCES

- [1] "Rehabilitation Engineering," 2017. [Online]. Available: <https://www.anatomicalconcepts.com/youbike/>. [Accessed 18 Februaty 2017].
- [2] "Rehabilitation Engineering," 2017. [Online]. Available: <http://www.berkelbike.co.uk/>. [Accessed 18 February 2017].
- [3] "US patent," 2017. [Online]. Available: <https://docs.google.com/viewer?url=patentimages.storage.googleapis.com/pdfs/US20120329611.pdf>. [Accessed 18 February 2017].
- [4] "CPM Machine after knee replacement," 2017. [Online]. Available: <https://www.verywell.com/do-i-need-a-cpm-following-knee-surgery-2548662>. [Accessed 18 February 2017].
- [5] "Online auction," 2017. [Online]. Available: https://www.alibaba.com/product-detail/Continuous-Passive-MotionNew-Products-Health-Leg_60361849022.html. [Accessed 18 February 2017].
- [6] "Rehabilitation Engineering," 2017. [Online]. Available: <http://www.chinesport.com/catalogue/rehabilitation-equipment/continuous-passive-motion-lower-limbs/XRI003-fisiotek-3000e/>. [Accessed 18 February 2017].
- [7] "The James Dyson Foundation," 2017. [Online]. Available: <http://www.jamesdysonaward.org/en-GB/projects/powerd-leg-brace/?cookies=true>. [Accessed 18 February 2017].
- [8] A. M. Dollar and H. Herr, "Design of a Quasi-Passive Knee Exoskeleton to Assist Running," Acropolis Convention Center, 22-26 September 2008. [Online]. Available: https://www.eng.yale.edu/grablab/pubs/dollar_IROS08.pdf. [Accessed 18 Feruary 2017].
- [9] M. R. Tucket, A. Moser, O. Lambercy, J. Sulzer and R. Gassert, "Design of a Wearable Perturbator for Human Knee," 2013 IEEE International Conference on Rehabilitation Robotics, 24-26 June 2013. [Online]. Available: <https://infoscience.epfl.ch/record/189717/files/Tucker%20MR%202013%20Design%20of%20a%20wearable%20perturbator%20for%20human%20knee%20impedance%20estimation%20during%20gait.pdf>. [Accessed 18 February 2017].
- [10] K. Goher and S. Fadlallah, "Design, Modelling, and Control of a Portable Leg Rehabilitation System," Journal of Dynamic Systems, Measurement, and Control, 2017. [Online]. Available:

- <http://dynamicsystems.asmedigitalcollection.asme.org/pdfaccess.ashx?url=/data/journals/jdsmaa/0/ds-16-1410.pdf>. [Accessed 18 February 2017].
- [11] E. Garcia, D. Sanz-Merodio, M. Cestari, M. Perez and J. Sancho, "An active knee orthosis for the physical therapy," Centre for Automation and Robotics, CSIC-UPM, 28500 Arganda del Rey, Madrid,, [Online]. Available: <http://digital.csic.es/bitstream/10261/133286/1/603130.pdf>. [Accessed 18 February 2017].
- [12] Y. Park, B. Chen, D. Young, L. Stirling, R. Wood, E. Goldfield and R. Nagpal, "Bio-inspired Active Soft Orthotic Device for Ankle Foot Pathologies. In Proceedings of the International Conference on Robots and Systems (IROS)," 25-30 September 2011. [Online]. [Accessed 25 February 2017].
- [13] Mohd Azuwan Mat Dzahir and Shin-ichihiro Yamamoto, "Recent Trends in Lower-Limb Robotic Rehabilitation Orthosis: Control Scheme and Strategy for Pneumatic Muscle Actuated Gait Trainers," *Robotics*, no. 3, p. 130, 2014.
- [14] K. Onogi, I. Kondo, E. Saitoh, M. Kato and T. Oyobe, "Comparison of the effects of sliding-type and hinge-type joints of knee-ankle-foot orthoses on temporal gait parameters in patients with paraplegia," *Japanese Journal of Comprehensive Rehabilitation Science*, vol. I, pp. 1-6, 2010.
- [15] S. Sargsyan, V. Arakelian and S. Briot, "ROBOTIC REHABILITATION DEVICES OF HUMAN EXTREMITIES: DESIGN CONCEPTS AND FUNCTIONAL PARTICULARITIES," in *11th Biennial Conference on Engineering Systems Design and Analysis*, Nantes, 2012.
- [16] S. Banala, S. Kim, S. Agrawal and J. Scholz, "Robot Assisted Gait Training With Active Leg Exoskeleton (ALEX)," *IEEE Transactions on Neural Systems and Rehabilitation Engineering*, vol. XVII, no. 1, pp. 2-8, February 2009.
- [17] "Rehabilitation Engineering," [Online]. Available: <http://www.yobotics.com>. [Accessed 09 March 2017].
- [18] J. Pratt, S. Collins, B. Krupp and C. Morse, "The RoboKnee: An Exoskeleton for Enhancing Strength and Endurance During Walking," in *Proceeding of the IEEE International Conference on Robotics & Automation*, New Orleans, LA, 2004.
- [19] "Rehabilitation Engineering," [Online]. Available: <http://www.litegait.com/>. [Accessed 09 March 2017].
- [20] "Rehabilitation Engineering," [Online]. Available: <http://www.ropox.com/>. [Accessed 09 March 2017].

- [21] P. Métrailler, R. Brodard, Y. Stauffer, R. Clavel and R. Frischknecht, "Cyberthesis: Rehabilitation Robotics With Controlled Electrical Muscle Stimulation," *Rehabilitation Robotics*, pp. 303-318, 2007.
- [22] "Rehabilitation Engineering," [Online]. Available: <http://www.musclepower.com/>. [Accessed 09 March 2017].
- [23] "Rehabilitation Engineering," [Online]. Available: <http://www.hocoma.com/>. [Accessed 09 March 2017].
- [24] P. Métrailler, "Système robotique pour la mobilization des membres inférieurs d'une personne paraplégique," Ecole Polytechnique Fédérale de Lausanne, 2005.
- [25] H. Schmidt, "HapticWalker - A novel haptic device for walking simulation," *Proceedings of EuroHaptics*, pp. 60-67, 5-7 June 2004.
- [26] "Rehabilitation Engineering," [Online]. Available: <https://www.hocoma.com/solutions/erigo/>.
- [27] F. P. Moersch and H. W. Wolman, "Progressive fluctuating muscular rigidity and spasm ("stiff-man syndrome"): report of a case and some observations in 13 other cases," *Mayo Clin Proc* 31, pp. 421-427, 1956.
- [28] R. A. Barker, T. Revesz, M. Thom, C. D. Marsden and P. Brown, "Review of 23 patients affected by the stiff man syndrome: clinical subdivision into stiff trunk (man) syndrome, stiff limb syndrome, and progressive encephalomyelitis with rigidity," 1998. [Online]. Available: <http://jnnp.bmjjournals.org/content/jnnp/65/5/633.full.pdf>. [Accessed 22 March 2017].
- [29] P. Brown and C. D. Marsden, "The stiff man and stiff man plus syndromes," *Journal of Neurology*, no. 246, pp. 648-652, 1999.
- [30] P. D. Thopmson, "The stiff-man syndrome and related disorders," [Online]. Available: <http://www.sciencedirect.com/science/article/pii/S1353802001000293>. [Accessed 22 March 2017].
- [31] T. Bartsch, J. Herzog, R. Baron and G. Deuschl, "The stiff limb syndrome – a new case and a literature review," *Journal of Neurology*, no. 250, pp. 488-490, 2003.
- [32] P. Brown, J. C. Rothwell and C. D. Mardsen, "The stiff leg syndrome," *Journal of Neurology, Neurosurgery, and Psychiatry*, no. 62, pp. 31-37, 1997.
- [33] A. Hajjioui, K. Benbouazza, M. E. Alaoui Faris, A. Missaoui and N. H. Hassouni, "Stiff limb syndrome: a case report," *Cases Journal*, no. 3, p. 60, 2010.
- [34] D. A. Winter, Biomechanics and motor control of human movement, 3d edition ed., Hoboken, N.J.: Wiley, 2005, p. 325 lk..

- [35] M. Lintsi and K. Helje, "Growth of Estonian seventeen-year-old boys during the last two centuries," *Economics and Human Biology*, no. 4, pp. 89-103, 2006.
- [36] M. F. Bobbert, "Why is the force-velocity relationship in leg press tasks quasi-linear rather than hyperbolic?," *J Appl Physiol*, no. 112, pp. 1975-1983, 2012.
- [37] S. J. Piazza, "The influence of muscles on knee flexion during the swing phase of gait," *J. Biomechanics*, vol. 29, no. 6, pp. 723-733, 1996.
- [38] S. K. Thorpe, Y. Li, R. H. Crompton and A. R. McNeill, "Stress in human leg muscles in running and jumping determined by force plate analysis and from published magnetic resonance images," *The Journal of Experimental Biology*, no. 201, pp. 63-70, 1998.
- [39] R. M. Erskine, D. A. Jones, C. N. Maganaris and H. Degens, "In vivo specific tension of the human quadriceps femoris muscle," *Eur J Appl Physiol*, no. 106, pp. 827-838, 2009.
- [40] R. J. Maughan, J. S. Watson and J. Weir, "Strength and cross-sectional area of human skeletal muscle," *J. Physiol.*, no. 338, pp. 37-49, 1983.
- [41] T. L. Wickiewicz, R. R. Roy, P. L. Powell and R. V. Edgerton, "Muscle architecture of the human lower limb," *Clinical orthopedics and related research*, no. 179, pp. 275-283, 1983.
- [42] R. D. Sacks and R. R. Roy, "Architecture of the hind limb muscles of cats: Functional significance," *Journal of morphology*, vol. 173, no. 2, pp. 185-195, 1982.
- [43] S. L. Delp, "Surgery Simulation: A Computer Graphics System to Analyze and Design Musculoskeletal Reconstructions of the Lower Limb," Ph.D., Department of Mechanical Engineering, Stanford, CA: Stanford University, 1990.
- [44] M. E. Arnold, R. S. Ward, L. R. Lieber and L. S. Delp, "A Model of the Lower Limb for Analysis of Human Movement," *Annals of Biomedical Engineering*, vol. 38, no. 2, pp. 269-279, 2010.
- [45] T. Fukunaga, R. R. Roy, F. G. Shellock, J. A. Hodgson and V. R. Edgerton, "Specific tension of human plantar flexors and dorsiflexors," *Journal of Applied Physiology*, vol. 80, no. 1, pp. 158-165, 1996.
- [46] P. L. Powell, R. R. Roy, P. Kanim, M. A. Bello and R. V. Edgerton, "Predictability of skeletal muscle tension from architectural determinations in guinea pig hindlimbs," Brain Research Institute and Neuromuscular Research Laboratory, University of California, Los Angeles, 1984.
- [47] M. F. Systems, "MiniTec," [Online]. Available: <http://www.minitecframing.com/index.htm>. [Accessed 09 March 2017].

- [48] M. F. Systems, "Aluminum profile 45 x 45 UL," [Online]. Available: http://www.minitecframing.com/Products/Aluminum_Profiles/Aluminum_Profile_Catalog_Pages/20.1063_Aluminum_Profile_45x45_UL.html. [Accessed 09 March 2017].
- [49] M. F. Systems, "Power lock fastener," [Online]. Available: http://www.minitecframing.com/Products/Profile_Fasteners/T-Slotted_Fastener_Catalog_Pages/21.0818_Power-Lock_SF.html. [Accessed 09 March 2017].
- [50] M. (Estonia), "Minitec Profile Systems," [Online]. Available: <http://www.automation.ee/en/services/minitec-profile-systems>. [Accessed 10 March 2017].
- [51] California Department of Social Services, "California Department of Social Services," [Online]. Available: http://www.cdss.ca.gov/agedblinddisabled/res/VPTC2/11%20Use%20of%20DME%20in%20the%20Home/Types_of_Wheelchairs.pdf#page=2. [Accessed 10 Maarch 2017].
- [52] M. F. Systems, "Roller element," [Online]. Available: http://www.minitecframing.com/Products/Lifting_Sliding_Doors/catalog_pages/21.1782_Roller_Element.html. [Accessed 10 March 2017].
- [53] M. F. Systems, "Slide LWN 32x45-45," [Online]. Available: http://www.minitecframing.com/Products/Linear_System_LG/Catalog_Pages/28.0192_Slide_LWN_32x45-45.html. [Accessed 10 March 2017].
- [54] M. F. Systems, "Angle bracket fixable," [Online]. Available: http://www.minitecframing.com/Products/Hinges_Links/Hinges_Links_Catalog_Pages.html/21.2010_Angle_Bracket_Fixable.html. [Accessed 14 March 2017].
- [55] M. F. Systems, "Angle bracke for floor fastening," [Online]. Available: http://www.minitecframing.com/Products/Floor_Mounting/Floor_Mounting_Catalog_Pages/21.1112_Angle_Bracket_For_Floor_Fastening.html. [Accessed 14 March 2017].
- [56] M. F. Systems, "Leveling foot," [Online]. Available: http://www.minitecframing.com/Products/Leveling_Feet_Mounting_Plates_Casters/Catalog_Pages/Leveling_Feet_PA/21.1872_M10_Plastic_Lev_45mm.html. [Accessed 14 March 2017].
- [57] M. F. Systems, "Shaft 20 mm," [Online]. Available: http://www.minitecframing.com/Products/Linear%20System%20LB/Catalog_Pages/17.1744_Shaft_20.html. [Accessed 14 March 2017].

- [58] M. F. Systems, "Support Bearing," [Online]. Available: http://www.minitecframing.com/Products/Belt_And_Roller_Conveyors/Catalog_Pages/50.0128_Support_Bearing_20.html. [Accessed 14 March 2017].
- [59] n. milk, "GrabCAD," [Online]. Available: <https://grabcad.com/library/wheelchair-10>. [Accessed 14 March 2017].
- [60] A. J. Bennet Wilson and S. R. McFarland, "California Department of Social Services," Reprinted from Wheelchairs: A Prescription Guide, [Online]. Available: http://www.cdss.ca.gov/agedblinddisabled/res/VPTC2/11%20Use%20of%20DME%20in%20the%20Home/Types_of_Wheelchairs.pdf. [Accessed 14 March 2017].
- [61] M. F. Systems, "Slide LR6 Compact," [Online]. Available: http://www.minitecframing.com/Products/Linear%20System%20LR/Catalog_Pages/28.0140_Slide_LR6_Compact.html. [Accessed 14 March 2017].
- [62] M. F. Systems, "Rail LR6 Compact," [Online]. Available: http://www.minitecframing.com/Products/Linear%20System%20LR/Catalog_Pages/28.0119_Rail_LR6_Compact.html. [Accessed 14 March 2017].
- [63] MiniTec Framing Systems, "Door Hinge Small," [Online]. Available: http://www.minitecframing.com/Products/Hinges_Links/Hinges_Links_Catalog_Pages.html/21.0973_Door_Hinge_Small.html. [Accessed 27 April 2017].
- [64] A. V. Hill, "The heat of shortening and dynamics constants of muscles," *Proc. R. Soc. Lond.*, no. 126(843), pp. 136-195, 1938.
- [65] Y.-C. Fung, "Biomechanics: Mechanical Properties of Living Tissues," *Springer-Verlag*, p. 568, 1993.
- [66] H. S. Milner-Brown, "The elderly recruitment of human motor units during voluntary isometric contractions," *J. Physiol.*, no. 230, pp. 359-370, 1973.
- [67] Parker motion, "The Straight Story on Linear Actuators," [Online]. Available: <http://www.parkermotion.com/bbs/newsletter/AW0308/LinearActuators.pdf>. [Accessed 07 April 2017].
- [68] Progressive Automations, "Progressive Automations," [Online]. Available: <https://www.progressiveautomations.com/>. [Accessed 08 April 2017].
- [69] Progressive Automations, "Track Linear Actuator," [Online]. Available: <https://www.progressiveautomations.com/track-linear-actuator>. [Accessed 08 April 2017].
- [70] Progressive Automations, "Technical specifications," [Online]. Available: https://www.progressiveautomations.com/media/catalog/pdf/Track_Actuator_PA-18.pdf#page=2. [Accessed 08 April 2017].

- [71] Progressive Automations, "DC Speed Controller for Electric Actuators," [Online]. Available: <https://www.progressiveautomations.com/ac-14>. [Accessed 08 April 2017].
- [72] Progressive Automations, "Rocker Switch Momentary," [Online]. Available: <https://www.progressiveautomations.com/rc-03>. [Accessed 08 April 2017].
- [73] Progressive Automations, "Relay 12 VDC DPDT," [Online]. Available: <https://www.progressiveautomations.com/ac-22>. [Accessed 08 April 2017].
- [74] Progressive Automations, "Power Supply - 120-220 VAC - 12 VDC - 25A," [Online]. Available: <https://www.progressiveautomations.com/ps-11>. [Accessed 08 April 2017].
- [75] Progressive Automations, "Wiring Kit," [Online]. Available: <https://www.progressiveautomations.com/ac-17>. [Accessed 08 April 2017].
- [76] Progressive Automations, "Wiring diagram for speed control," [Online]. Available: <https://www.progressiveautomations.com/media/catalog/pdf/DC%20Speed%20Controller%20One%20Direction%20Wiring%20Diagram.pdf>. [Accessed 08 April 2017].
- [77] Progressive Automations, "Push Button External Limit Switch," [Online]. Available: <https://www.progressiveautomations.com/ac-24>. [Accessed 08 April 2017].
- [78] Progressive Automations, "110 VAC - 12 VDC Control Box - 2 Channels," [Online]. Available: <https://www.progressiveautomations.com/pa-22>. [Accessed 08 April 2017].
- [79] Progressive Automations, "12 VDC - Synchronized Dual Hall Effect Actuator Contro," [Online]. Available: <https://www.progressiveautomations.com/pa-40>. [Accessed 08 April 2017].
- [80] T. Instruments, "MSP430 LaunchPad Value Line Development kit," [Online]. Available: <http://www.ti.com/tool/MSP-EXP430G2#1>. [Accessed 04 April 2017].
- [81] Newport, "Low Noise Air Compressor, 3.5 Liter Capacity, 220 VAC," [Online]. Available: <https://www.newport.com/p/ACGP-02#>. [Accessed 04 April 2017].
- [82] Festo, "Linear drives DGC-K," [Online]. Available: https://www.festo.com/cat/en-gb_gb/data/doc_ENGB/PDF/EN/DGC-K_EN.PDF. [Accessed 04 April 2017].
- [83] Ebay.com, "FESTO DGC-K-25-450-PPV-A-GK 450MM 25MM RODLESS PNEUMATIC CYLINDER D551947," [Online]. Available: <http://www.ebay.com/itm/FESTO-DGC-K-25-450-PPV-A-GK-450MM-25MM-RODLESS-PNEUMATIC-CYLINDER-D551947-/381977059848?hash=item58ef9b6208>. [Accessed 04 April 2017].
- [84] plccenter.co.uk, "Festo DGC-K-25-250-PPV-A-GK," [Online]. Available: <http://www.plccenter.co.uk/Buy/FESTO%20ELECTRIC/DGCK25250PPVAGK?redirect=true>. [Accessed 04 April 2017].

- [85] T.-O.-M. Inc., "BC2 repair sect 01," [Online]. Available: <https://www.youtube.com/watch?v=YDhZsEfUtj4>. [Accessed 04 April 2017].
- [86] Parker, "Rodless Pneumatic Cylinders Magnetically Coupled," [Online]. Available: <http://www.seall.cz/uploads/files/linearni-bezpistnicove-pneumaticke-valce-s-magnetickym-prenosem-serie-p1z/parker-pneumatic-p1z-rodless-cylinders-pde2522tcuk-pdf.pdf#page=21>. [Accessed 04 April 2017].
- [87] Ebay.co.uk, "Speed Control Valve Push to Connect One Touch Air Fitting," [Online]. Available: <http://www.ebay.co.uk/itm/3-8-OD-x-1-2-90-Speed-Control-Valve-Push-to-Connect-One-Touch-Air-Fitting-/232059342887?var=&hash=item3607d09027:m:mrACub0mWa-jKQ8aSWIjoFg>. [Accessed 04 April 2017].
- [88] Ebay.co.uk, "Electrical Solenoid Pneumatic Air Control," [Online]. Available: <http://www.ebay.co.uk/itm/12V-24V-220V-5-Way-2-Position-1-4-1-8-Solenoid-Valve-Pneumatic-Air-Control-/162216028156?var=&hash=item25c4d427fc:m:mb5kJOAMRboIkvzvPpz-65Q>. [Accessed 04 April 2017].
- [89] Ebay.co.uk, "Manual Lever Pneumatic Air Control," [Online]. Available: <http://www.ebay.co.uk/itm/1-4-Bsp-5-3-Manual-Lever-Lever-Valve-Sealed-Mid-Position-HUK-/132076851619?hash=item1ec064d1a3:g:xAIAAOsw9GhYiIYo>. [Accessed 04 April 2017].
- [90] FrightProps, "How to Control the Speed of a Pneumatic Cylinder," [Online]. Available: <https://www.youtube.com/watch?v=cYBIq74IikE>. [Accessed 18 May 2017].
- [91] W. Parandyk, M. Ludwicki, B. Zagrodny and J. Awrejcewicz, "The Positioning of Systems Powered by McKibben Type Muscles," *Advances in Intelligent Systems and Computing*, no. 317, pp. 133-140, 2015.
- [92] Ebay.co.uk, "Geared 4 phase Stepper Motor with Driver Board," [Online]. Available: http://www.ebay.co.uk/itm/Geared-4-phase-Stepper-Motor-with-Driver-Board-28BYJ-48-ULN2003-x1-x2-x5-/121679687346?var=&hash=item1c54acaeb2:m:mPGg5Uah-Vsqkha_W4HpcVw. [Accessed 04 April 2017].
- [93] J. Fernández de Cañete, C. Galindo and I. García Moral, "System Engineering and Automation," in *System Engineering*, Málaga, Springer-Verlag Berlin Heidelberg, 2011, p. 245.
- [94] adafruit.com, "Adafruit VL53L0X Time of Flight Distance Sensor," [Online]. Available: <https://www.adafruit.com/product/3317>. [Accessed 05 May 2017].

- [95] adafruit.com, "Lithium Ion Polymer Battery - 3.7v 150mAh," [Online]. Available: <https://www.adafruit.com/product/1317>. [Accessed 05 May 2017].
- [96] autokalagoen.no, "Valeo 533 serien," [Online]. Available: http://www.autokatalogen.no/wls/view_article_info.do?articleIdNo=1774978&nodeIdNo=2941794. [Accessed 05 May 2017].
- [97] adafruit.com, "Lithium Ion Battery Pack - 3.7V 6600mAh," [Online]. Available: <https://www.adafruit.com/product/353>. [Accessed 05 May 2017].
- [98] ebay.com, "12 V -> 3 V voltage converter," [Online]. Available: <http://www.ebay.com/itm/Waterproof-DC-DC-Converter-12V-Step-Down-to-3V-3A-15W-Power-Supply-Module-New-/122033281687>. [Accessed 09 May 2017].
- [99] store.ti.com, "MSP-EXP430G2-MSP430 LaunchPad Value Line Development kit," [Online]. Available: <https://store.ti.com/ProductAccessories.aspx?ProductId=2031>. [Accessed 06 May 2017].
- [100] dim.molle.com, "Spring T32860," [Online]. Available: <http://dim.molle.com/dettagli.asp?id=2137>. [Accessed 06 May 2017].
- [101] Unbrako, "Unbrako fasteners price list," [Online]. Available: <http://www.ubk.it/unbrakopricelisteuro.pdf>. [Accessed 06 May 2017].
- [102] powerstream.com, "12 V -> 3 V voltage converter," [Online]. Available: <http://www.powerstream.com/dc6.htm>. [Accessed 06 May 2017].
- [103] powerstream.com, "3V -> 12V voltage converter," [Online]. Available: <http://www.powerstream.com/Product9.htm>. [Accessed 06 May 2017].

Appendix 1
Approximate estimated cost of standard parts of the project

#	Name	Price per unit, €	Units needed	Total price, €
Minitec Estonia standard parts				
1	Profile 45x45 UL20.1063/0	12,15 / m	15,755 m	191,5
2	Angle 45x90 GD-Z21.1397/0	4,9 / pc	4 pcs	19,6
3	Angle-bracket for floor fastening ST 21.1112/0	7,55 / pc	8 pcs	60,4
4	Support bearing 20 50.0128/0	11,65 / pc	4 pcs	46,6
5	Shaft Ø 20 mm 17.1744/0	11,48 / m	1,74 m	19,98
6	Power lock fastener 45 SF 21.0818/0	2,85 / pc	22 pcs	62,7
7	End cap 45x45 Z grey 22.1004/1	0,62 / pc	6 pcs	3,72
8	Foot M08 D 45 21.1871/0	4,4 / pc	2 pcs	8,8
9	Square nut M8 galvanized 21.1351/0	0,26 / pc	22 pcs	5,72
10	Angle bracket fixable 21.2010/0	20,15 / pc	2 pcs	40,3
11	Door hinge small 21.0973/0	14,65 / pc	1 pc	14,65
12	Roller element 21.1782/0	5,05 / pc	4 pcs	20,2
13	Slide LWN 32x45-45 28.0192/0	41,3 / pc	1 pc	41,3
14	Hex socket cap screw M8x16 galvanized 21.1200/0	0,13 / pc	2 pcs	0,26
15	Square nut M6 galvanized 21.1330/0	0,26 / pc	8 pcs	2,08
			Total	537,81
Progressive Automations electrical parts				
16	Linear actuator PA-18-24-450	176 / pc	2 psc	352
17	Rocker switch RC-03	17 / pc	1 pc	17
18	Relay AC-22	16 / pc	2 pcs	32
19	Power supply PS-11	81 / pc	1 pc	81
20	Wiring kit AC-17	28 / kit	1 kit	28
21	Shipping from US			-
			Total	510+shipping
Intellectual work (one time investment)				
22	Creating of program algorithm for microcontroller MSP 430	30 / hr	40 hrs	1200
23	Creating of mathematical and physical models	30 / hr	40 hrs	1200
			Total	2400
Valeo [96] (for reference only)				
24	NC switch Valeo serien 533 S533000	6,32 / pc	1 pc	6,32
			Total	6,32

3d party fasteners [101] (for reference only)				
25	DIN 912 M2,5x18	53,8 / 200 pcs	2 pcs	53,8
26	DIN 912 M6x18	6,6 / 200 pcs	8 pcs	6,6
27	DIN 912 M6x40	10,15 / 200 pcs	8 pcs	10,15
28	DIN 912 M8x20	10,68 / 200 pcs	20 pcs	10,68
29	DIN 912 M8x40	17,50 / 200 pcs	6 pcs	17,50
30	DIN 912 M10x65	38,50 / 200 pcs	2 pcs	38,50
31	DIN 912 M10x130	84 / 200 pcs	4 pcs	84
32	DIN 125A M6	30,24 / 200 pcs	16 pcs	30,24
33	DIN 125-1A M8	32,13 / 200 pcs	28 pcs	32,13
34	DIN 125 M10	37,80 / 200 pcs	4 pcs	37,80
35	DIN 934 M2,5	-	2 pcs	-
36	DIN 934 M6	11,41 / 200 pcs	4 pcs	11,41
37	DIN 934 M8	17,15 / 200 pcs	2 pcs	17,15
38	DIN 934 M10	25,90 / 200 pcs	6 pcs	25,90
			Total	375,86

Electronics

39	Texas Instruments Launchpad MSP 430 [80]	9 / pc	1 pc	9
40	Voltage converter 12 – 3 V [102]	18,95 / pc	1 pc	18,95
41	Voltage converter 3 - 12 V [103]	24,5 / pc	1 pc	24,5
42	Sensor Adafruit VL53LOX	13,6 / pc	1 pc	13,6
43	Adafruit battery pack 150 mAh	5,4 / pc	1 pc	5,4
44	Shipping from US			-
			Total	71,45+ shipping

Custom parts and processing (available on demand from concrete vendor)

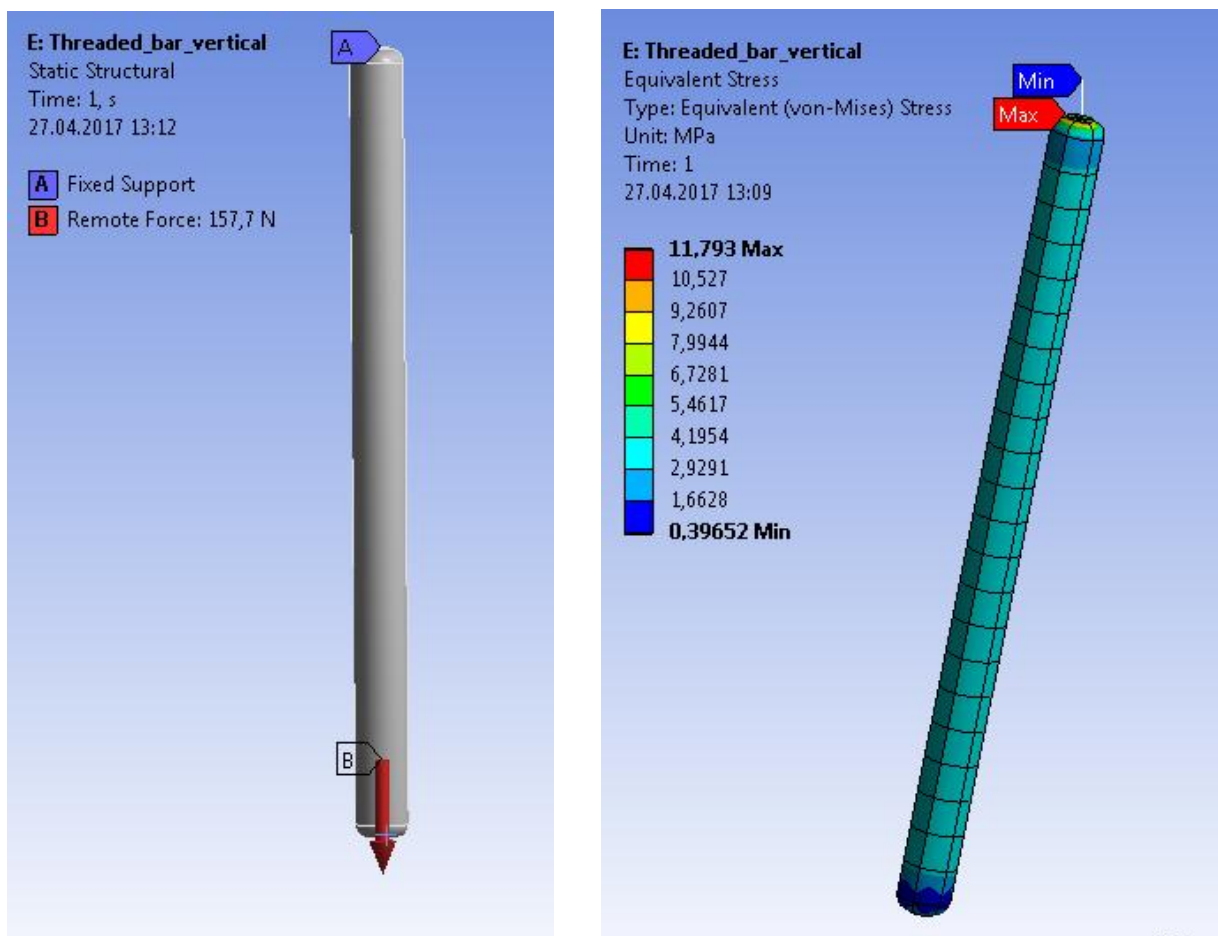
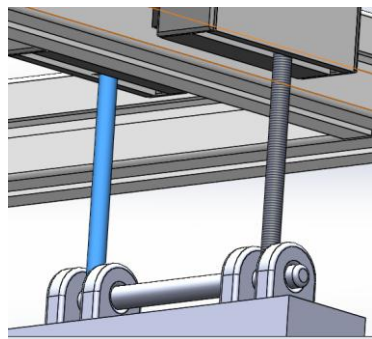
45	Plastic 3D printing (ABS)	-	-	-
46	Rubber 3D printing (Shore 27A)	-	-	-
47	Milled and welded aluminum slab	-	-	-
48	Plasma cut steel alloy sheet metal	-	-	-
49	Drilled steel bar 8x140	-	1 pc	-
50	Threaded steel bar 8x119	-	2 pcs	-
51	Milled steel bar 12x305	-	2 pcs	-
			Total	-

Extension spring (for reference only)

52	T32860 [100]	7,35 / pc	4 pcs	29,4
----	--------------	-----------	-------	------

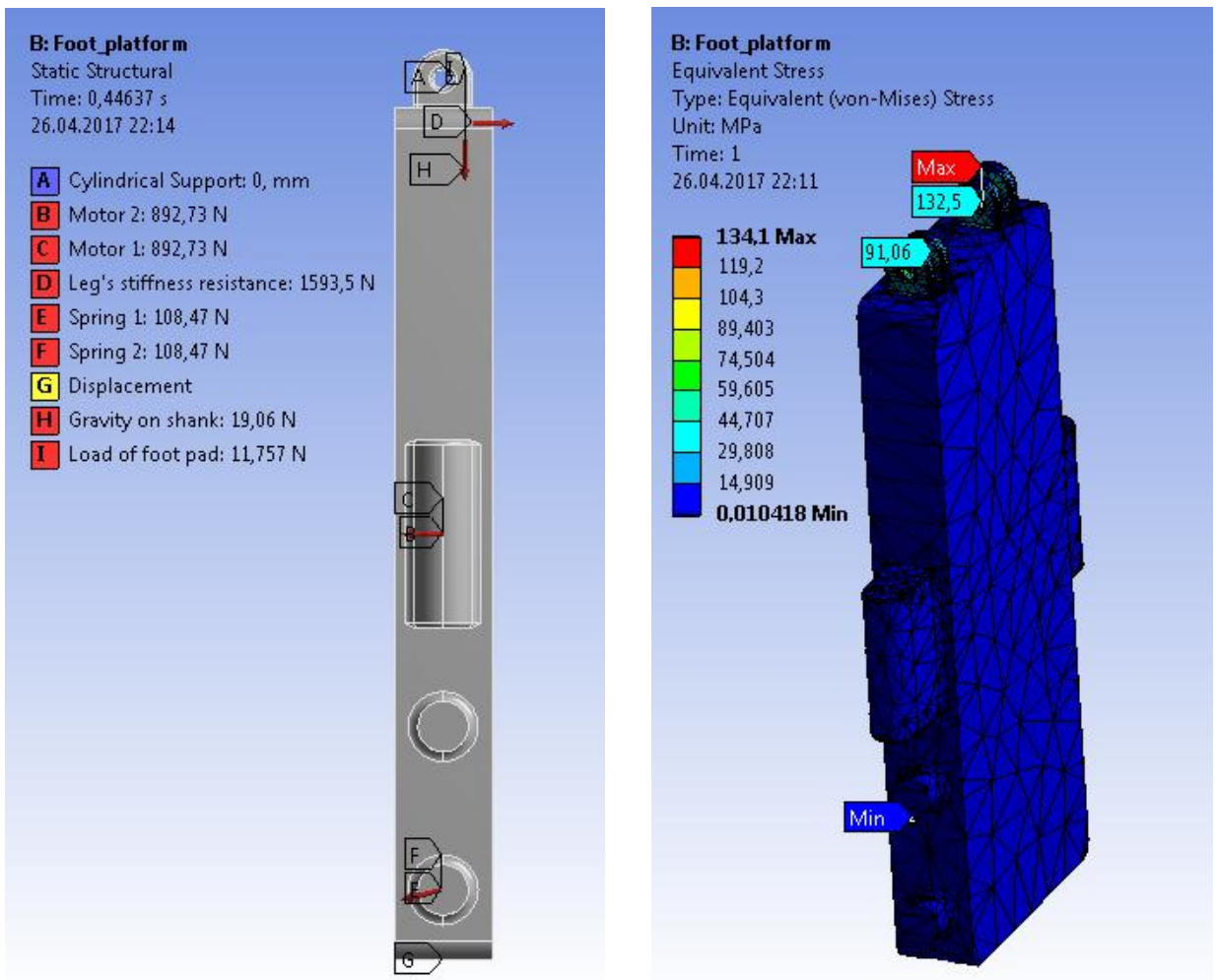
			Total	29,4
			Grand total	3930,84

Threaded bar force distribution and equivalent stress



The ultimate tensile strength for given steel alloy is 723,83 MPa.

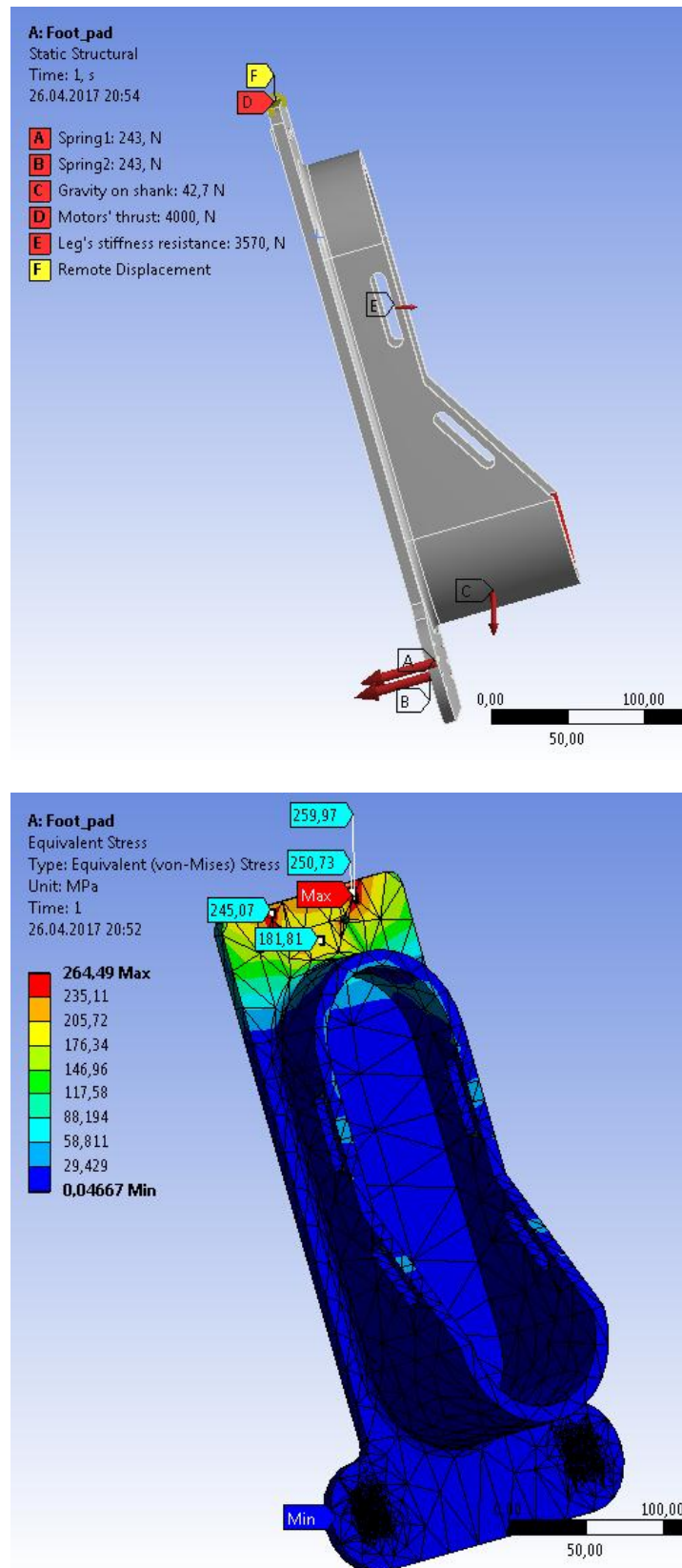
Foot platform force distribution and equivalent stress



The ultimate tensile strength for aluminum alloy 6061-T6 (SS) is 310 MPa.

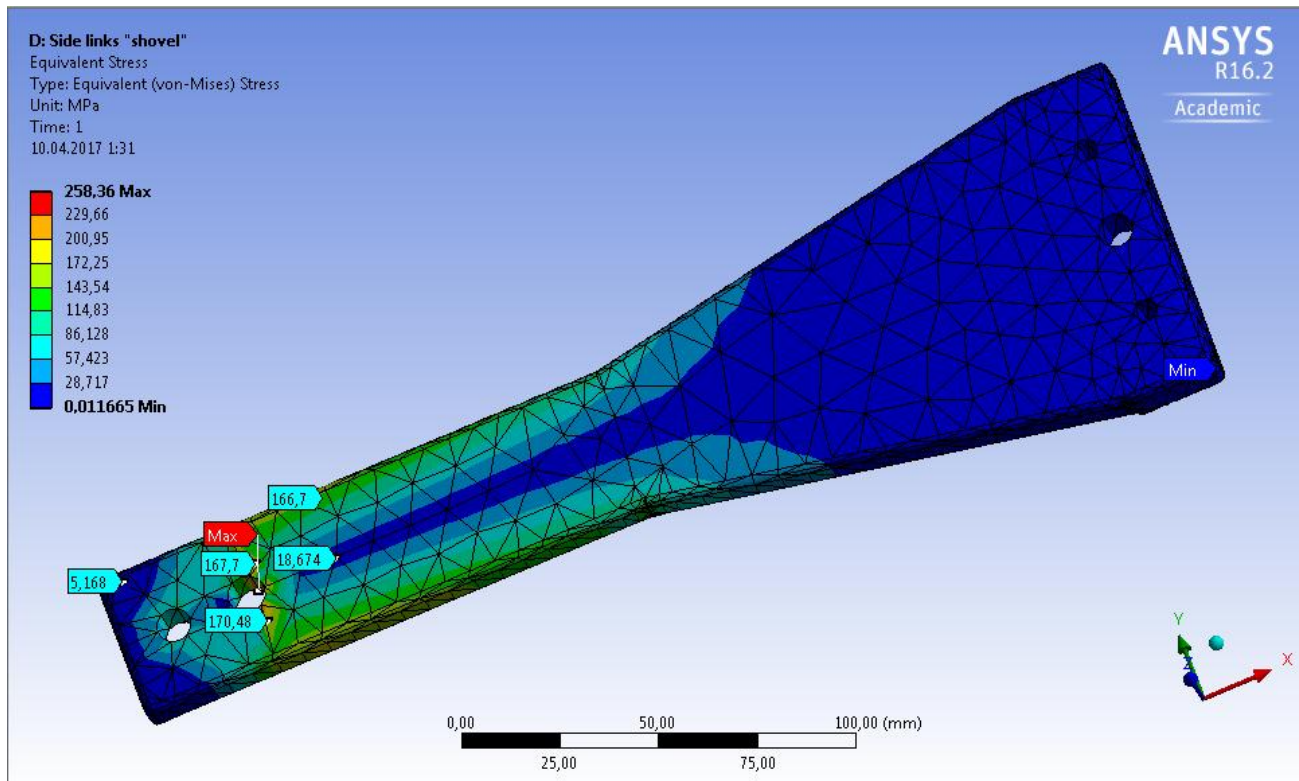
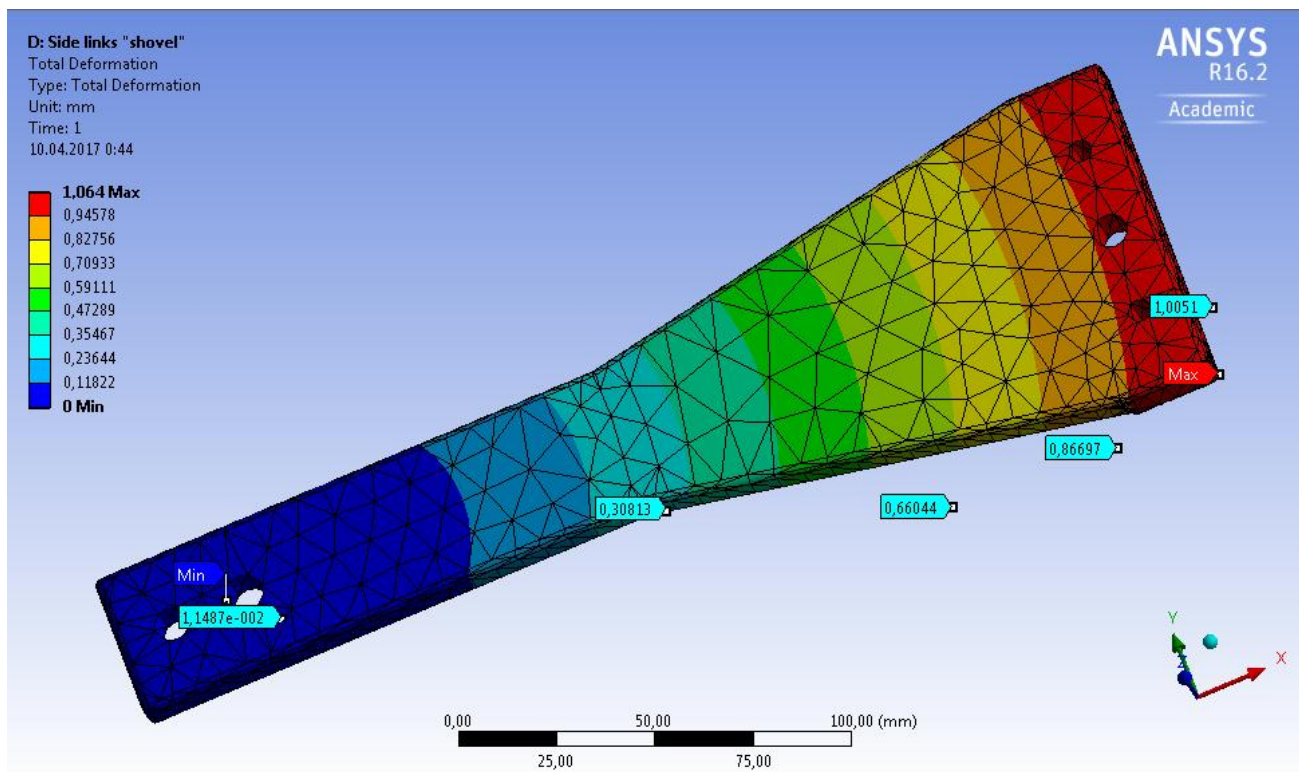
Because of restrictions of academical version of Ansys Workbench, the geometry of the model had to be simplified. Specifically, perforations across the whole area of the platform were suppressed to decreased the amount of nodes in mesh model.

Moving foot pad force distribution and equivalent stress



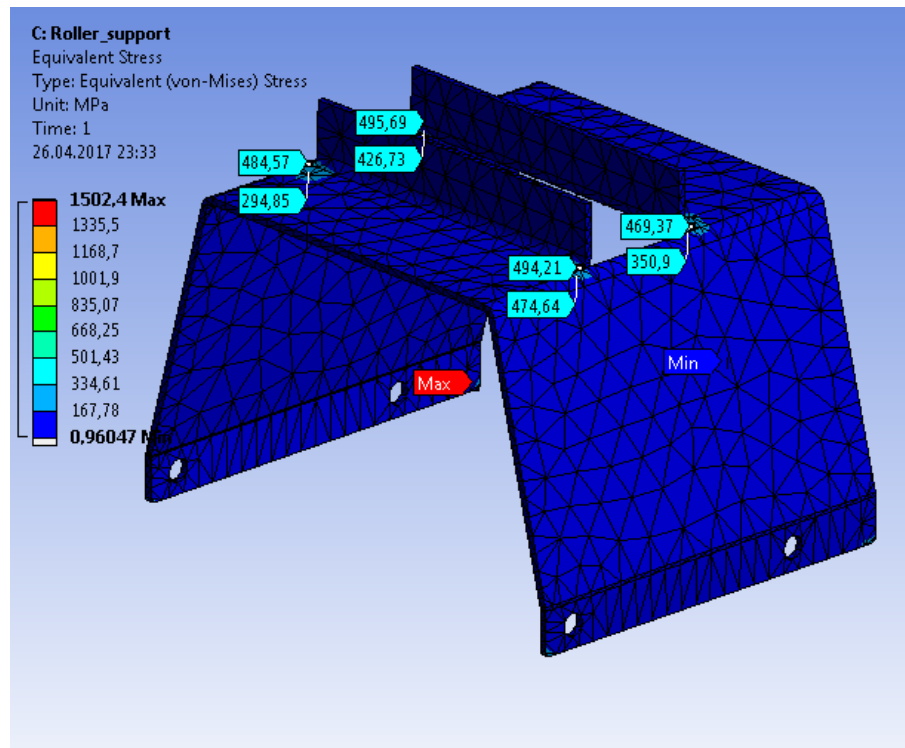
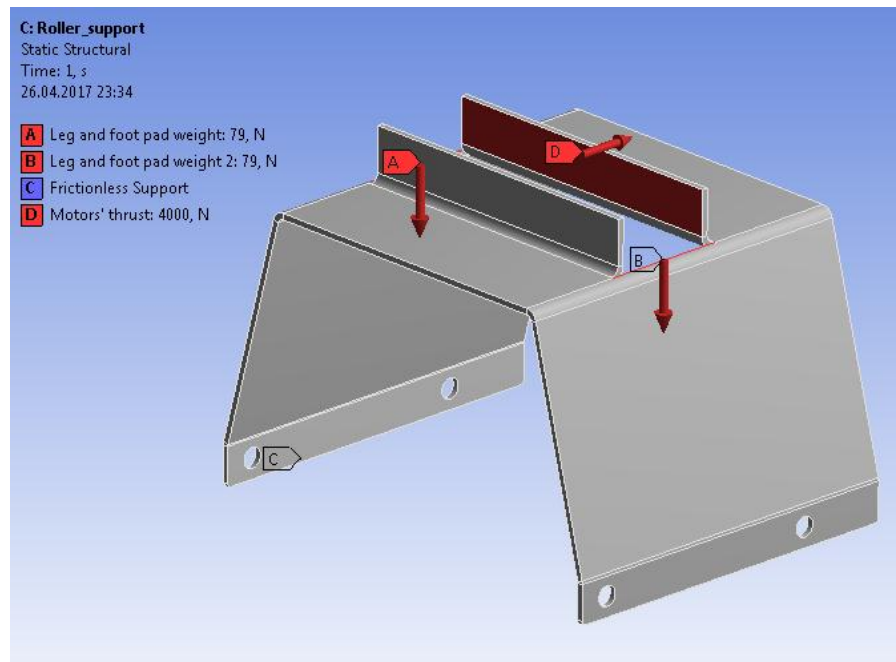
The ultimate tensile strength for aluminum alloy 6061-T6 (SS) is 310 MPa.

Connecting link total deformation and equivalent stress



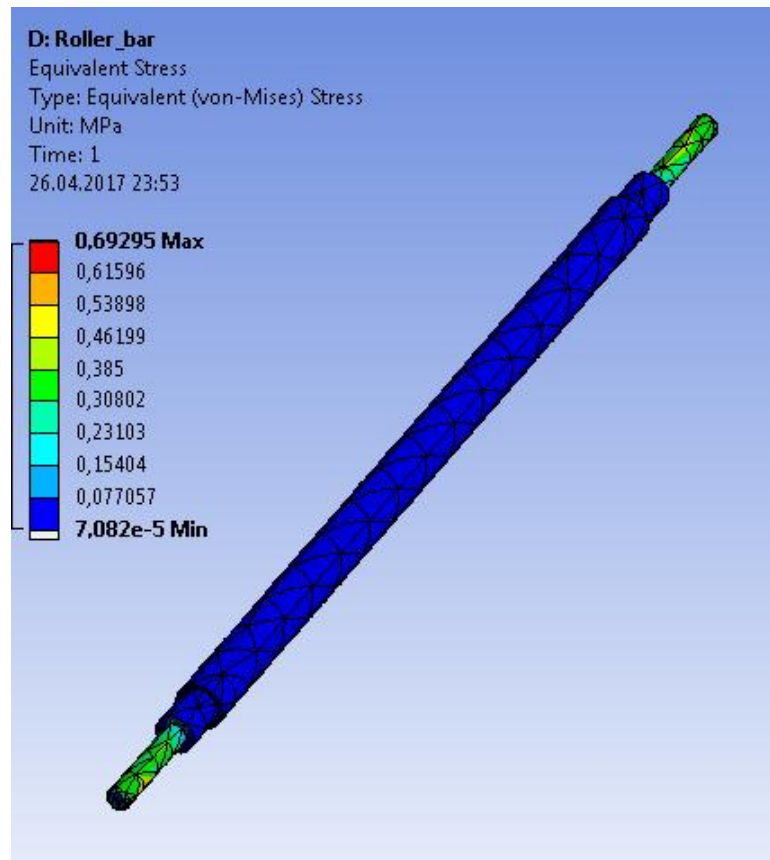
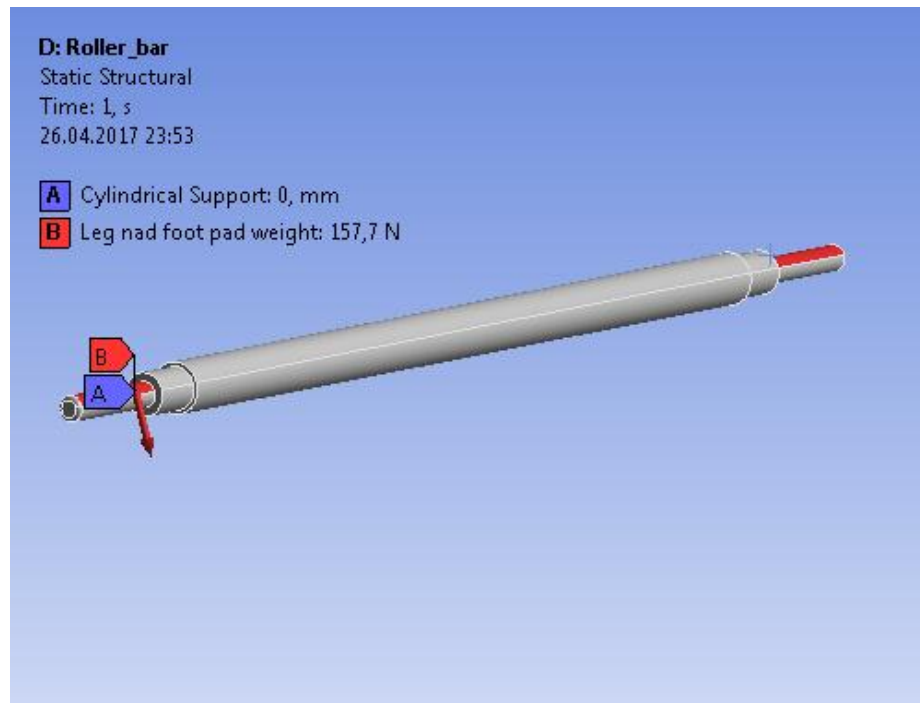
The ultimate tensile strength for given steel alloy is 723,83 MPa.

Base support force distribution and equivalent stress



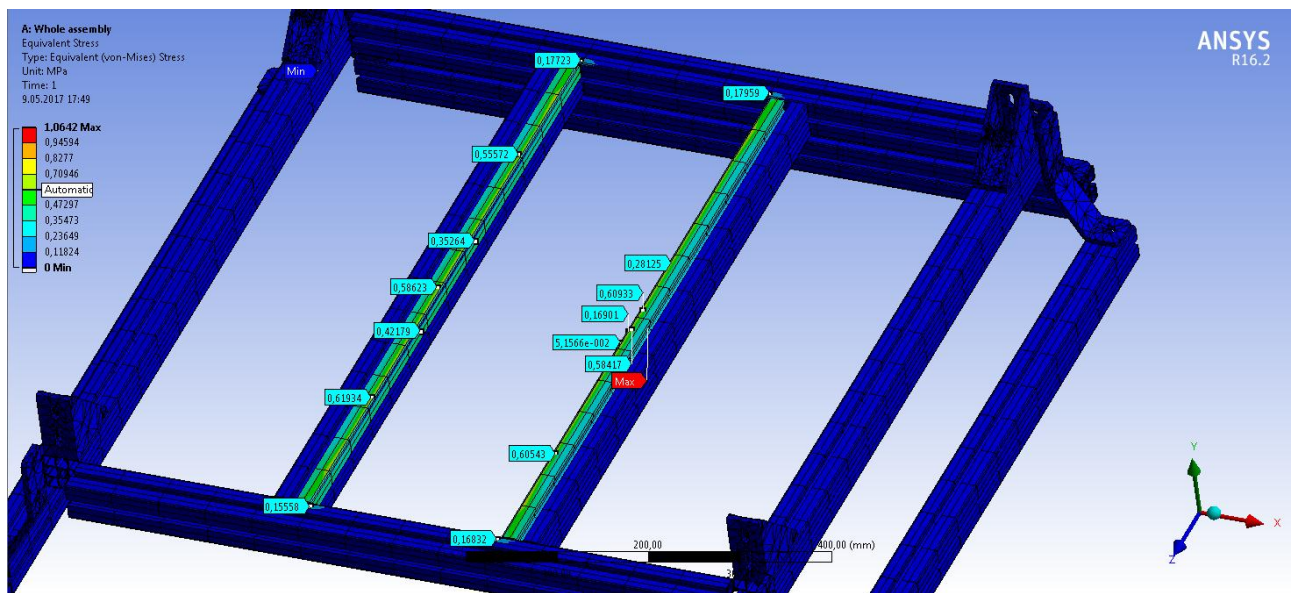
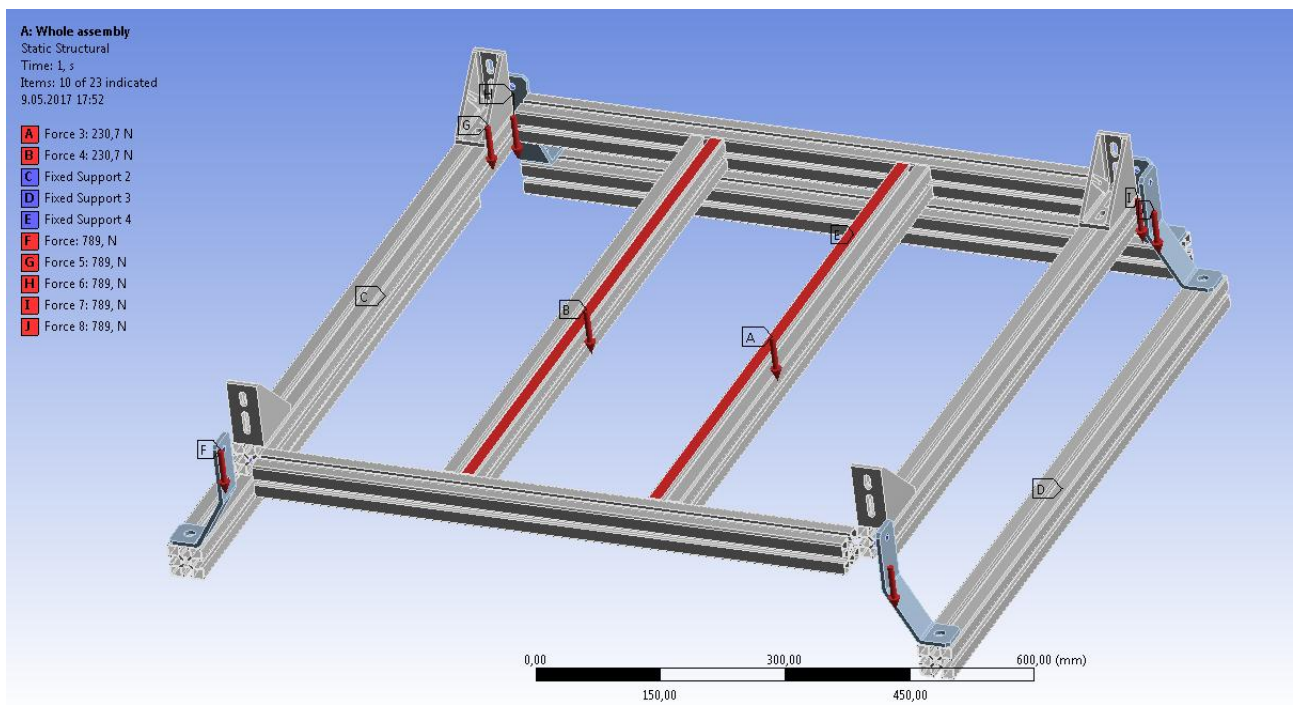
The ultimate tensile strength for given steel alloy is 723,83 MPa. In critical places stress stays within boundaries.

Base support axis force distribution and equivalent stress



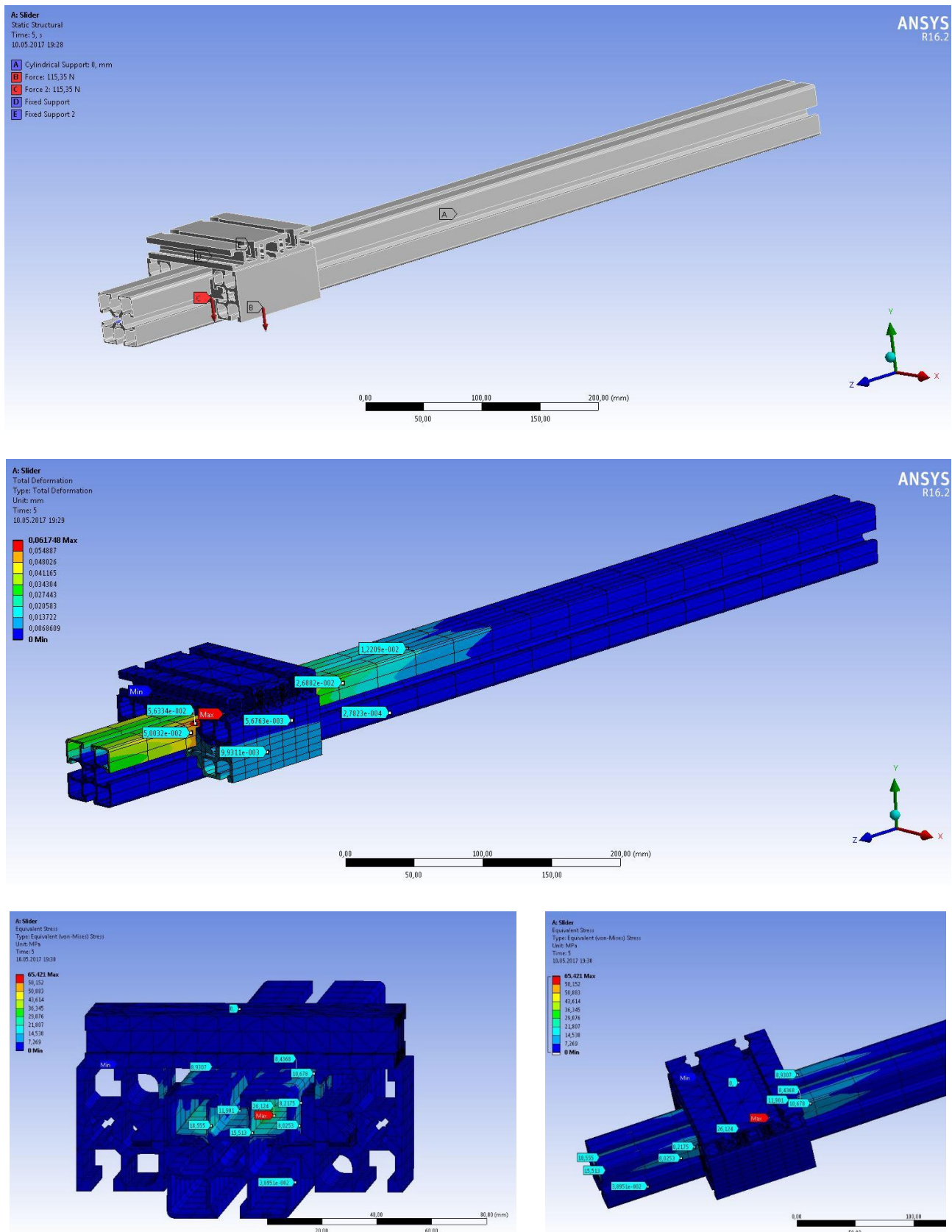
The ultimate tensile strength for given steel alloy is 723,83 MPa.

Base of frame force distribution and equivalent stress



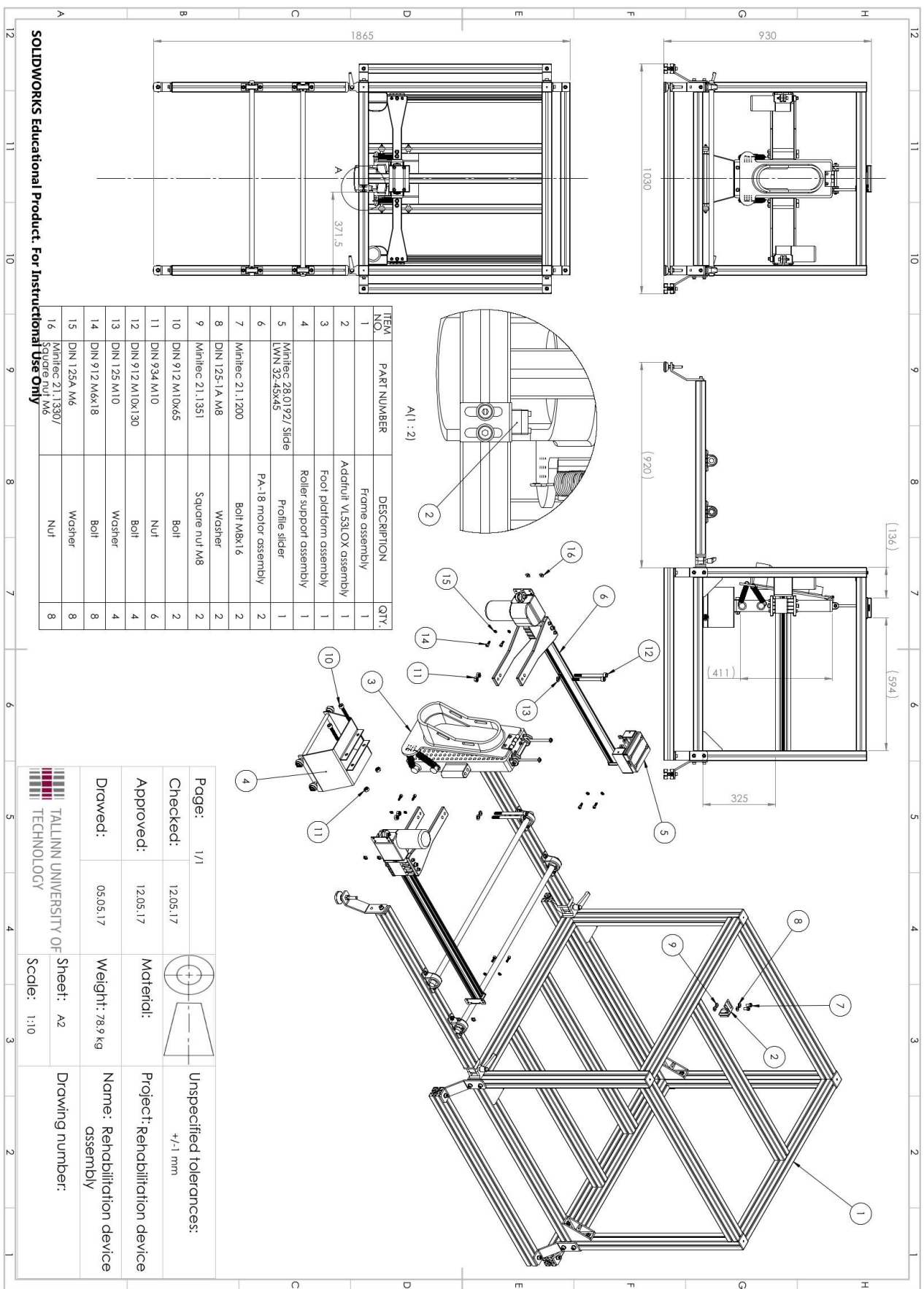
The ultimate tensile strength for given aluminum alloy is 310 MPa.

Upper slider with aluminum profile force distribution, total deformation and equivalent stress

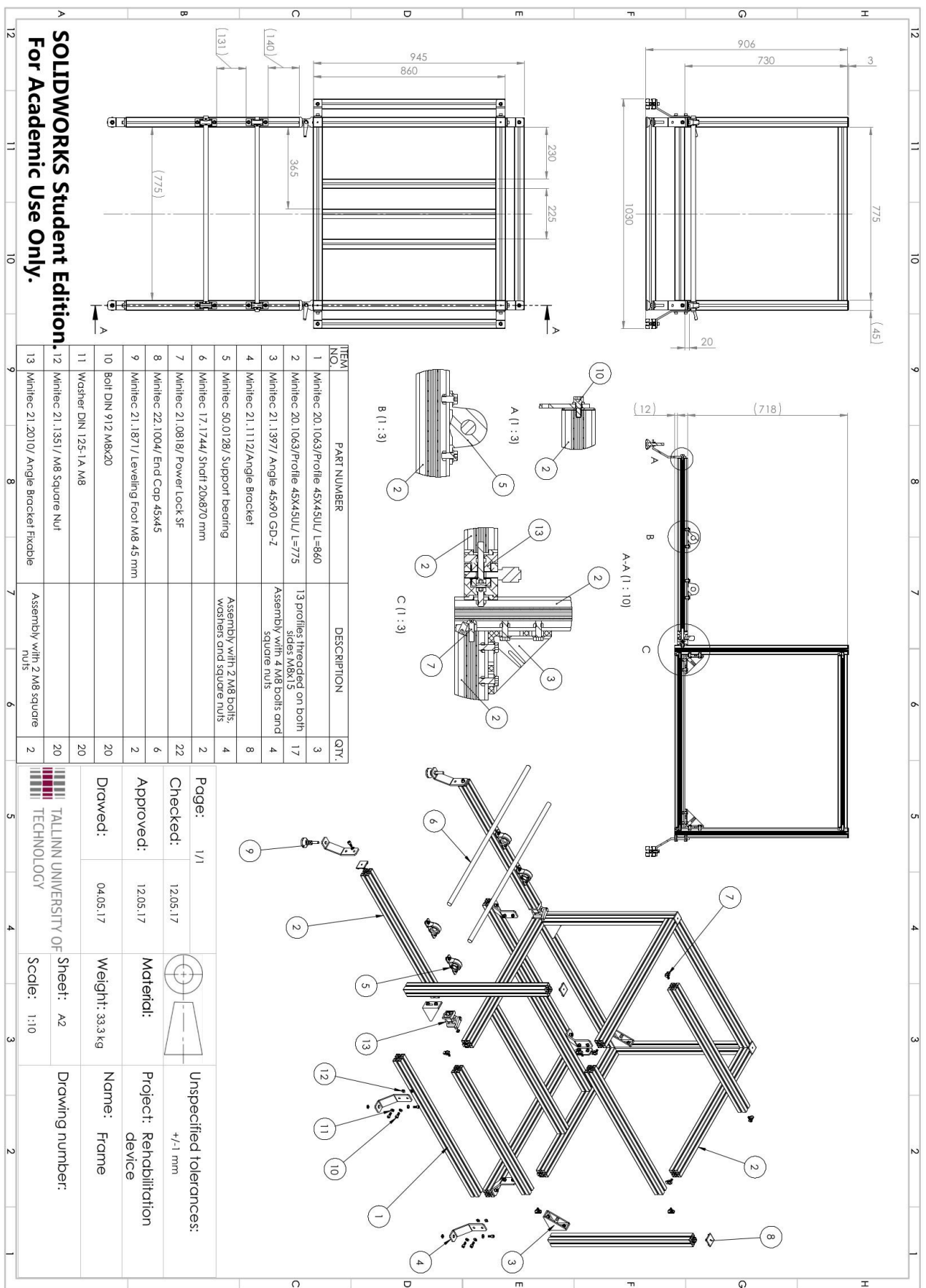


The ultimate tensile strength for given aluminum alloy is 310 MPa.

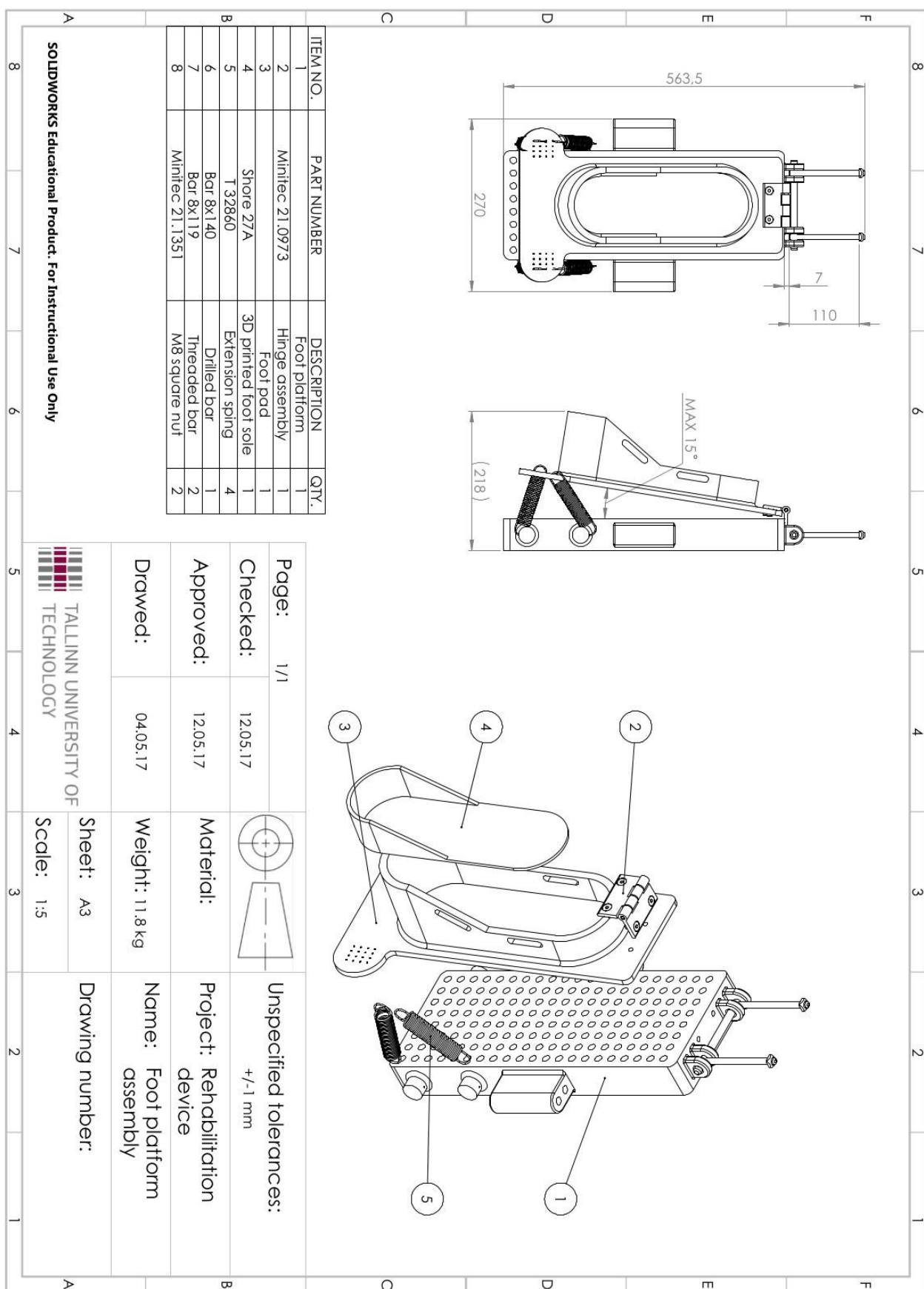
Assembly drawing of the whole system



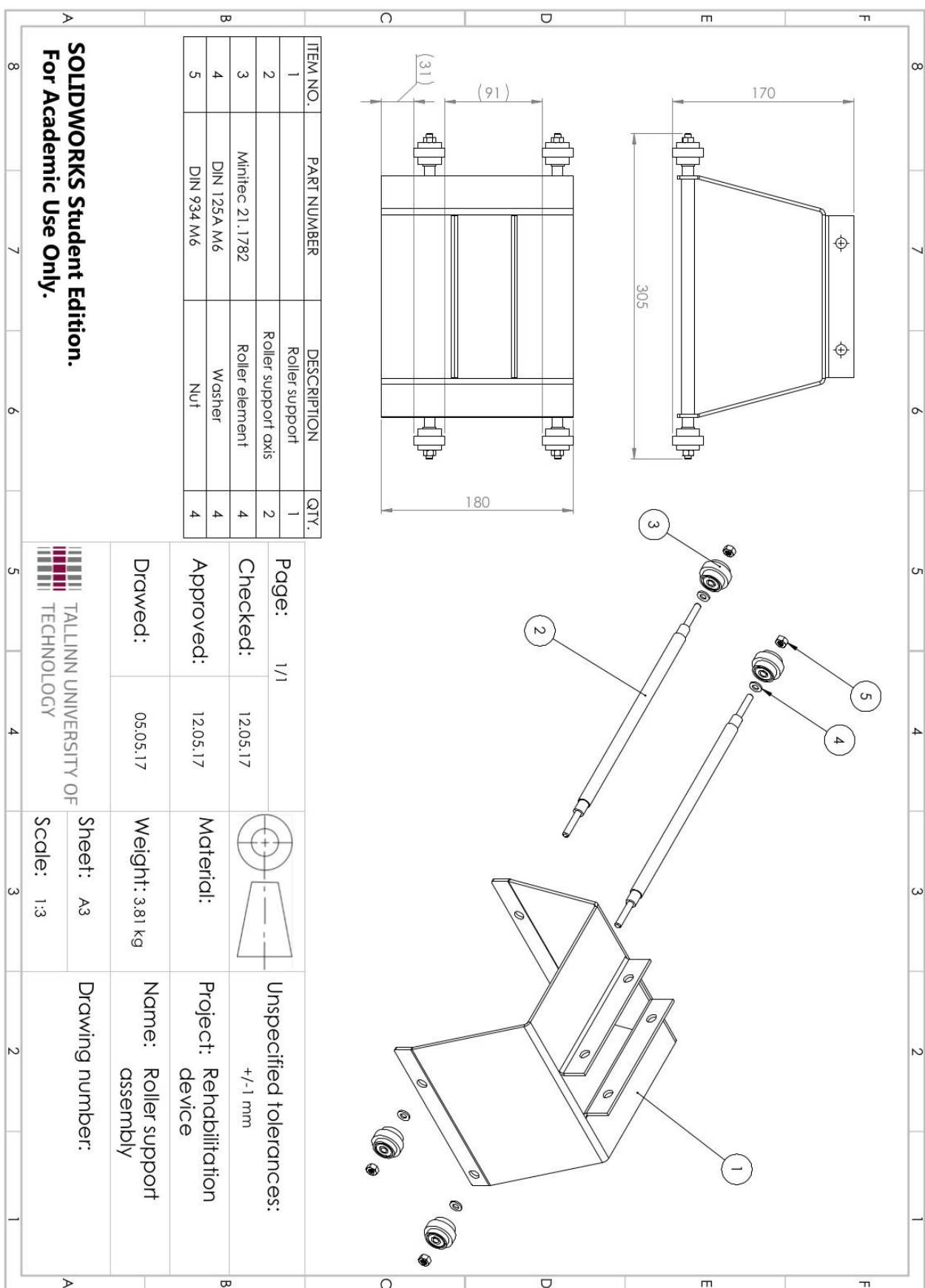
Assembly drawing of the frame



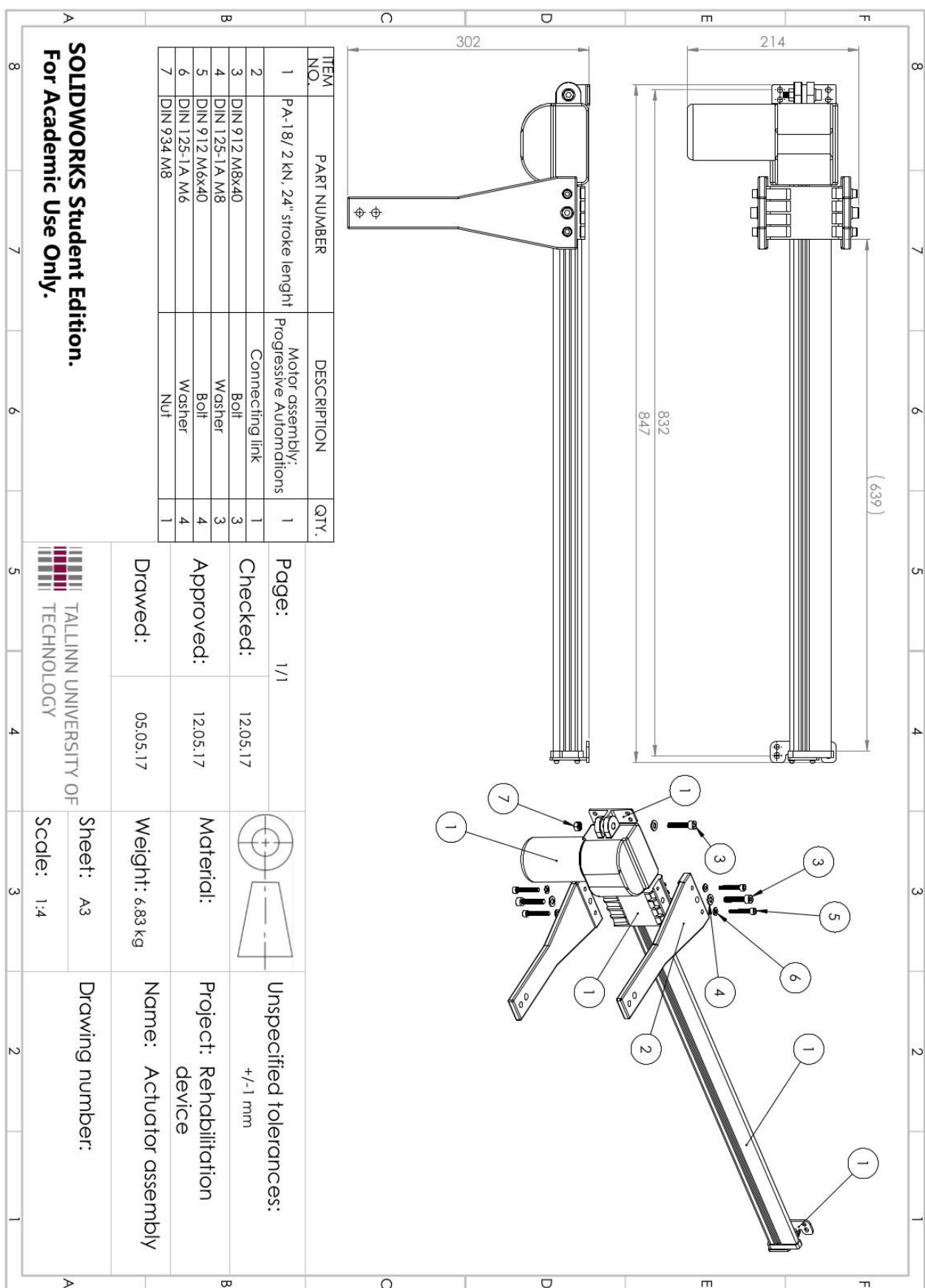
Assembly drawing of the foot platform



Assembly drawing of the roller support



Assembly drawing of the actuating equipment



SOLIDWORKS Student Edition
For Academic Use Only.

Assembly drawing of the position sensor and its enclosure

Front View Dimensions:

- Width: 63 mm
- Height: 35 mm
- Depth: 15 mm
- Base width: 49 mm
- Base height: 6 mm

Rear View Exploded View:

The drawing shows the rear view of the device assembly with callouts numbered 1 through 7, corresponding to the parts listed in the bill of materials.

Bill of Materials (BOM) - Part A:

ITEM NO.	PART NUMBER	DESCRIPTION	QTY.
1		Enclose base; 3D printed	1
2		Enclosure cover; 3D printed	1
3	DIN 934 M2.5	Nut	2
4		Sensor mounting bracket	1
5	Adafruit VL53L0X	Position sensor	1
6	Adafruit 3.7 V 150 mAh	Battery pack	1
7	DIN 912 M2.5x18	Bolt	2

Page: 1/1 **Checked:** 12.05.17 **Material:** Project: Rehabilitation device

Unspecified tolerances: $+/-1$ mm

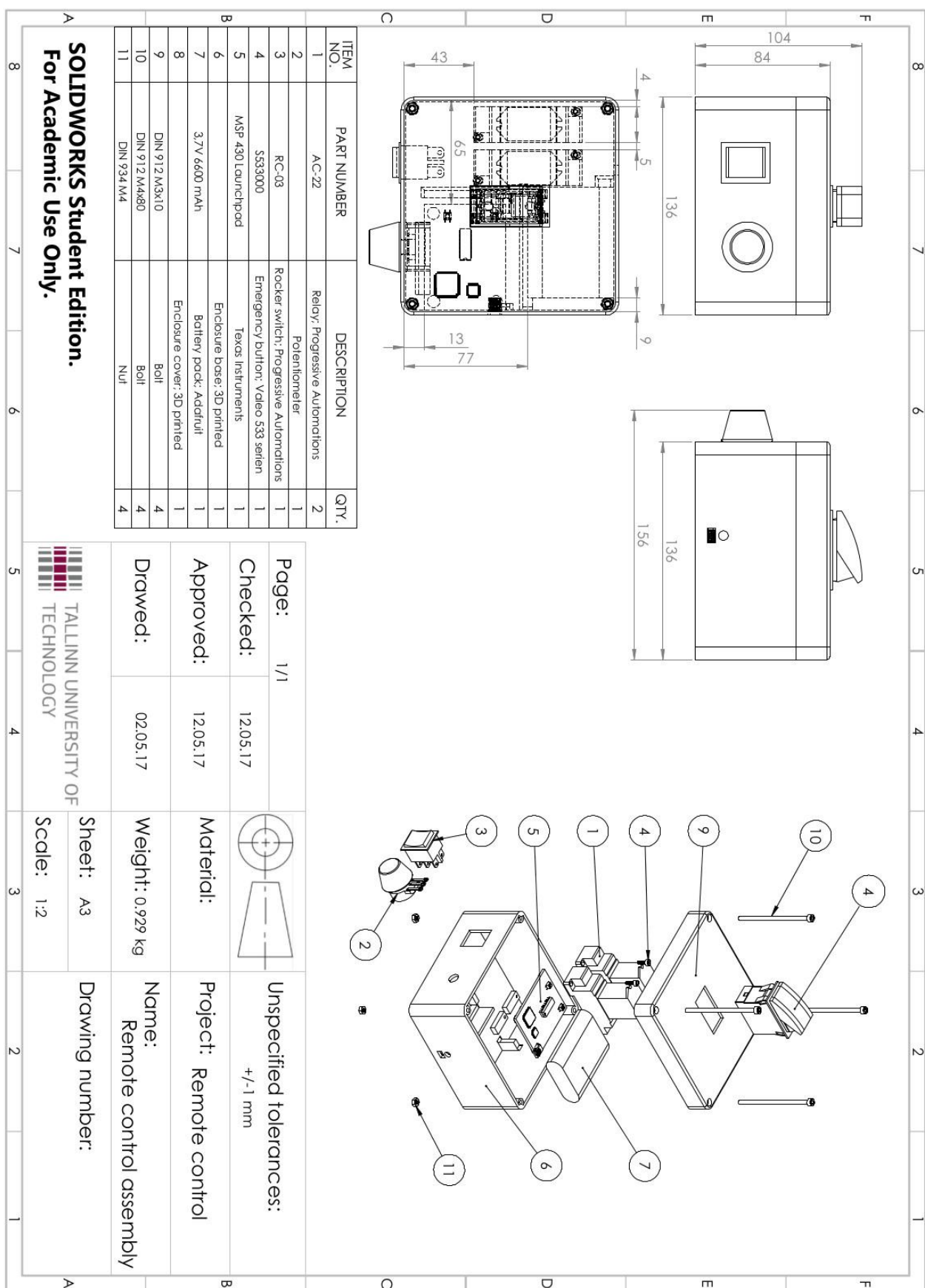
Approved: 12.05.17 **Drawn:** 03.05.17 **Weight:** 0.035 kg **Name:** Adafruit VL53L0X assembly

Sheet: A3 **Scale:** 1:1 **Drawing number:** A

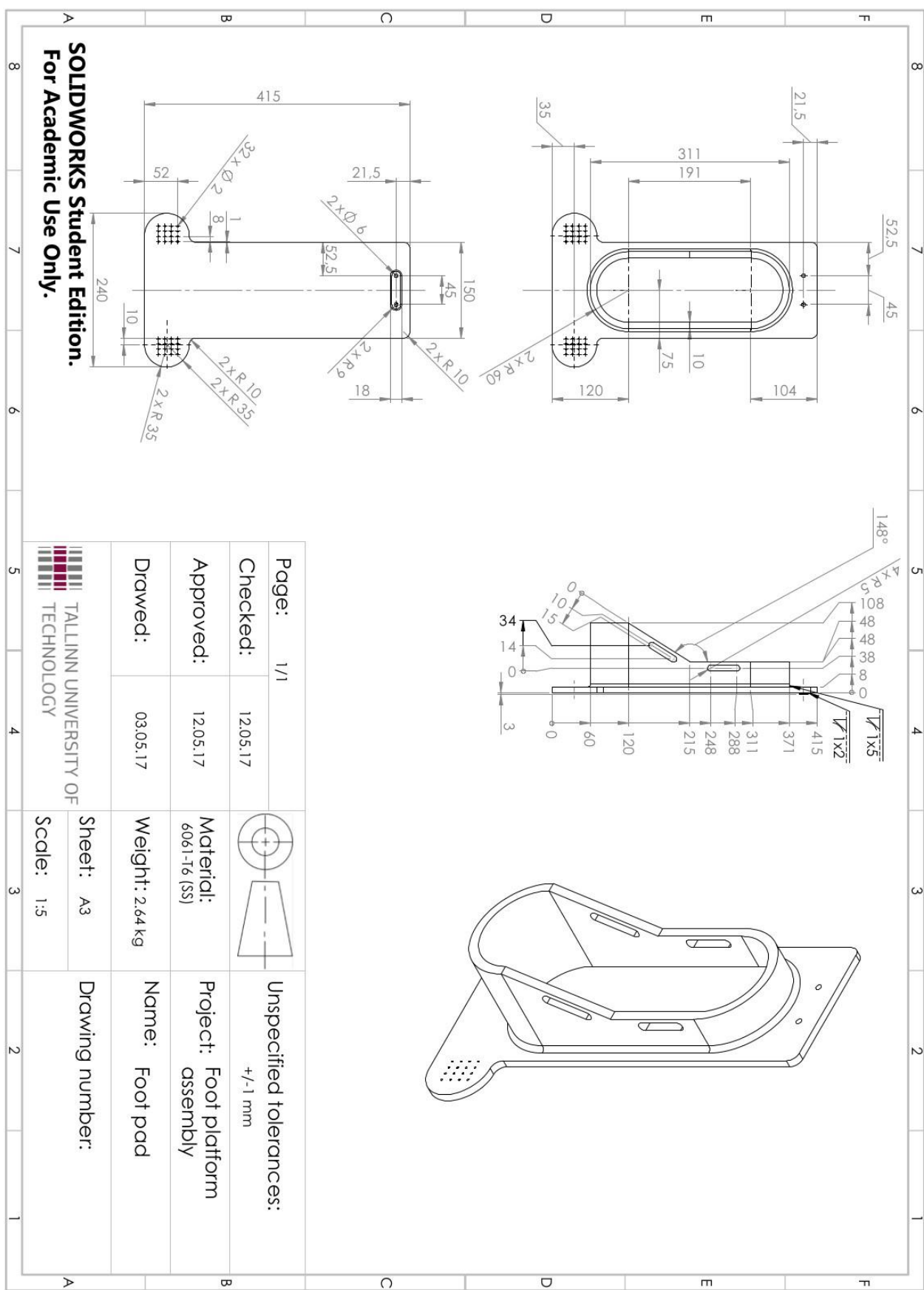
**SOLIDWORKS Student Edition
For Academic Use Only.**

TALLINN UNIVERSITY OF TECHNOLOGY

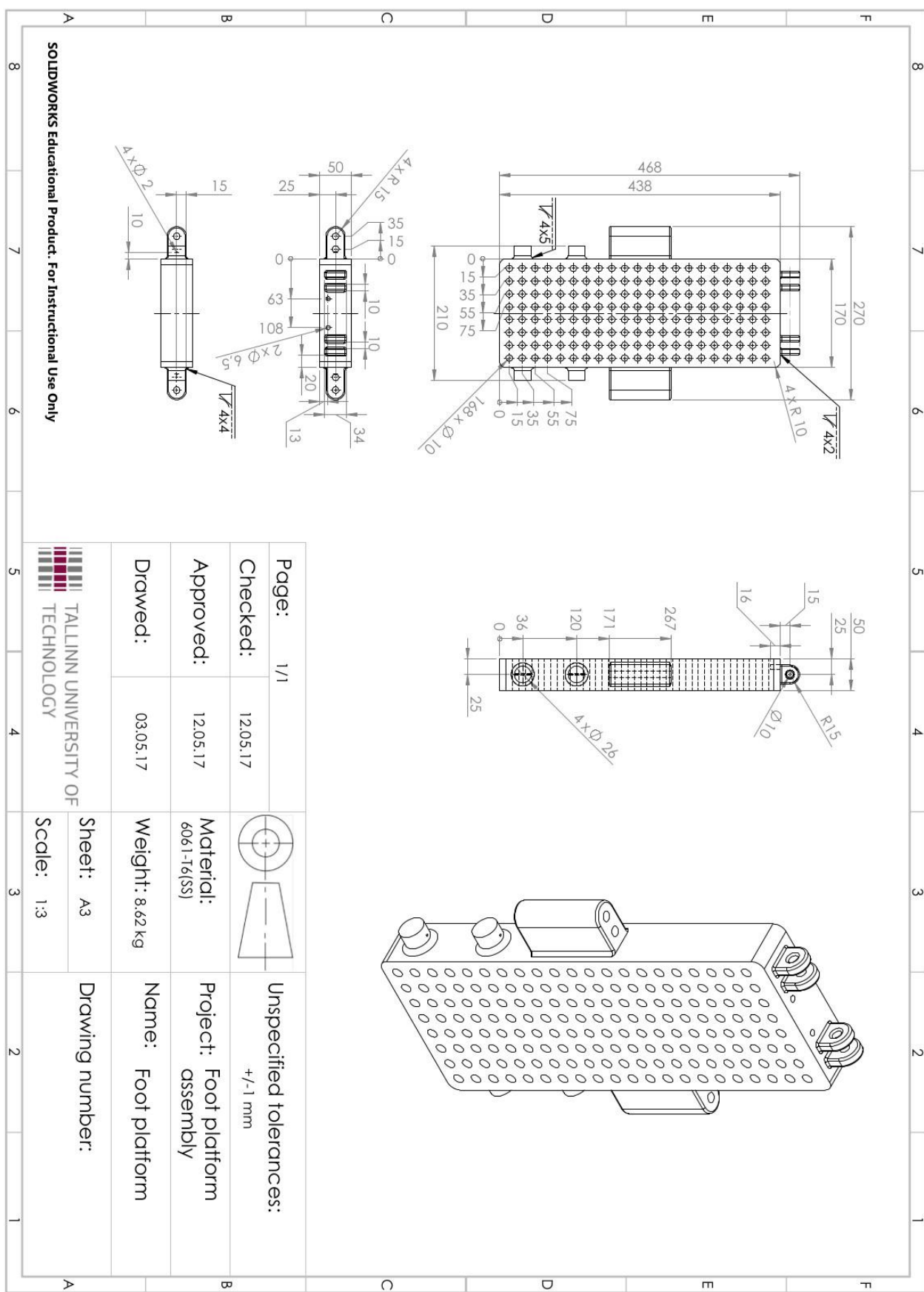
Assembly drawing of the remote control enclosure and respective electronics



Production drawing of the foot pad



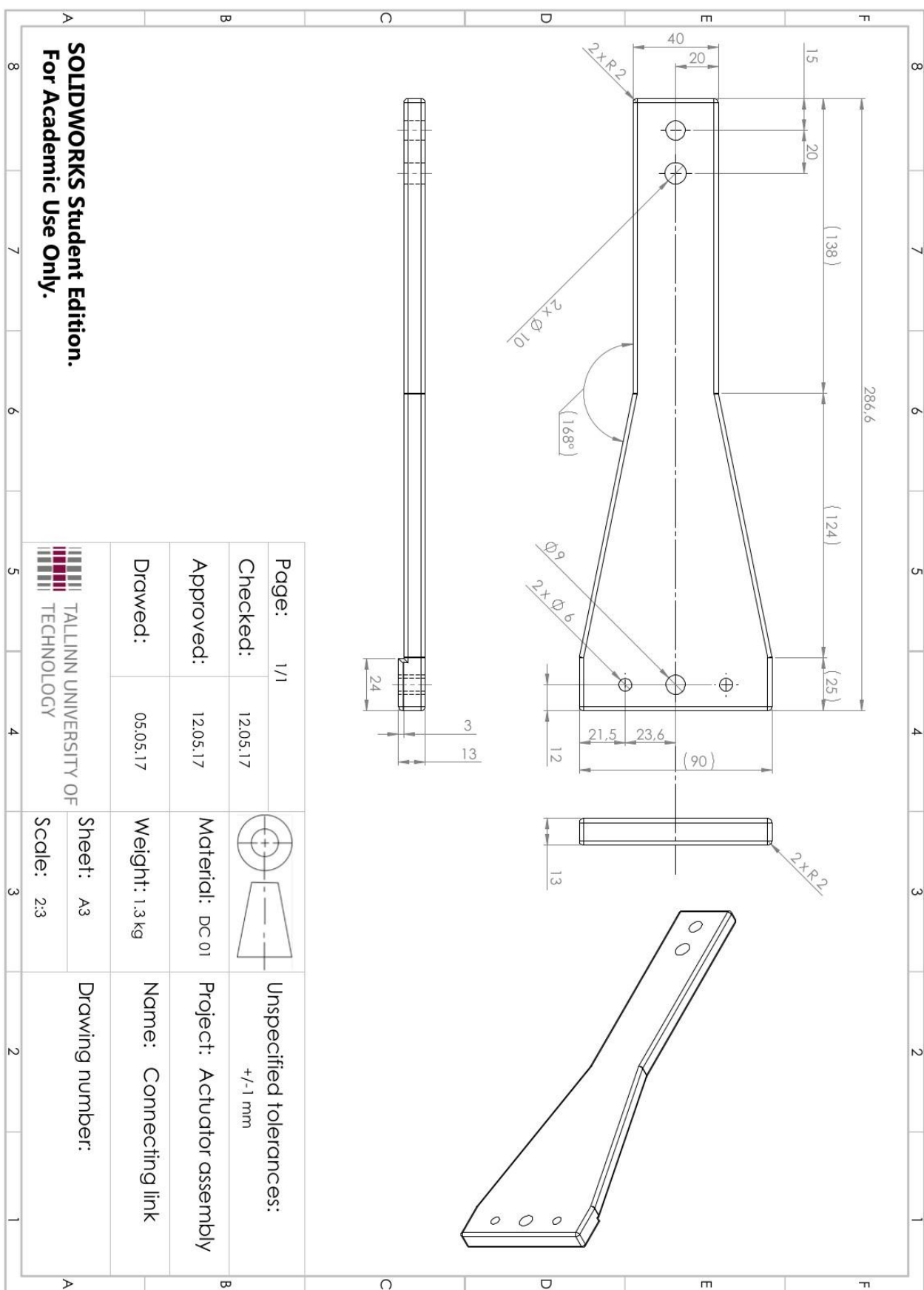
Production drawing of the foot platform



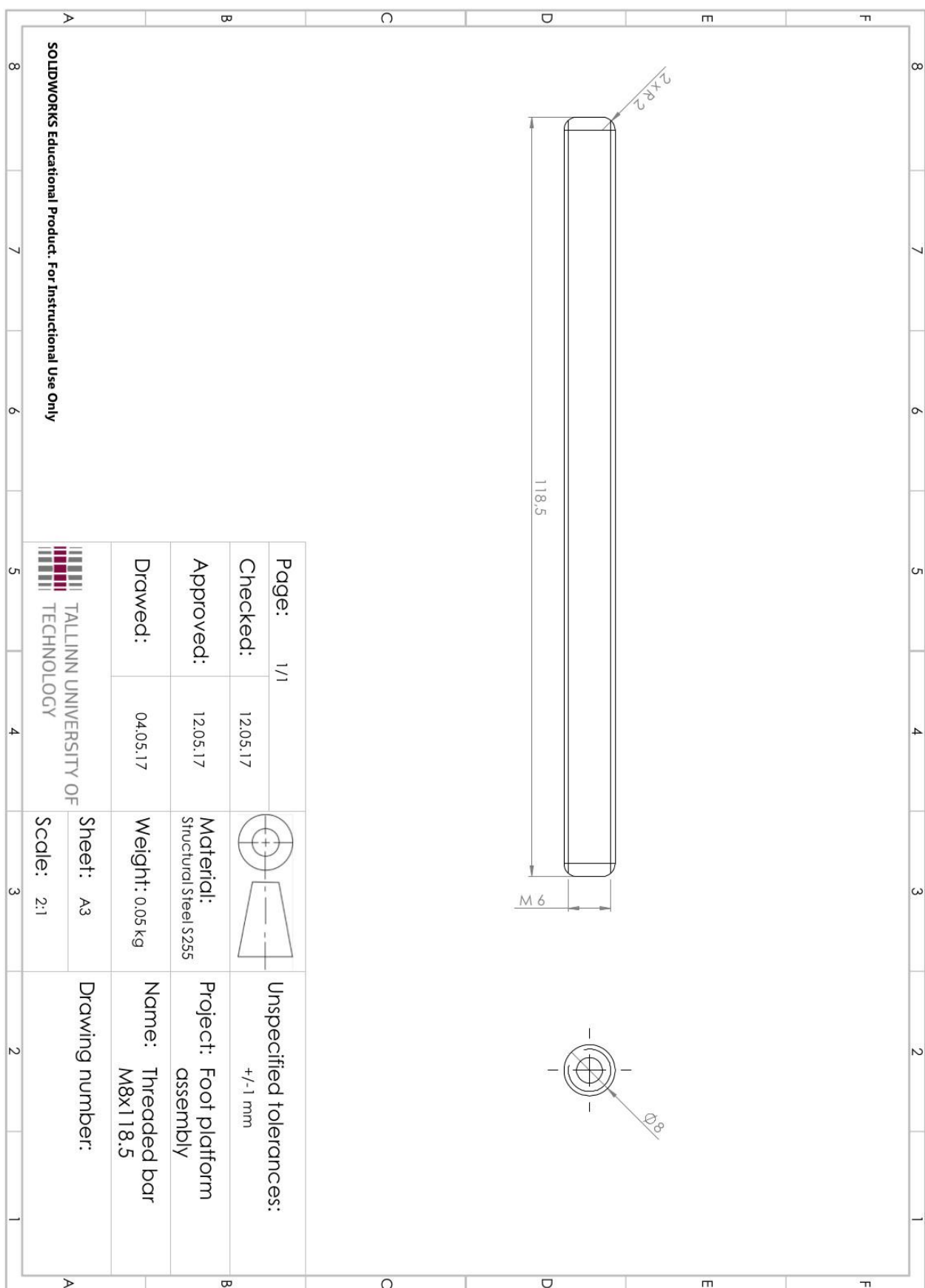
A SOLIDWORKS Educational Product. For Instructional Use Only

TALLINN UNIVERSITY OF
TECHNOLOGY

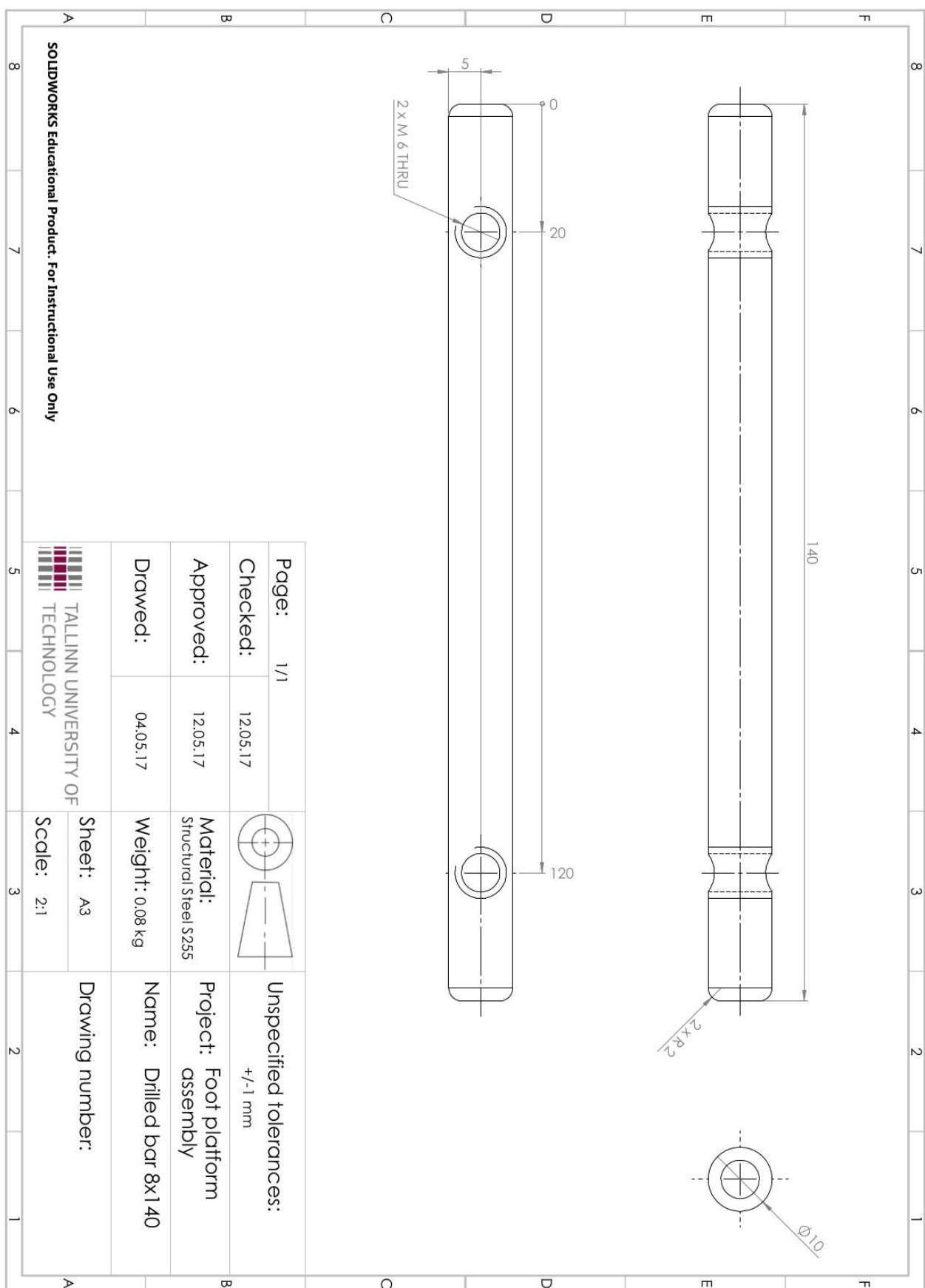
Production drawing of the connecting link



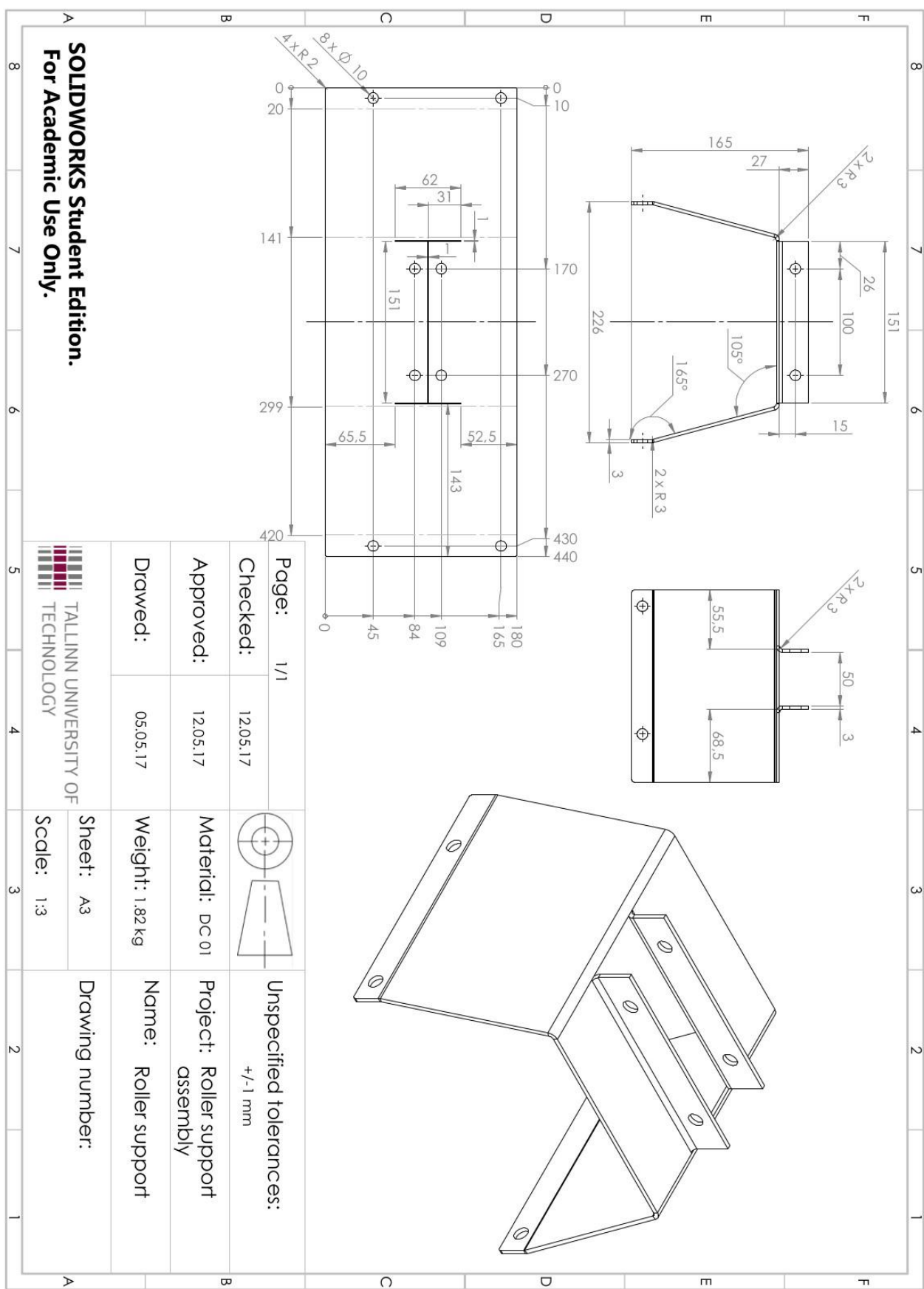
Production drawing of the connecting threaded bar



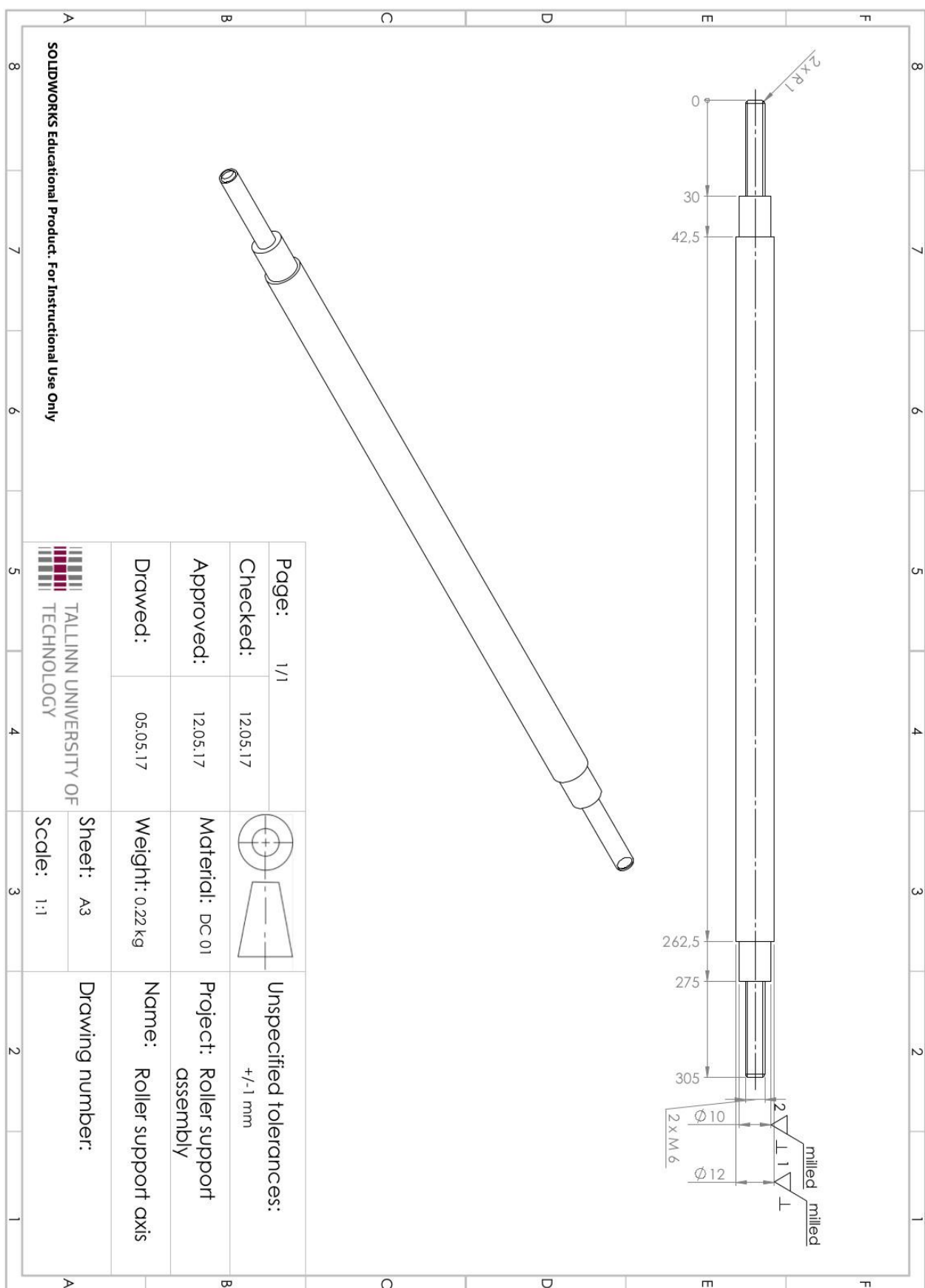
Production drawing of the connecting drilled bar



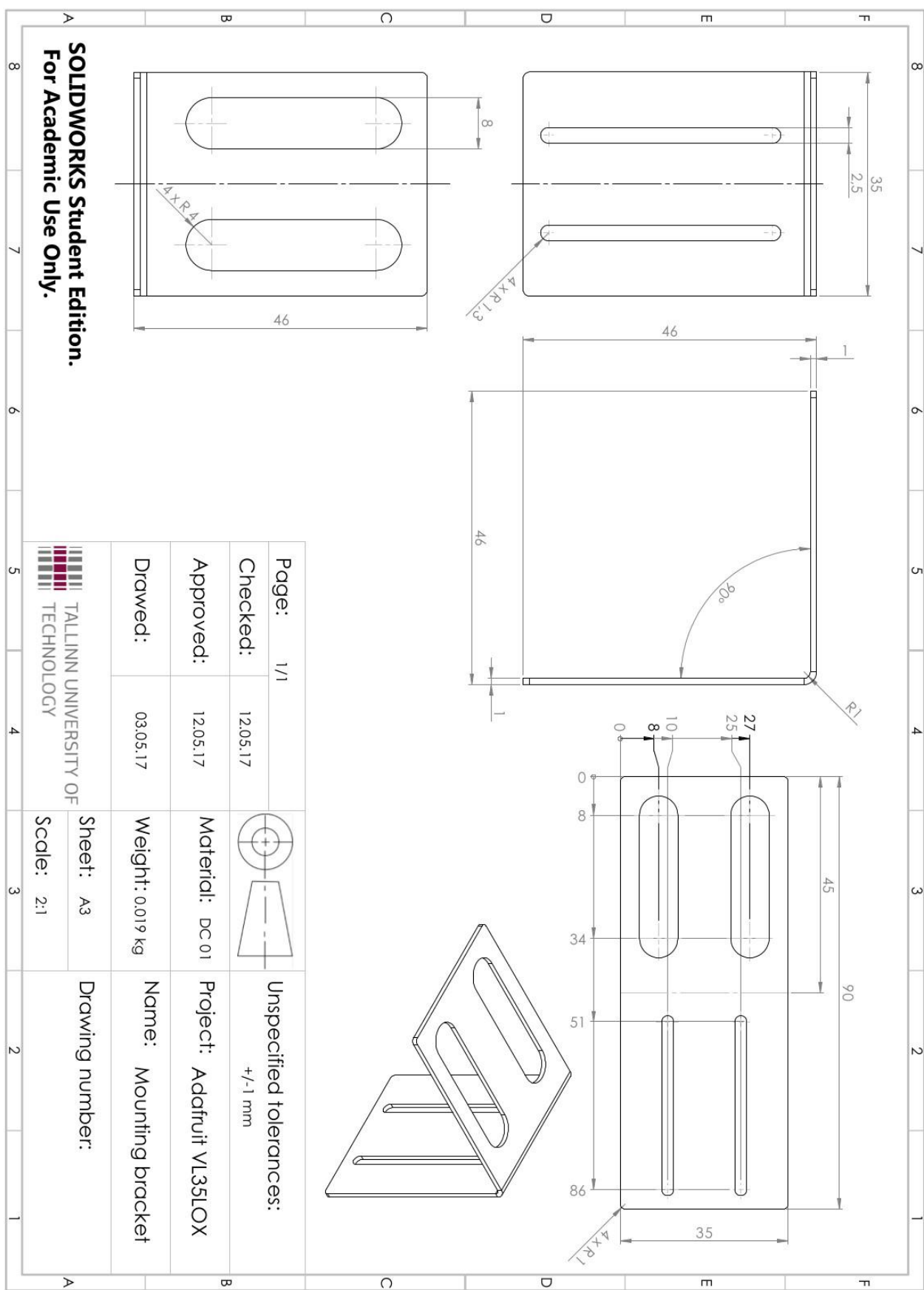
Production drawing of the roller support sheet metal



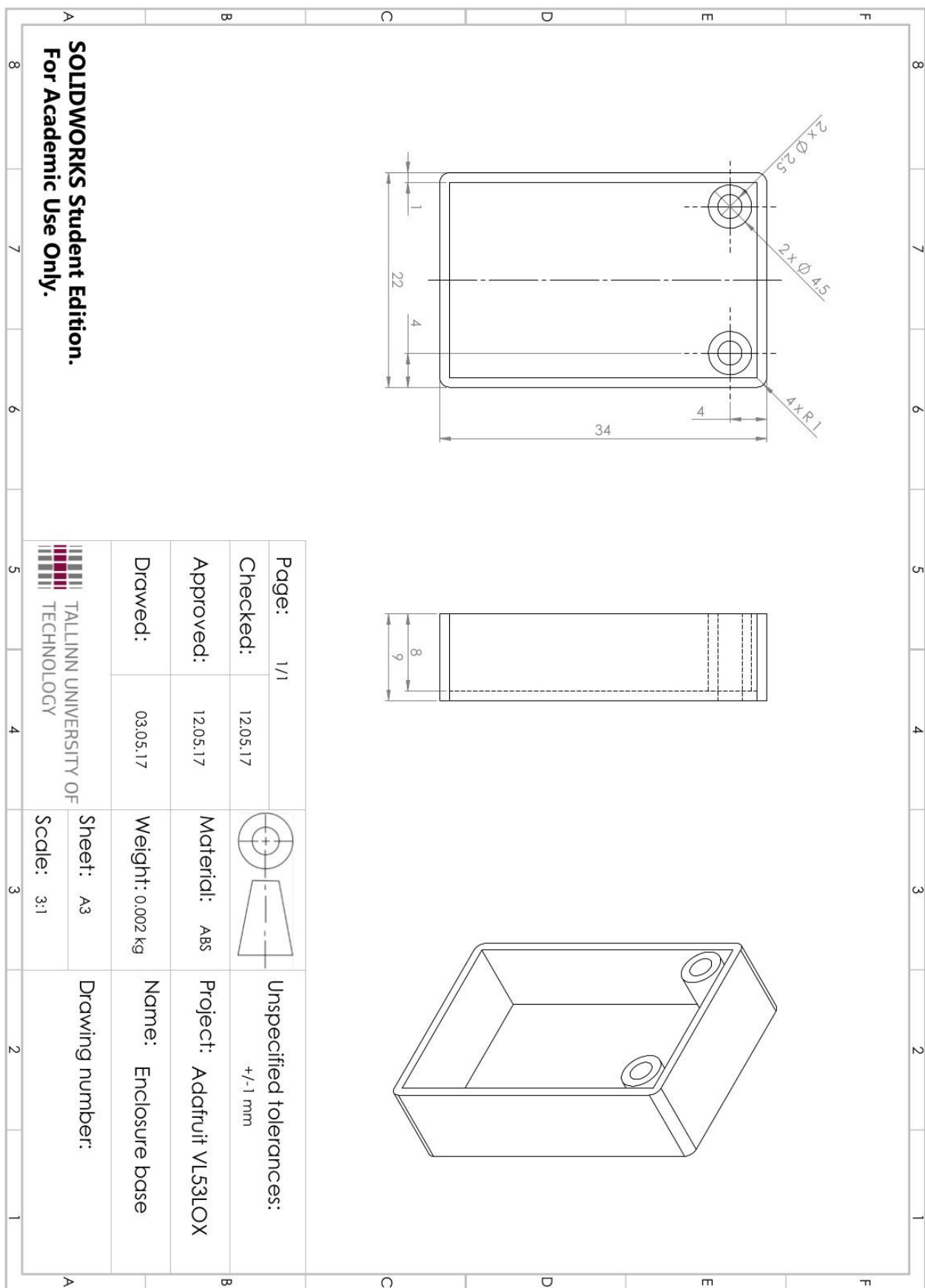
Production drawing of the roller support axis



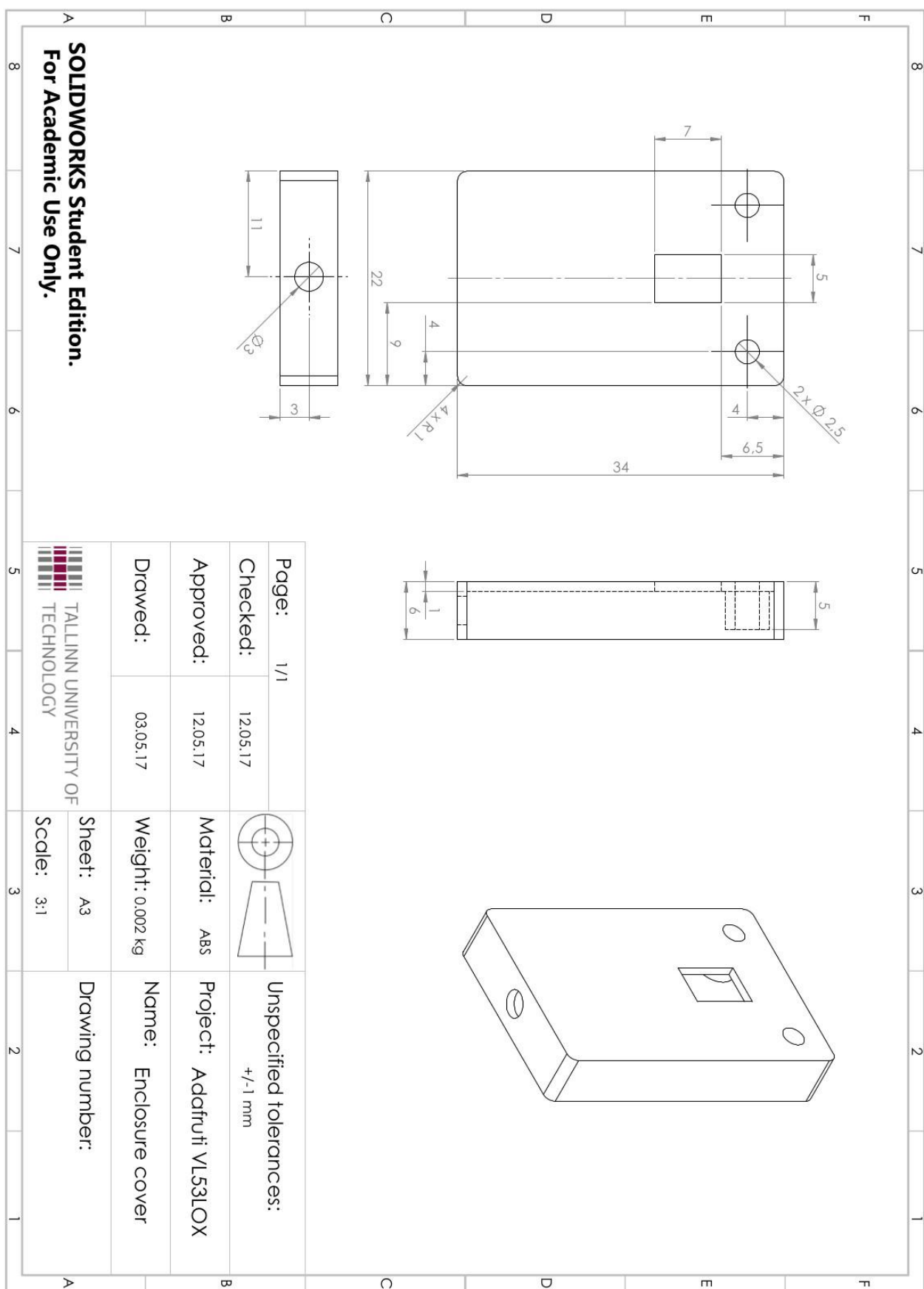
Production drawing of the position sensor mounting bracket



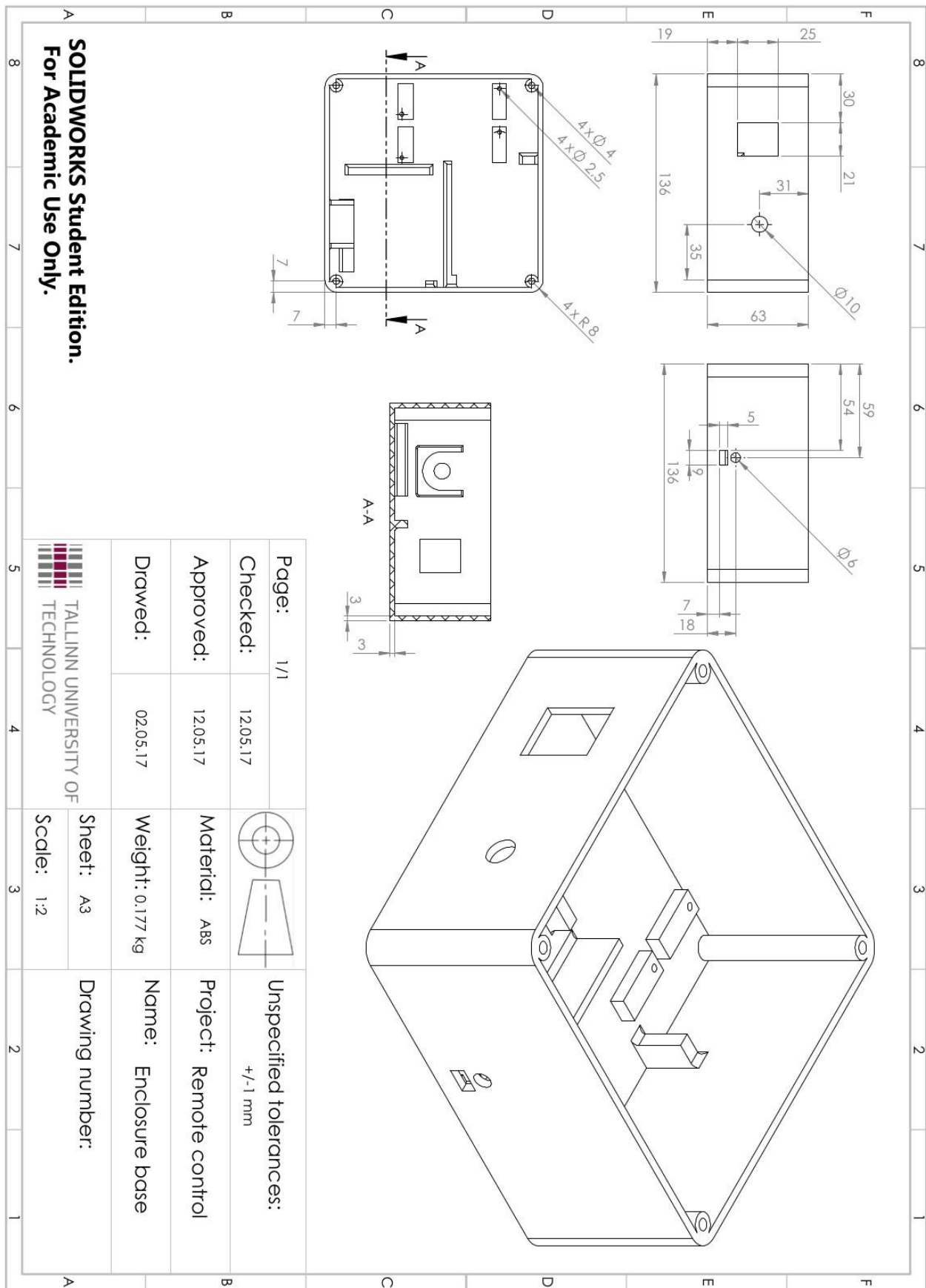
Production drawing of the position sensor enclosure base



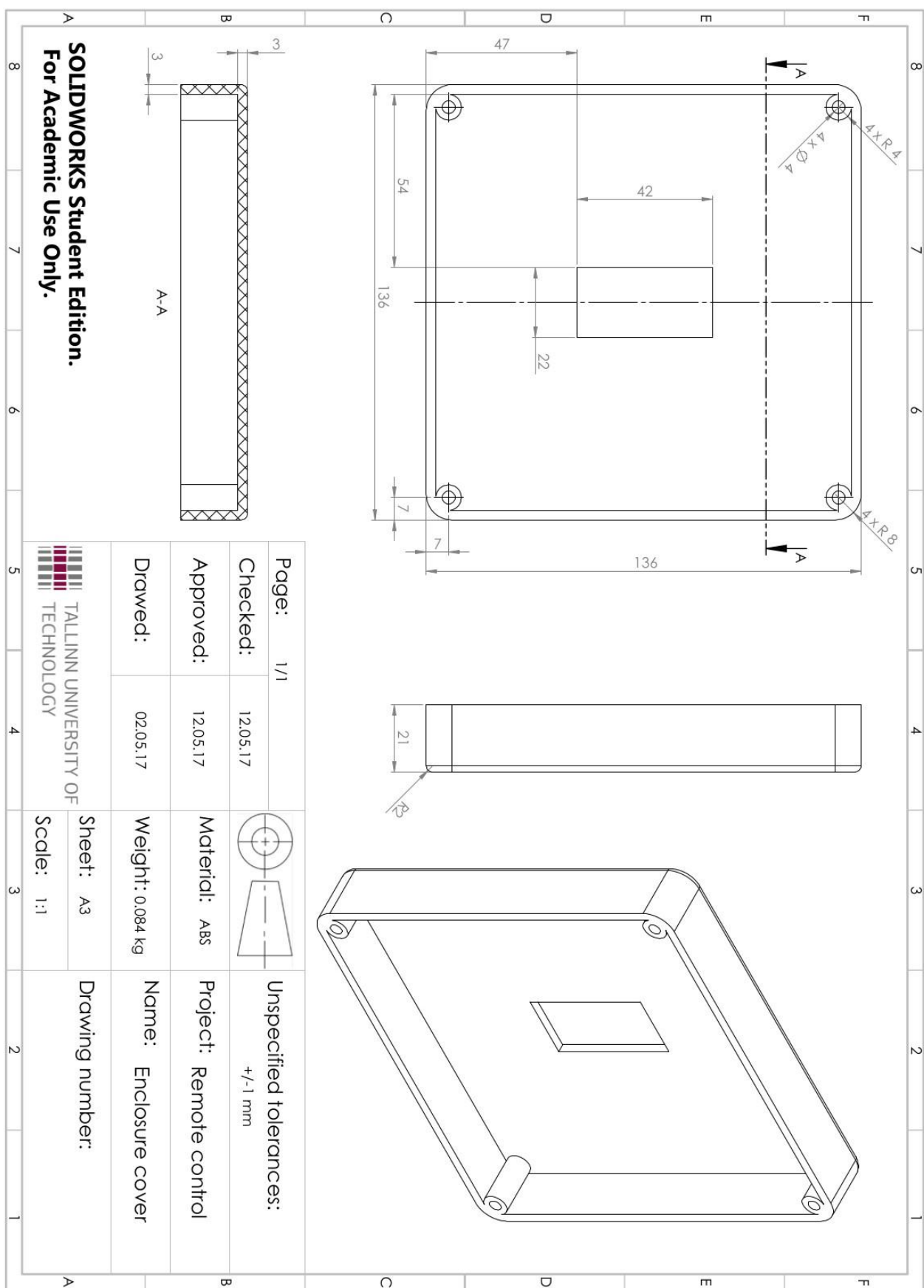
Production drawing of the position sensor enclosure cover



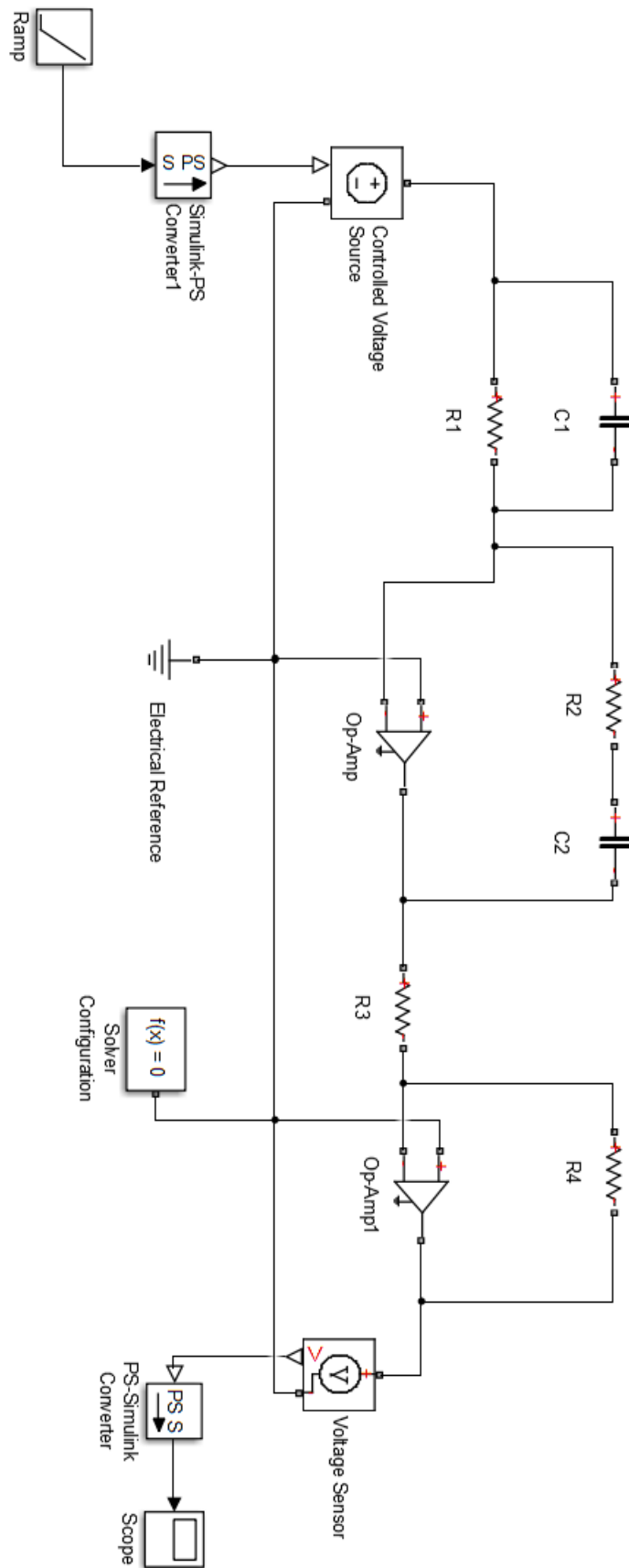
Production drawing of the remote control enclosure base



Production drawing of the remote control enclosure cover



PID controller built on operational amplifiers



Validation model using Simscape libraries

